

MODELLING AND SIMULATION OF THE BIOLOGICAL AND PHYSICAL PROCESSES OF SLOW SAND FILTRATION

A thesis submitted to the University of London
for the degree of Doctor of Philosophy and for the Diploma of the
Imperial College of Science, Technology and Medicine



By

Luiza Cintra Campos

Department of Civil and Environmental Engineering
Imperial College of Science, Technology and Medicine
London, SW7 2BU

May 2002

*Blessed is the man who finds wisdom,
the man who gains understanding...*

Proverbs 3.13

To those who were there for me.

ABSTRACT

Slow sand filtration (SSF) is the earliest form of engineered potable water treatment and remains one of the most efficient processes for improving the physical, biological and chemical quality of water. However, whilst widely used throughout the world, knowledge of the filtration mechanisms remains limited. This is important in understanding and managing the processes that are responsible for gradually blocking the filter reducing its operational life and filtration efficiency.

The objective of this thesis was to develop a mechanistic simulation model of the fundamental physico-chemical and biological processes responsible for the filtration mechanisms operating in slow sand filters. The model solves a set of equations describing schmutzdecke development above the sand and microbial biomass growth within the sand. The model assumes that the schmutzdecke layer contributes to the water purification process and its growth is described as linear function in relation to time. The dynamic interactions between the principal groups of microorganisms including: algae, bacteria and protozoa, were modelled using Monod-type kinetic equations. The filtration performance of the filter media was defined in the model by the removal of particulate material from water and was represented by a combination of headloss and filtration coefficient functions.

The model was calibrated and verified using data from full and pilot plant-scale SSF operated by Thames Water Utilities Ltd. Simulation results showed that interstitial biomass was the smallest part of the bulk specific deposit in both covered and uncovered filters. However, microbial dynamics played an important role in the filtration performance. Schmutzdecke development had a major influence on the operation of uncovered filters and was responsible for the significant increase of headloss observed during operation. The model provides a representation of the fundamental nature of SSF processes and could form the basis of an operational management system to optimise SSF.

ACKNOWLEDGEMENTS

To God, who is able to do immeasurably more than all we ask or imagine. To Him are the glory, the power, and the honour for now and forever.

The financial support provided by the *Fundação Coordenação de Aperfeiçoamento de Pessoal de Nível Superior – CAPES / Brazil* and the *Universidade Federal de Goiás – UFG / Brazil* are gratefully acknowledged.

Sincere thanks are expressed to my supervisors Professor Nigel Graham and Dr. Stephen Smith for their invaluable support and advice throughout this research. In particular, I am grateful to Professor Graham for his expert guidance and to Dr. Smith for his generous assistance and direction. I share with them the credits for this achievement.

The encouragement and support of Professor Luiz Di Bernardo of *Escola de Engenharia de São Carlos*, University of São Paulo-USP / Brazil, was fundamental in the preparatory stage of the research project.

Thanks are due to Professor Steven Chapra at the Civil and Environmental Engineering Department of Tufts University, USA, for his assistance and discussion on microbial modelling during the first year of this research. Dr. Adrian Butler and Dr. Matthew Lees are acknowledged for helping with general modelling and calibration issues.

Many thanks to Thames Water Utilities Ltd. for providing the extensive data from the pilot plant at Kempton Park, and for allowing access to the full-scale slow sand filter beds at Walton treatment works. In particular, I am grateful to Dr. Michael Chipps and Martin Skull. Dr. Roger Wotton and his student, Steve Hurley, at the Department of Biology of University College London, are also acknowledged for assistance during part of the experimental work.

I am indebted to my dear friend and colleague Dr. Manfred Schütze for always being ready to help me with many issues, in particular, during the computer program development. I thank him for his patience in assisting me in learning programming skills.

Of some colleagues who generously helped me with discussion of ideas and information I would like to acknowledge Maria Almeida, Gabriel Coutinho, Didia Covas, Frederico Ferreira, Bojana Jankovic, Neil McIntery, Luis Nieto-Barajas, and Thorsten Wagener. I am also grateful to Elaine Benelli, Emma Bowen, Ugo Cocchini, Sharon Jasim, James Lau, Fayyaz Memom, and Ivan Stoianov for their continuous support and encouragement.

Thanks are due to staff at Civil and Environmental Engineering Department who indirectly contributed to the development of this thesis, in particular: Andy Chippling, Frank Cock, Mark Ferrie, Dr. Geoffrey Fowler, Angela Frederick, Ruth Harrison, Dr. Steve Lambert, Jon Sison, Mark Soole, and Susanna Parry. I am also very grateful to all my English teachers from the English Language Support Programme-ELSP at Imperial College. In particular, I am indebted to Su Peneycad for kindly proof-reading this thesis.

I express my heartfelt thanks to those who were there when I most needed a friendly shoulder. I acknowledge my flatmates at the community flat, my friends from the Hinde Street Methodist Church, Cecile Andre, Monica and Fernando Buarque, Lisa and Tim Parkinson, and Teresa Oliveira. I hope our friendship continues throughout the years.

Special thanks are reserved for my parents Izaías Campos and Odávia Luiza Borges. Their love and undying support were very important in attenuating difficult moments of my living in London. Many thanks are also due to my sister Izabela Campos for being my representative in Brazil during my period abroad.

Finally, I am deeply indebted to Dr. Jonathan Parkinson for his fair criticism, encouragement and advice over the last 2 years. Jonathan, I thank you very much for your love, patience, and invaluable support during the hard stages of my PhD.

1 - INTRODUCTION

1.1 - Motivation behind the research

Slow sand filtration (SSF) is the earliest technology to water treatment. It was initially developed by John Gibb at Paisley in Scotland in 1804 to obtain pure water. His design was improved by Robert Thom in 1827 and was later employed by James Simpson at the Chelsea Water Company in 1829 (Baker, 1949). After John Snow linked the outbreak of diseases such as cholera and typhoid to waterborne contamination, slow sand filters became a legal requirement for all potable water extracted from the River Thames from 1852 (Huisman and Wood, 1974). Further convincing proof of the effectiveness of SSF at controlling waterborne disease was provided in 1892 by the experience of two neighbouring cities, Hamburg and Altona, which both abstracted drinking water from the River Elbe. The former delivered drinking water from the river untreated, while the latter filtered the whole of its supply. When the river water became infected with cholera organisms, Hamburg suffered from a cholera epidemic, while Altona escaped the epidemic. Slow sand filtration was the sole method of water treatment until the advent of rapid sand filtration at the end of 19th Century (Ellis, 1985).

The introduction of chlorination and chemical coagulation techniques in water treatment followed by the development of rapid sand filters led to a decline in the use of slow sand filters (Bowles *et al.*, 1983). The disadvantages of SSF are the relatively large area needed, the high cost of cleaning, and, the low-turbidity raw water required. These are also cited as the cause for the decline in SSF systems for water treatment (Rachwal *et al.*, 1986; Barret *et al.*, 1991; Fox *et al.*, 1994). Whilst the construction of SSF plants has been largely abandoned in the United States, many other countries (e.g. Germany, the Netherlands, United Kingdom, France, India, Peru, and Colombia) have continued to use and construct slow sand filters. Despite the recent technological advances in the field of water treatment, SSF remains one of the most efficient unit filtration processes at improving the physical, biological and chemical quality of potable water (Poynter and Slade, 1977; Schuler *et al.*, 1991; Welte and Montiel, 1996).

During the last 3 decades, there has been a resurgence of interest in the application of SSF throughout the world. In particular, SSF is recognised as appropriate technology

for treating water for rural and small communities due to its simplicity of construction, operation and maintenance. Major advances have been also achieved in pre-treatment methods to overcome raw water quality problems, especially in developing countries (Smet and Visscher, 1989). In Europe and North America, the efficient removal of problematic pathogenic microorganisms such as *Giardia* and *Cryptosporidium* cysts (Bellamy *et al.*, 1985a; Fogel *et al.*, 1993), and dissolved organic matter after pre-oxidation (Graham, 1999), by SSF is acknowledged as a major advantage of SSF, compared to rapid filtration and other advanced water treatment methods.

Despite the wide spread re-emergence of SSF as a water treatment method, operational strategies and the knowledge of the filtration mechanisms remain limited. Indeed there is comparatively little scientific literature on SSF, compared with the volume of material published on rapid sand filtration processes. The main areas of investigation on SSF during the past 25 years have focused on (a) the ecology of slow sand filters, (b) pre-treatment methods, and (c) process performance and development. Relatively little attention has been given to the process modelling of SSF. The principal interest has been the development of new process designs and process control systems and there has been relatively little achievement in scientific understanding of the fundamental mechanisms operating during SSF.

Over the last 10 years, process simulation has become an increasingly powerful tool for optimising the operation of water and wastewater treatment systems within the water industry. A range of models (e.g. WEASEL¹, SANDMAN², GACMAN³) have been developed for a variety of purposes such as preliminary design, refinement and

¹ WEASEL is a water treatment process simulation package designed by the Water Research Centre (WRc) to perform dynamically, responding to changes in water quality, flow and operating parameters (Head, 1998).

² The Sand and GAC Management System (SANDMAN) is a PC-based decision support system used by Thames Water, which helps process managers schedule slow sand filter bed maintenance activities (Mann and Rock, 1996).

³ GACMAN is a computer model developed by WRc that calculates the GAC saturation volume (i.e. the volume of water GAC has treated) based on the concentration of pesticides in the water to be treated and the flow profile of each filter bed (Mann and Rock, 1996).

optimisation of design, commissioning, operational decision support and training. Simulation models for potable water treatment processes are usually carried out with a time series of influent data, such as water flow and quality parameters. The output generated by these models consists of the treated water quality and several operational parameters of the different treatment process including the points in time of backwashing a rapid filter, the total amount of dosed chemical, the loading of activated carbon, etc.

Despite the relative advance in modelling of process performance and control of water treatment works, considerable benefits in terms of operational plant control, and of understanding of the SSF mechanisms could be obtained using an adequately computer-based simulation model. The major potential for developing a sensitive simulation model for SSF is that it will identify and describe the significant mechanisms occurring in the filter media and their dynamic nature. Finally, improved understanding of SSF process mechanisms through simulation models could potentially stimulate its use in developing countries. This could establish SSF in those countries (e.g. Brazil) where slow sand filters have been replaced by other technologies (i.e. rapid filtration) causing, apart from the supply of inadequately treated water, a loss in the development and improvement of SSF.

1.2 - Overview of modelling of SSF mechanisms

The first attempt at SSF modelling was made by Iwasaki (1937), which incorporated two basic filtration equations including the kinetic and continuity functions to describe the filter capacity. The kinetic equation assumed that the removal of suspended particles was proportional to the concentration of particles present in the influent water, and the continuity equation represented the relationship between the suspended particles concentration in the water and the accumulating deposit in the filter, i.e. the particle mass balance. Iwasaki (1937) had difficulties in describing the removal of bacteria by filtration and a modification of the continuity equation was suggested by Slade (1937) to account for bacterial growth in slow sand filter beds.

Following the pioneering work of Iwasaki (1937), the next developments in modelling of the SSF were by Woodward and Ta (1988), who proposed a simple empirical model to predict flows and headloss for a SSF bed network at the Ashford Common water treatment plant operated by Thames Water Utilities Ltd. The model did not make use of the Iwasaki (1937) equations but was successfully used in the simulation of headloss and flow. The continuity equation of Woodward and Ta (1988) assumed that all particles were removed from the influent water. Although a general growth rate term was included, the model did not take into account any dynamic of biological growth. It is generally observed that in operational slow sand filters the clean headloss is recovered after scraping the top 2 cm of the media including the schmutzdecke. This indicates that the upper layers of the sand bed contribute mainly to the headloss development. Therefore, a uniform distribution of material across the entire media depth as assumed by Woodward and Ta (1988) appears to be unrealistic. Another limitation of this model is that it does not predict the spatial variation of headloss across the filter bed.

Ojha and Graham (1991, 1994) simulated SSF using combinations of headloss and filtration coefficient relationships. Their filtration coefficient was based on an assumed headloss model similar to that of Woodward and Ta (1988). The model simulated overall headloss development of a filtration run, but the prediction of headloss distribution with depth was poor and, subsequently, the derivation of the filtration coefficient model was found to be invalid for simulation of slow sand filters. However, alternative headloss and filtration coefficient models suggested by Ojha and Graham (1994) provided a basis for a satisfactory simulation of slow sand filter performance. The model structure included a simple representation of biomass development, but the influence of schmutzdecke was ignored.

A numerical scheme for evaluating the role of the schmutzdecke was proposed by Ojha and Graham (1993a), using a combination of filtration coefficient and headloss models. Increasing headloss was assumed to be related to the development of a schmutzdecke layer on the surface of the media and deposits in the top 2 cm of the media bed. The headloss across the schmutzdecke and the top 2 cm of the media was derived by subtracting the clean bed headloss of the lower layers from the total headloss. Following

this approach, the *schmutzdecke* layer was identified as the major contributor to headloss development and the removal of particulate matter. However, the assumption that the sand bed beneath the upper 2 cm was clean may not be in accordance with real systems since microorganisms and other impurities are known to penetrate to deeper layers of the sand bed (Bellinger, 1979; Toms, 1996).

Retamoza *et al.* (1994) proposed an empirical model for slow sand filters based on the production of biofilm and deposit of particles within the sand bed. The model incorporated one modified equation of continuity and two kinetic equations, a substrate removal function and an equation to describe particle removal within the interstitial sand. A relationship between the filtration coefficient and substrate removal was established, based on the assumption that removal of substrate was caused by the accumulation of bacteria within the sand bed. Apart from bacteria growth, the model did not take into account any other biological growth. A headloss model was derived using Boucher's law which relates headloss with volume of filtered water. A limitation of the model is that it does not predict the spatial variation of headloss across the filter bed.

Ojha and Graham (1996a) used numerical algorithms to investigate the significance of the *schmutzdecke*. Their approach was based on the comparison of two parallel, pilot-scale slow sand filters. One filter was covered and the other was uncovered. Both filters were started at the same time with the same initial conditions and were subjected to the same influent water concentrations. *Schmutzdecke* development in the uncovered filter was assumed to be entirely due to algal growth, whilst *schmutzdecke* was absent in the covered filter. The model was calibrated for the covered filter and this model was used to predict the performance of the uncovered filter. As would be expected, there was good agreement between observed and simulated values of headloss for the covered filter, but the model substantially underestimated headloss in the uncovered filter. Thus the model did not take full account of the effects of the *schmutzdecke* layer on headloss development. The model was calibrated using one a single data set with very short filtration run lengths of 19 days for the covered filter and 12 days for the uncovered system. However, this is unrealistic of operational practice where filtration periods may be several weeks or months. Furthermore, dynamics of microbial and *schmutzdecke* growth were not considered in the model structure.

Ojha and Graham (1996b) later included microbial growth and changes in the bulk specific deposit due to microbial activities within the developing modelling framework. The approach partitioned the influent concentration into inert and biologically active components. The biologically active part was further divided into algae, bacteria and protozoa. Changes in the bulk specific deposit of these various components due to microbiological activity were considered, taking into account interactions between the microorganisms and their substrates. The changes in the concentrations of these components were predicted using Monod-type kinetic equations. Different weighting factors were assumed in the calculation of the bulk specific deposit, as the amount of the various components participating in different interactions was unknown. Substrates were assumed to be in the dissolved state and to be removed by adsorption, following the kinetics of filtration theory. The same value of bulk factor was used for the various components and different filtration coefficients were determined for each component (inert material, algae, bacteria, protozoa and substrates). In the presence of microbiological interactions, the filtrate quality was found to improve and the headloss to reduce. This model simulated the apparent variations in observed microbial biomass within the filter layers, although the possible contribution of the schmutzdecke layer to water purification was ignored. The relative importance of empirical model parameters was investigated, but the model could not be calibrated because of the lack of experimental data on microbial interactions and their influence on water filtration processes.

Shiba (1996) proposed a simple mathematical model to predict the filtrate concentration of both slow and rapid filters. The model contains an empirical parameter estimated from input and output water quality data, and assumes that the removal of particles is uniform across the filter depth. The model successfully simulated the operational performance of a rapid sand filter. However, the model was not verified for SSF, probably because of the difficulty in estimating the empirical water quality parameter since the distribution of deposit is non-uniform with depth and time. The model is physically based and is unlikely to be applicable to slow sand filters because important biological kinetics and processes are not considered.

Chu (1998) applied the fundamental ideas of Ojha and Graham (1994, 1996b) in developing a computer-based numerical model of SSF which included microbial interactions and the kinetics of microbial growth of algae, bacteria and protozoa populations in the filter bed. The behaviour of the schmutzdecke was simulated as a single layer and was conceptualised as a non-woven fabric layer. The growth of the schmutzdecke was represented by an algal growth function based on temperature, nutrients and light. Interactions between the schmutzdecke and other microorganisms were not considered in the model. All particles were considered to be the same size and, consequently, had same initial filtration coefficient. The model was developed to simulate uncovered slow sand filters, but could not be calibrated due to lack of experimental data on physico-chemical and biological activities in slow sand filter systems.

Despite recent progress in developing models of SSF mechanisms, current models fail to adequately integrate the biological process with filtration theory in slow sand filters. Existing approaches (Ojha and Graham, 1994-1996; Chu, 1998) have improved the representation of the schmutzdecke and provided a more comprehensive description of the microbial dynamics. This is important in understanding and managing the processes that are responsible for gradually blocking the filter and its operational efficiency. However, the contribution of the schmutzdecke to the headloss development remains undefined and unquantified and this is principally due to the lack of experimental data for model calibration and verification, as emerged in some previous works (Ojha and Graham, 1994-1996; Chu, 1998). Experimental data are therefore a critical constraint to further development and validation of SSF models.

1.3 - Objectives of the thesis

The purpose of this thesis is to contribute to the understanding and description of the complex and fundamental interactions between the biological and physico-chemical processes operating in slow sand filters. The focus of the work was to model and simulate physico-chemical and biological phenomena in order to predict the process performance of both uncovered and covered filters.

To achieve this purpose the specific objectives were:

- (1) develop a computer-based model to simulate the most relevant processes of SSF including particle removal, microbial dynamics, schmutzdecke and sand biomass, and headloss development using existing mathematical models of filtration theory and microbial dynamics;
- (2) identify the most important model parameters by sensitivity analysis and to calibrate these parameters using Monte Carlo techniques;
- (3) examine the applicability of the model using field data from operational covered and uncovered slow sand filters;
- (4) define and quantify the contribution of the schmutzdecke to headloss development.

1.4 - Outline of the thesis

Chapter 2 presents a review of the literature of those areas that are of relevance to the research. Section 2.2 provides a general description of the slow sand filter, including the functioning of the process, mechanisms of filtration, and biological aspects. Section 2.3 describes the nutrition and growth conditions of microorganisms, as well as the general mathematical representation of microbial dynamics. Section 2.4 summarises the main issues that are relevant for the development of the SSF model.

Chapter 3 contains a description of the data set provided by Thames Water and used for model calibration. Section 3.2 contains a background of data measurements, while the main characteristics of these data are illustrated in Section 3.3. Section 3.4 contains an analysis of the data carried out by determining the coefficient of correlation between the water quality parameters. The processing of the data is explained in Section 3.5. Section 3.6 contains a summary of the quality and quantity of the data provided by Thames Water.

Chapter 4 describes an experimental investigation to determine schmutzdecke and interstitial sand biomass in full-scale slow sand filters at the Walton Advanced Water Treatment (AWT) works, operated by Thames Water. Section 4.2 contains a description

of the treatment works, methods and analysis utilised. Section 4.3 presents and discusses the results obtained from this investigation, and Section 4.4 summarises the main conclusions. This work was of primary importance for the understanding of the influence of microbial growth and dynamics on SSF processes, and the subsequent analysis and application of the SSF model.

Chapter 5 describes the development of the SSF model, from its basic concepts (Section 5.2) to the elaboration of the computer program (Section 5.5). Section 5.3 presents the mathematical formulation of important processes occurring within a filter, including growth of the schmutzdecke, microbial dynamics in the supernatant water and in the filter bed, and filtration mechanisms. The limitations of the SSF model, including the initial and boundary conditions, the process of filter cleaning, and the model parameters and data required are included in Section 5.4. Section 5.5 provides the numerical solution of the differential equations and the computer program is described in Section 5.6. The procedures for model calibration are included in Section 5.7. Section 5.8 summarises the characteristics of the SSF model.

Chapter 6 describes the application and analysis of the SSF model. Section 6.2 contains the sensitivity analysis of the model with respect to changes in time step, sand depth discretization, 'growing time' of the schmutzdecke, number of Monte Carlo samples, and model parameters. The calibration of the model in relation to biomass development and headloss is presented in Section 6.3. Section 6.4 contains a description of the process of model verification. Section 6.5 provides an assessment and overview of the general performance of the SSF model.

Chapter 7 describes the further development of the SSF model structure to improve the prediction of headloss development in uncovered filters. Section 7.2 describes the characteristics of the improved SSF model. Section 7.3 identifies the most important parameters to headloss development and Section 7.4 considers the calibration of the improved model for headloss development during winter and summer seasons. Section 7.5 presents the process of model verification incorporating temperature correction factors for model parameters. Section 7.6 summarises the results of the calibration and verification procedures for the improved SSF model.

Chapter 8 examines the fundamental insights into SSF mechanisms from the simulation model. Section 8.2 illustrates the simulation of headloss in the schmutzdecke and sand bed with time and depth, as well as defining the contribution of the schmutzdecke to headloss development in slow sand filters. The importance of the distribution of the bulk specific deposit with depth is shown in Section 8.3. Section 8.4 explains the significance of the simulation of biomass growth. Section 8.5 presents simulation results for the various microbial interactions predicted by the model and elucidates the importance of the microbial dynamics in the SSF processes. The variation in the filtration coefficient of the slow sand filters is described in Section 8.6. Section 8.7 examines the role of the schmutzdecke in uncovered filters and Section 8.8 considers the importance of the initial conditions of the sand bed to the SSF simulation process. Simulated changes in the supernatant water of uncovered filters are presented in Section 8.9 and Section 8.10 shows the potential of the SSF model at predicting the influence of filtration rate and temperature in the SSF process. A general summary of the insights into SSF process from the simulation model is presented in Section 8.11.

Chapter 9 contains the conclusions and recommendations for further research. Section 9.1 summarises the characteristics and potential of the SSF model. Section 9.2 outlines the main achievements and results of this work. Finally, recommendations for future work are presented in Section 9.3.

2 - +LITERATURE REVIEW

2.1 - Introduction

The objective of this literature review is to describe the main aspects of the SSF and the mathematical modelling of microbial growth considered to be relevant for the SSF model development, summarised in Figure 2.1.

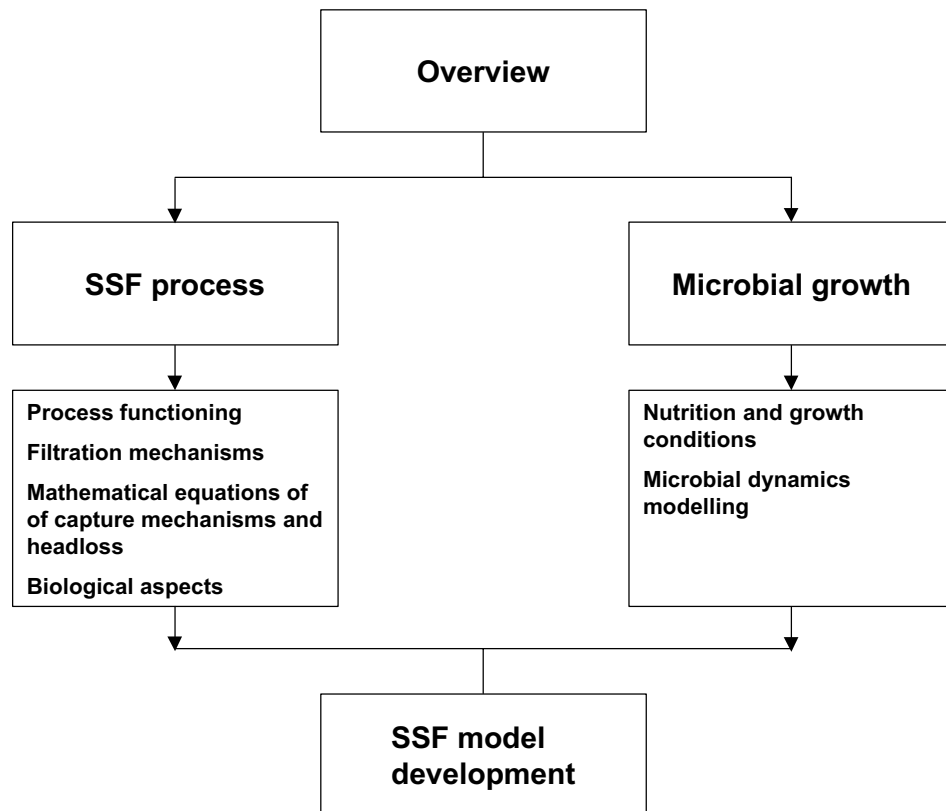


Figure 2.1 - Areas covered by the literature review

2.2 - Slow sand filtration processes

2.2.1 - Characteristics of the SSF processes

The basic components of a slow sand filter are: supernatant water layer, sand bed, underdrain system, and flow control system (Figure 2.2). The supernatant water layer provides a head of water that is sufficient to drive the water through the filter bed, whilst creating a retention period of several hours for the water. Sand is the usual filter medium because of its low cost, durability and availability, although other granular materials such as diatomaceous earth can be used. The sand has a relatively fine grain size (effective size 0.15-0.3 mm) with a uniformity coefficient of preferably less than 3

(Visscher, 1990). The underdrain system provides an unobstructed passage for treated water from the filter bed and supports the filter sand bed. The outlet flow control maintains submergence of the medium during operation to minimise potential air-binding problems.

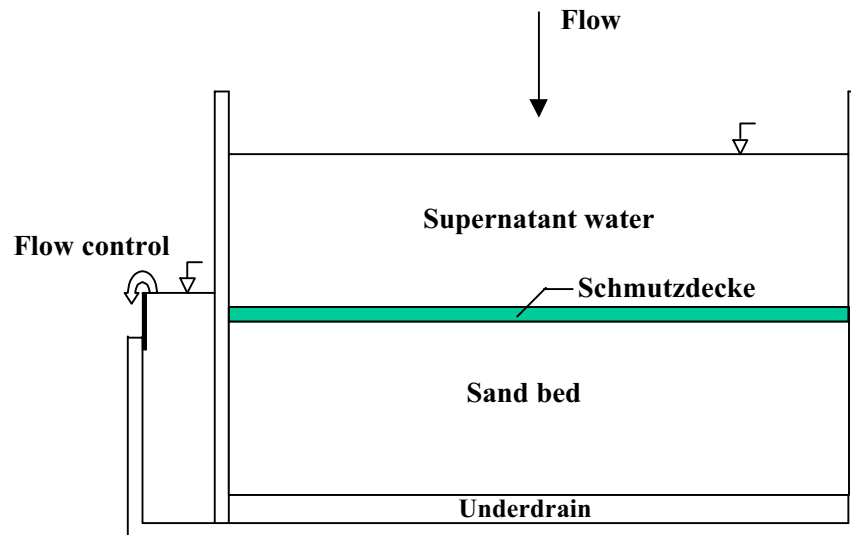


Figure 2.2 - Schematic representation of a slow sand filter

Water percolates slowly through the porous sand medium, and inert particles, organic material, and microorganisms such as bacteria, viruses and cysts of *Giardia* and *Cryptosporidium* enteroparasites are removed (Ellis, 1985; Fogel *et al.*, 1993). An algal mat forms on the surface of the sand bed of uncovered filters and this is termed 'schmutzdecke' (see Figure 2.2). The long hydraulic retention time of water above the sand bed (3-15 h) in slow sand filters permits the development of a substantial biological community. Therefore, the particle deposit on the top of the sand includes microorganisms, which contribute to the development of the schmutzdecke. After several weeks or months of operation, the surface area of the filter bed becomes clogged due to deposition of suspended solids. The deposit of captured inert particles and microorganisms, together with the growth of biological populations, gives rise to increasing hydraulic resistance to flow manifested as an increasing process pressure headloss. Final headloss occurs when, with the maximum water head above the sand and the outlet valve fully open, it is no longer possible to achieve the designed flow rate and cleaning of the filter bed is required to restore the filtration rate. The filter bed is cleaned by scrapping off the top 2-3 cm of the sand including the schmutzdecke layer

(Plate 2.1). After successive scrapings the depth of the sand bed is reduced to its minimum design level (usually 0.5-0.6 m), and a resanding is necessary.



Plate 2.1 - Cleaning a full-scale slow sand filter at Walton, Thames Water

Slow sand filtration is regarded as an effective and appropriate treatment technology for good quality surface waters with turbidity less than 10 NTU and colour less than 5 CU (Sharpe *et al.*, 1994). However, several pretreatment techniques, such as micro-straining, roughing filters, and pre-ozonation, have been suggested to overcome the raw water quality limitation of slow sand filters. Moreover, slow sand filters can be modified with non-woven fabric mats and surface amendment to enhance operational and treatment performance (McNair *et al.*, 1987; Graham and Mbwette, 1990).

In practice, there are some cases where slow sand filters are covered to minimise winter freezing problems, especially in Europe and the USA (Plate 2.2). Plastic membranes provide greater flexibility as covering materials, compared with solid structures (Lloyd, 1974). Insulation, such as an earthen embankment around a filter structure, and heating can also prevent freezing problems (Logsdon, 1991). Furthermore, covering a slow sand filter reduces algal growth in the supernatant water and schmutzdecke development by minimising or eliminating solar radiation. In climates where seasonal algal blooms are prevalent, covering improves filter run lengths under these conditions (Houghton, 1970; Haarhoff and Cleasby, 1991; Stedman, 2000). Uncertainty remains as to whether this

effect is due solely to the absence of algae in the surface deposits, or in conjunction with the absence of algae in the sand media (Graham, 1991). In contrast, some authors (Huisman and Wood, 1974) argue that the decreased biological activity of the schmutzdecke observed in covered filters may potentially compromise the effectiveness of the sand bed at water filtration.

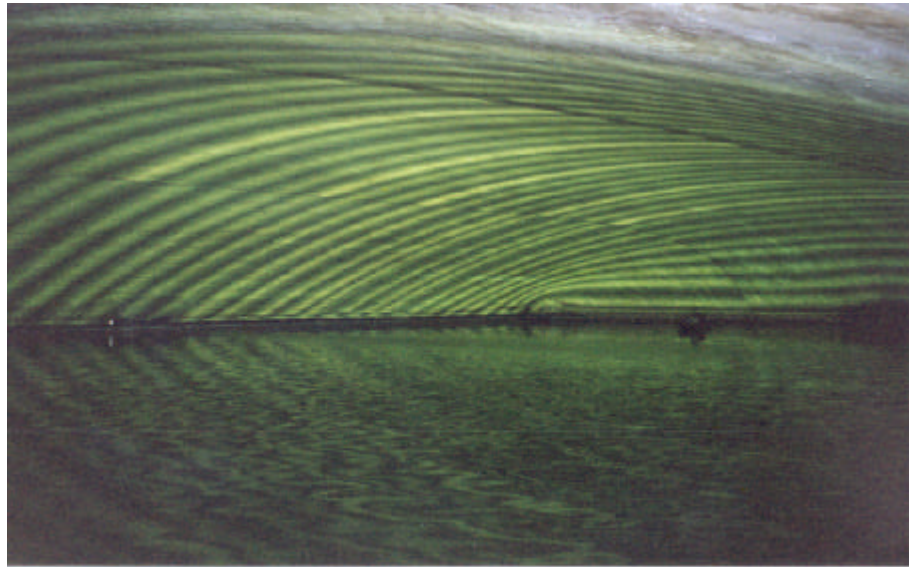


Plate 2.2 - Internal view of a slow sand filter covered by plastic film supported by positive air-pressure at Walton, Thames Water

Slow sand filtration systems vary considerably depending on raw water quality, the level of pretreatment and the local conditions including the availability of construction materials. Table 2.1 summarises the main characteristics of different SSF systems reported by various authors.

2.2.2 - Mechanisms of filtration

Filtration is used primarily to remove suspended particulates, including pathogens, in the production of potable water. Table 2.2 lists the variety particles found in raw waters. Particle removal efficiencies in the range 99 % to 99.99 % are reported in the literature for biologically mature slow sand filters (Bellamy *et al.*, 1985a), particularly from surface waters of relatively low turbidity. A limited amount of research has focused on the filtration mechanisms operating during SSF (Edwards and Monke, 1967; Cleasby *et*

al., 1984; Lloyd, 1996; Weber-Shirk and Dick, 1997ab), and knowledge of the process mechanisms remains restricted.

Table 2.1 - Characteristics of slow sand filters (adapted from Galvis *et al.*, 1998)

Characteristics	Ten States Standard USA (1997)	Huisman and Wood (1974)	Visscher <i>et al.</i> (1987)	CINARA, IRC (1997)
Time of operation (h d ⁻¹)	n.s.	24	24	24
Filtration rate (m h ⁻¹)	0.08 – 0.24	0.1 – 0.4	0.1 – 0.2	0.1 – 0.3
Sand depth (m)				
Initial	0.8	1.2	0.9	0.8
Minimum	n.s.	0.7	0.5	0.5
Effective sand size (mm)	0.30 – 0.45	0.15 – 0.35	0.15 – 0.30	0.15 – 0.30
Uniform coefficient of sand	≤ 2.5	< 3	< 5	< 4
Water above top of sand (m)	≥ 0.9	1 – 1.5	1	0.75
Maximum surface areas (m ²)	n.s.	n.s.	< 200	< 100

n.s.: not specified

Table 2.2 - Particles found in ambient waters (adapted from Hendricks, 1991)

Category	Group/name	Size (µm)
Mineral	Clays (colloidal)	0.001 - 1
	Silicates	no data
	Non-silicates	no data
Biological	Viruses	0.001 – 0.1
	Bacteria	0.3 – 10
	<i>Giardia lamblia</i> cysts	10
	Algae, unicellular	30 – 50
	Parasite eggs	10 – 50
	Nematode eggs	10
	<i>Cryptosporidium</i> oocysts	4 – 5
	Biological concentrate from 5 µm cartridge filter	mixture
Other particles	Amorphous debris, small	1 – 5
	Amorphous debris, small	5 – 500
	Organic colloids	no data

In general, filtration occurs by physical (straining and transport) and chemical mechanisms (attachment). Flow in the filter pores is laminar in both rapid and SSF (Cleasby and Bauman, 1962; Ives, 1980) and all these mechanisms are likely to operate during SSF (Ellis, 1985). Additionally, biological processes are important purification mechanisms operating in SSF (Huisman and Wood, 1974; Hendricks, 1988).

Sub-section 2.2.2.1 briefly describes the physico-chemical mechanisms of filtration. However, further information on filtration mechanisms can be found in Ives (1960, 1967, 1969, 1970, and 1980) and Ison and Ives (1969). Published research on biological mechanisms operating in SSF are summarised in Sub-section 2.2.2.2. Mathematical models describing mechanisms of particulate capture are presented in Sub-section 2.2.2.3 and numerical descriptions of headloss development in SSF are described in Sub-section 2.2.2.4.

2.2.2.1 - Physico-chemical mechanisms

Straining is the principal mechanism of removal for particles larger than grain pores. Some researchers (Herzig *et al.*, 1970) suggest that straining is important for particle removal when the ratio of the particle size to the medium grain size is greater than 0.2. Straining is an important filtration mechanism that operates in SSF because slow sand filter beds have small effective sand size (0.2 mm) preventing the penetration of larger particles into the sand bed. Indeed, the building up of the *schmutzdecke* layer is, in part, a consequence of the straining mechanism operating in SSF.

Transport mechanisms are responsible for removing particles out of their flow streamlines into the proximity of the grain surfaces. These mechanisms include inertia, sedimentation, diffusion, interception and hydrodynamic action (Figure 2.3). The significance of the various transport mechanisms depends principally upon the flow rate, particle size, grain size and temperature (Ives, 1970). However, several transport mechanisms usually act simultaneously on a particle during the filtration process.

The attachment of particles to grain surfaces is caused by physico-chemical and molecular forces (Ives, 1969). These forces include electrical attraction (Van der Waals' forces) and adherence. Electrical forces (electrostatic or electrokinetic) are either

attractive or repulsive, according to the physico-chemical conditions of the suspension, but Van der Waals' forces are always attractive (Herzig *et al.*, 1970). Adherence takes place in the 'slimy' material (i.e. active bacteria, detritus, and assimilated organic material) deposited on the filter surface and in the pores during the filtration process (Huisman and Wood, 1974).

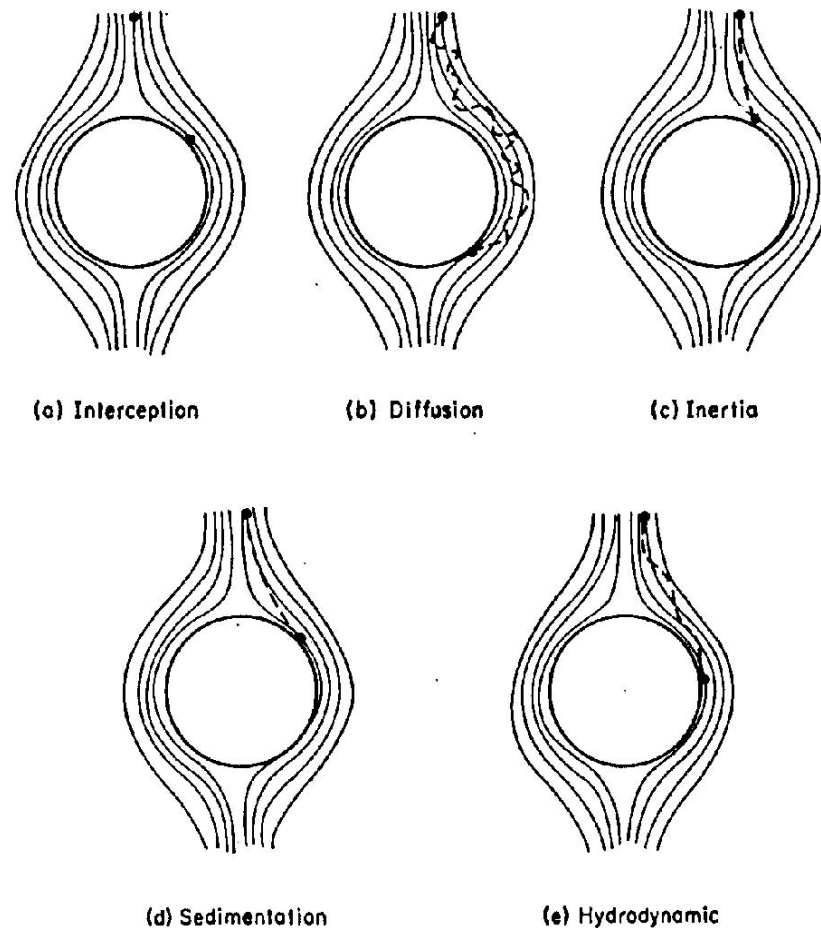


Figure 2.3 - Various transport mechanisms (Ives, 1975)

2.2.2.2 - Biological mechanisms

Pathogenic microorganisms including viruses and bacteria, and cysts of enteroparasites may be effectively removed by SSF (Burman, 1962; Poynter and Slade, 1977). This is partly explained by the slow filtration rate of water and fine sand used, but also attributed to biological mechanisms in the schmutzdecke and within the upper layers of the sand bed (Huisman and Wood, 1974). Among the several biological mechanisms operating in slow sand filters, predatory activities associated with the maturity of the

filter bed are suggested as the main process responsible for removing and inactivating microbial pathogens during SSF.

Haarhoff and Cleasby (1991) concluded from a review of published literature that predation, scavenging, natural death/inactivation and metabolic break down are the principal biological mechanisms responsible for particle removal by SSF. For example, bacteria removal in SSF has been attributed to grazing by protozoa. Burman and Lewin (1961) examined the bacterial condition of water before, during and after filtration at the Walton treatment works, in London. This showed that coliform and *E. coli* counts decreased in the supernatant water during the hydraulic retention time above the sand. This was attributed to bacterial grazing by protozoa or other predators migrating from the filter surface. Coliform counts increased at the sand surface, but lower *E. coli* counts were found, suggesting that growth of coliform bacteria may occur in the filter mat on the sand surface but there was no evidence for the growth of *E. coli* in the filter. In another study at Walton on colonisation of a resanded slow sand filter, the numbers of *E. coli* bacteria in the filtered water were inversely related to the size of numbers of flagellate and ciliate populations in the filter, suggesting that protozoa were important agents for bacteria removal (Richards, 1974).

Although Lloyd (1974, 1996) suggested that the primary process of removing bacteria was adsorption onto positively charged surfaces, a significant secondary role was attributed to the sand grazing members of the interstitial fauna, particularly the protozoan ciliates. Grazing activities were suggested because of the saturability of all adsorption systems and the ability of bacteria to grow in the sand bed and detach again. In addition to bacteria removal, disappearance of algae during SSF was attributed to grazing by protozoa. However, rotifers, crustacea and insect larvae may also feed on algae, particularly filamentous species (Brook, 1954, 1955).

Weber-Shirk and Dick (1997a) investigated physico-chemical and biological particle removal mechanisms in slow sand filters at a laboratory scale. The comparative roles of physico-chemical and biological particle removal mechanisms were evaluated by measuring *E. coli* and particle removal in the presence and absence of sodium azide (used to inhibit biological activity). Physico-chemical particle removal mechanisms

were important for the removal of particles over 0.75-10 μm . Particle removal efficiency increased with particle accumulation within the filter bed. Decreased removal of both *E. coli* and particles smaller than 2 μm in the presence of sodium azide indicated that biological mechanisms improved slow sand filter performance (Weber-Shirk and Dick, 1997b). The grazing of bacteria by protozoa was found to be the only significant biological removal mechanism.

Maturity of the sand bed is a critical factor influencing particle and microorganism removals in SSF. A filter is 'mature' when coliform removal reaches its optimum level (Barret *et al.*, 1991). Poynter and Slade (1977) found that SSF was highly efficient at removing bacteria and viruses from contaminated reservoir water. During their experiments, one of the two filters under investigation was taken out of use for repairs. The filter was refilled with clean sand and put back into use afterwards. A significant difference in performance and virus removal was observed between the two filters with the old filter indicating a removal efficiency ten times greater than the new sand bed. The maturity of the sand was important in controlling the removal of *Giardia* and *Cryptosporidium* cysts, and bacteria and turbidity by slow sand and diatomaceous earth filtration (Schuler *et al.*, 1991). Both filtration systems removed more than 99 % of the cysts applied, and exhibited satisfactory removal of coliform (> 90 %) and turbidity (0.2-0.3 NTU).

Fogel *et al.* (1993) also studied the removal of *Giardia* and *Cryptosporidium* cysts by full-scale operational slow sand filters. Results demonstrated an average 93 % removal of *Giardia* cysts by the filtration plant, whilst an average 48 % removal of *Cryptosporidium* cysts was removed. Low water temperature and reduced biological activity within slow sand filter beds affected the removal efficiency of *Cryptosporidium* from contaminated water.

The removal of algae by SSF was investigated in a pilot plant installed at São Carlos Engineering School of São Paulo University in Brazil (Di Bernardo *et al.*, 1990). Different concentrations of the diatom *Melosira italica* (750, 1500, and 7500 cells ml^{-1}) were inoculated into raw water and the extent of algal removal efficiency for algae was

found to be dependent on filter maturation period, raw water algae concentration and specific algae characteristics.

In addition to the maturity of the sand bed, the development of the schmutzdecke layer on the top of the sand is an important process of removing particles and microorganisms. For example, Bellamy *et al.* (1985ab) found that microbiological maturity of the sand bed was important for the removal of *Giardia* cysts and coliform bacteria. However, schmutzdecke was important for the removal of coliform bacteria and had no influence on the removal of *Giardia* cysts. Nevertheless, the schmutzdecke development was correlated with significant increases in particle removal over the experimental period of 54 days carried out by Hirschi and Sims (1991) using SSF columns in laboratory. They suggested that the growth of the schmutzdecke increased the 'stickiness' of the filter medium, and thus raised the filtration efficiency value. McNair *et al.* (1987) also observed that filamentous algae greatly increase the specific surface area of the filter by expanding the sorptive and interceptive capabilities of the filter bed above the water-sand interface up to the surface of the filamentous algal mat.

Wotton and Hirabayashi (1999) showed that midge larvae (*Chironomidae*) were abundant on the surface of the slow sand filters at Ashford Common works, England. Larvae ingested the schmutzdecke on the sand surface and excreted faecal pellets that were compacted and bounded with mucopolysaccharides. These findings suggested that midge larvae may have an important role as agents of organic matter removal in purification of drinking water in SSF process.

Collins *et al.* (1994) evaluated the capacity of covered slow sand filters in removing organic precursor materials as quantified by dissolved organic carbon (DOC), ultraviolet (UV) absorbance and trihalomethane formation potential (THMFP). Removal of natural organic matter (NOM) and organic precursor material were related to filter biomass and increased with increasing biomass concentrations in the filter. Average NOM and organic precursor removals for the slow sand filters evaluated during the study were 15 ± 5 %. Unexpected strong correlation between DOC removed and headloss led to the conclusion that DOC removals contributed to headloss development directly due to the fouling potential of concentrated and hydrophobic

NOM fractions and indirectly by supporting elevated bacterial populations at the sand-water interface which could further enhance particulate removal.

2.2.2.3 - Mathematical models of capture mechanisms

The physico-chemical mechanisms described in Sub-section 2.2.2.1 are regarded collectively as the capture or clarification process. The empirical interaction between a uniform suspension and a uniform filter medium has been used as the basis for filtration clarification theory. This is described as the filtration coefficient (Iwasaki, 1937) and depends on particulate transport and attachment mechanisms, which are a function of the characteristics of the particles in suspension, dissolved salt concentrations, water temperature, interstitial velocity, and grain surface (Ives, 1980).

The concentration of a suspension flowing through a filter progressively decreases with distance due to the effects of filtration. The rate that a suspension concentration diminishes with distance travelled through the filter is proportional to the local concentration in the filter pores (Equation 2.1).

$$\frac{\partial C_p}{\partial L} = -\lambda C_p \quad (2.1)$$

where

C_p = concentration of suspended particles (mg l^{-1})

λ = filtration coefficient (m^{-1})

L = depth (m)

Equation 2.1 assumes that for clean filter media containing no deposited material, all layers of the filter are equally efficient at removing particles from suspension, and that in every layer the suspension entering and leaving is uniformly dispersed and unchanged in nature (e.g. non-flocculating). The equation originally proposed by Iwasaki (1937) for slow sand filters has been validated theoretically by Litwiniszyn (1967) and experimentally by Ison and Ives (1969).

Suspended particles removed from the flow accumulate in the filter pores. The relation between the concentration of suspended particles in the flow and the accumulating deposit in the filter medium is expressed by the continuity equation (Iwasaki, 1937), which states that the material removed from the suspension is equal to that accumulated in the filter (Equation 2.2).

$$u \frac{\partial C_p}{\partial L} + \frac{\partial \sigma_a}{\partial t} = 0 \quad (2.2)$$

where:

- σ_a = absolute specific deposit (mg l^{-1})
- u = approach velocity of the water (m h^{-1})
- t = time (h)

However, the accumulation of specific deposit in the filter alters the geometry of the filter pores and changes the transport and attachment mechanisms. Therefore, the removal efficiency (λ) of the filter is modified with time and filter depth. A variety of models have been proposed to represent the changes in the filtration coefficient in relation to the specific deposit (Tien and Gimbel, 1982). The majority of these are derived from Equation 2.3, originally proposed by Ives (1960).

$$\ddot{\epsilon} = \ddot{\epsilon}_0 + a_1 \dot{\sigma} - \frac{a_2 \dot{\sigma}^2}{(\ddot{a}_0 - \dot{\sigma})} \quad (2.3)$$

where:

- λ_0 = initial filtration coefficient (m^{-1})
- ϵ_0 = initial porosity (dimensionless)
- σ = bulk specific deposit (vol vol^{-1})
- a_1 = empirical parameter (m^{-1})
- a_2 = empirical parameter (m^{-1})

Equation 2.3 indicates that at the beginning of filtration $\lambda = \lambda_0$, when $\sigma = 0$ for a clean filter containing no deposit, and $\lambda = 0$ when the accumulation of deposit in a filter layer

is so great that no more suspension is removed. However, Equation 2.3 assumes that λ increases before decreasing, ultimately to zero (Ives, 1960). This initial increase in filtration coefficient is attributed to increases in surface area of the sand grains due to the formation of domes of deposit.

Herzig *et al.* (1970) presented experimental values for filtration coefficients from various water filtration experiments with particles of diameter 1 to 25 μm and filter grains of diameter 100 to 800 μm . The filtration coefficient varied in magnitude according to the type and size of particles, as well as to the flow and size of sand grains. Iwasaki's values, for example, vary from 10 to 8 m^{-1} for bacteria removal at flow rates of 0.126 to 0.292 m h^{-1} , respectively, and for a sand grain size equal to 0.227 mm. For the same flow range and sand grain size equal to 0.104 mm, the filtration coefficient for bacteria varied from 51.2 to 45 m^{-1} , respectively. Thus, the filtration coefficient decreases with increasing flow rate and increases with decreasing sand grain size. For algae removal, the filtration coefficient varied from 199 to 140 m^{-1} at a flow rate of 0.126 to 0.292 m h^{-1} , respectively, and for a sand size of 0.227 mm. Therefore, the filtration coefficient also increases with increasing particle size.

Mbwette (1989) determined the clean bed filtration coefficient (λ_0) of non-woven synthetic fabrics and sand using kaolin particles in the range of 2.25 to 7.18 μm at a flow rate of 0.3 m h^{-1} . This provided further confirmation that the filtration coefficient increases with increasing diameter of particles in suspension and decreases with increasing filtration rate. Interestingly, the filtration coefficient was higher for fabric materials than in sand. For example, at a flow rate of 0.3 m h^{-1} the clean bed filtration coefficient of the sand (effective size = 0.3 mm) ranged from 106 to 214 m^{-1} , and for the fabric media (fibre diameter = 33 μm ; porosity = 0.89) it varied from 186 to 332 m^{-1} .

Ives and Sholji (1965) based on laboratory investigations of variables affecting rapid filtration with pvc microspheres, which were of bacterial size, determined the empirical constant values of a_1 and a_2 (Equation 2.3) equal to 190 and 380 m^{-1} for λ_0 equal to 2.65 m^{-1} . However, the values in the ranges 44.8 to 248.4 m^{-1} and 149 to 970 m^{-1} for a_1 and a_2 , respectively, have been experimentally measured using a suspension of hydrous

ferric floc with λ_0 in the range 9.7 to 14.4 m^{-1} (Fox and Cleasby, 1966). In the case of SSF, Ojha and Graham (1991) determined, through optimisation techniques, values of 6.1 and 26.5 m^{-1} for a_1 and a_2 , respectively, using an initial filtration coefficient of 50 m^{-1} . These results suggest that the values of a_1 and a_2 are dependent on the characteristics of the water varying from filtration system to filtration system.

In Equation 2.3, the bulk specific deposit (σ) represents the volume effectively occupied in the pores, including the porosity of the deposited particles. This term is obtained by multiplying the absolute specific deposit in mass by the bulk factor (Equation 2.4). The bulk factor therefore represents the ratio of the bulk volume of deposits and the solid volume (Ives and Pienvichitr, 1965).

$$\sigma = b\sigma_a \quad (2.4)$$

where:

b = bulk factor (l mg^{-1})

The bulk factor (b) has been assumed to be a constant value by some investigators (Camp, 1964; Ives and Sholji, 1965; Sembi and Ives, 1983). The empirical determination of the bulk factor for flocculent solids has been shown to be problematic, and bulk factors in the range 40×10^{-6} to $230 \times 10^{-6} \text{ l mg}^{-1}$ (Fox and Cleasby, 1966) and 50×10^{-6} to $262 \times 10^{-6} \text{ l mg}^{-1}$ (Mohanka, 1969) have been used to verify the conformity of mathematical models to experimental data. The empirical determination of the bulk factor may not be possible in practice since the floc size may change during filtration. Ojha and Graham (1993b) investigated the theoretical estimation of the bulk specific deposit in rapid filtration and found that the bulk factor varied from 0.377×10^{-6} to $19 \times 10^{-6} \text{ l mg}^{-1}$ during a filtration run. The uncertainty in empirical and theoretical values of the bulk factor for rapid filtration suggests that additional difficulties may be apparent in SSF since it also involves a dynamic biological process.

A consequence of the definition of the bulk specific deposit is that the local porosity is expressed by

$$\varepsilon = \varepsilon_0 - \sigma \quad (2.5)$$

where:

ε = effective porosity of the filter bed (dimensionless)

The approach velocity of the water through the media is represented by the ratio of flow rate and effective porosity of the media (Herzig *et al.*, 1970).

$$u = \frac{q}{\varepsilon} \quad (2.6)$$

where:

q = flow rate (m h^{-1})

2.2.2.4 - Mathematical models of headloss

Headloss is defined as the increase in flow resistance (i.e. loss of permeability) caused by the accumulation of suspended material in the medium pores, and headloss increases with filter run time in normal operational practice. In the case of slow sand filters, the precise contribution of the schmutzdecke to the rate of pressure headloss remains undefined and unquantified (Graham *et al.*, 1994). However, it is generally accepted that headloss increases ‘exponentially’ with time during the SSF process (Toms and Bayley, 1988; Retamoza *et al.*, 1994; Graham *et al.*, 1996). The filtration run usually ends when the total headloss reaches a predetermined limit, known as maximum or terminal headloss.

The resistance to flow observed with clean filter media is described as the initial headloss and this is also apparent with clean water. The headloss of clean filter is proportional to flow rate, following Darcy’s law and depends on grain size and porosity according to the Kozeny-Carman equation (Ives, 1980).

$$dH_0 = \frac{q\Delta L}{K} \quad (2.7)$$

where:

H_0 = initial headloss (m)

ΔL = depth increment (m)

K = hydraulic conductivity (m h^{-1})

As filtration progresses, the permeability of the filter bed decreases due to the deposit in the filter pores and under these conditions, the Kozeny-Carmam equation is invalid. Subsequently, headloss development becomes a function of the deposited material. Various mathematical models of headloss due to clogging by deposits are listed in Sakthivadivel *et al.* (1972) and Tien and Gimbel (1982). Those equations that have been applied to SSF are presented below.

Equation 2.8, which is similar to the model of Woodward and Ta (1988), was used by Ojha and Graham (1994) to simulate headloss development with time and depth during SSF. The principal contribution towards overall headloss development is generally considered to arise in schmutzdecke and the top 2 cm of the media (Huisman and Wood, 1974; Barret and Silverstain, 1988). However, Equation 2.8 could not explain all the contribution to headloss development in slow sand filter beds as observed by the poor prediction of headloss distribution with depth (Ojha and Graham, 1994).

$$\frac{H}{H_0} = f(\sigma, \varepsilon_0) = \frac{1}{(1 - a_c \sigma)} \quad (2.8)$$

where:

H = headloss (m)

a_c = empirical constant (dimensionless)

Equation 2.9 was proposed for describing headloss through any layer containing specific bulk deposit in rapid sand filtration (Sembi and Ives, 1983), and this function was also found to adequately represent headloss variation with time and filter depth in SSF (Ojha and Graham, 1994).

$$\left(\frac{\partial H}{\partial L}\right)_{L,t} = \left(\frac{\partial H}{\partial L}\right)_{L,0} \left(1 + \frac{\sigma}{(1 - \varepsilon_0)}\right)^{c_1} \left(\frac{\varepsilon_0}{(\varepsilon_0 - \sigma)}\right)^{c_2} \quad (2.9)$$

where:

c_1 = empirical parameter (dimensionless)

c_2 = empirical parameter (dimensionless)

The use of this equation requires the determination of the parameters c_1 and c_2 . Sembi and Ives (1983) proposed $c_1 = 1.33$ and $c_2 = 3$ for simulation of rapid sand filtration, but the experimental determination of these parameters was not described. Ojha and Graham (1994) optimised these parameters to $c_1 = 1.331$ and $c_2 = 3.402$ using Monte Carlo techniques for SSF.

Toms (1984), cited in Toms (1996), proposed Equation 2.10 to predict normalised headloss in slow sand filters at Coppermills, Thames Water. A normalised headloss is the effective headloss corrected to a standard flow of 0.2 m h^{-1} and was the nominal maximum rate at which slow sand filters were operated by Thames Water.

$$\frac{\text{NHL}}{\text{NHL}_0} = \exp(\text{BQ}) \quad (2.10)$$

where:

NHL = normalised headloss (m)

NHL_0 = initial normalised headloss (m)

Q = total quantity of water filtered per unit area of sand (m)

B = rate of increase of headloss (m^{-1})

2.2.3 - Biological aspects of SSF

Biological mechanisms have a significant role in the purification of water by SSF. Among the several biological mechanisms operating in SSF, schmutzdecke, predatory action and maturity of filter bed were identified as being critical to the water purification process as described in Sub-section 2.2.2. An understanding of the microbial dynamics and the growth of the schmutzdecke and sand biomass is required

to determine the fundamental nature of these complex biological mechanisms operating in SSF systems. The following sub-section presents an overview of the biological aspects of slow sand filters, including a description of the microorganisms found inhabiting these filtration systems and the characteristics of the schmutzdecke and sand biomass.

2.2.3.1 - Fauna and flora of slow sand filters

Several studies examined the biological aspects of slow sand filters. Most of these have focused on bacteria, algae, protozoa, nematodes and rotifers, inhabiting the interstitial sand, as well as the complex biological community in the schmutzdecke.

According to Huisman and Wood (1974), the water purification process in SSF begins in the supernatant water. During the day, under the influence of sunlight, algae absorb carbon dioxide, nitrates, phosphates, and other nutrients from the influent water to form new cellular material and oxygen. The oxygen dissolves in the water and reacts with organic compounds, rendering these, in turn, more assimilable by bacteria and other microorganisms. Dead algae from the supernatant water and living bacteria in the raw water are consumed within the schmutzdecke and inorganic salts are released. Organic nitrogen compounds are mineralised and oxidised to form $\text{NO}_3^- - \text{N}$ (nitrate nitrogen). After passing through the schmutzdecke, the water reaches the sand bed and particles, bacteria and viruses attach to the surface of the sand grains by mass attraction and electrical forces. The surfaces of the grain sand become coated with a sticky layer, similar in composition to the schmutzdecke, but without the larger particles and the algae, which have failed to penetrate. The living coating continues through some 40 cm of the sand bed, different life forms predominating at different depths, with the greatest activity, taking place near the surface, where food is abundant.

Bellinger (1968, 1979) examined the algal species inhabiting slow sand filters in the Thames Valley and divided the algal flora into three categories including those species living in the supernatant water, those present on the sand surface, and those algae living below the sand surface. The supernatant algae were mainly planktonic forms of small, fast growing species, which may or may not be motile. The benthic algae on the sand surface were mainly slow growing filamentous or non-filamentous species capable of

attachment including filamentous algae, pennate diatoms, and thalloid algae. Certain species of the diatom genera of *Nitzschia* and *Navicula* penetrated down to a depth of 30 cm or deeper and contributed to the chlorophyll-a content of the sand. Bellinger (1979) pointed out that algal populations of the supernatant water and surface of the sand released up to 30 % of their photosynthetic products as extra-cellular organic substances, which pass into the filter bed providing a readily metabolizable substrate source for the interstitial organisms, particularly bacteria.

Similar to Bellinger (1968, 1979), the spatial distribution of algae in slow sand filters was described by Haarhoff and Cleasby (1991), based on a review of published literature. Algae were characterised in three different zones of slow sand filters. The algae in the supernatant water contain planktonic species present in the water influent, as well as planktonic organisms that may grow within the supernatant reservoir itself. The highest concentration of algae anywhere in slow sand filters appears in the schmutzdecke layer on the top of the sand. The schmutzdecke is predominately composed of filamentous algae, attached organisms and detritus. Within the sand bed, the algal concentration is highest immediately below the schmutzdecke.

The seasonal characteristics of the algal flora on the sand surface and supernatant water of slow sand filters were investigated by Brook (1954, 1955) at the water treatment works operated by the Newcastle and Gateshead Water Company at Whittle Dene, England. The algal flora consisted mainly of filamentous diatoms. Non-filamentous species were also identified and populations of these organisms increased during May and June and the lowest abundance was observed in January and February. Brook (1954, 1955) suggested that this cycle may be related to seasonal factors and was probably in response to fluctuating seasonal temperature and light conditions. Differences in the composition of the algal flora were also observed within recently cleaned and mature sand beds. Certain species (e.g. *Melosira varians* and *Fragilaria capucina*) that were abundant in the recently cleaned beds were rarely found or were absent from mature beds.

Ridley (1967) also studied the seasonal characteristics of the algal flora at three water treatment works in the lower Thames Valley (Hanworth Road, Kempton Park, and

Ashford Common). Three stages of algal succession were observed during the spring and summer period:

- (1) there was proliferation of *Chlorophyceae* in the supernatant water during the first seven days of a filtration run;
- (2) after 5 days of operation the sand surface became seeded with diatoms;
- (3) after 10 days of operation there was proliferation of the larger species of filamentous algae including *Melosira*, *Cladophora*, *Hydrodictyon* and *Enteromorpha*.

A progressive increase in headloss was observed when the organisms of stage 1 dominated the flora throughout the filtration run and also during accumulation of diatoms of stage 2. Diatom populations on the sand surface (stage 2) declined when large amounts of filamentous algae from stage 3 were present in the supernatant water through reduced light penetration to the sand surface.

Anuradha *et al.* (1983) observed the biological forms for a period of 2 years in a slow sand filter pilot plant in India, which was subjected to different conditions of operation. Samples of schmutzdecke and top few centimetres of the sand were collected at the end of the filtration runs. Various phyto and zooplankton were observed in the raw and filtered waters, and a varied assemblage of micro and macro organisms such as algae, protozoa, rotifers, oligochaetes (worms), nematodes, crustaceans, and insect larvae was found in the schmutzdecke. The diatoms formed the bulk of the phytoplankton in the schmutzdecke. A pilot SSF study in Brazil (Di Bernardo *et al.*, 1990) also found that the largest amount of algae was in the schmutzdecke, but it decreased with depth in the sand bed. During the experiments of Anuradha *et al.* (1983), covering the filter suppressed the growth of algae on schmutzdecke due to exclusion of sunlight, but did not increase the filtration run lengths, contrasting other observations (Houghton, 1970; Stedman, 2000).

Investigations on microorganism distributions in slow sand filters operated by Thames Water indicated that population densities declined with depth. Lloyd (1974) investigated the interstitial micro-fauna in slow sand filters at Walton and Ashford Common treatment works. Protozoa and rotifers were present in most of samples collected. However, the largest organisms in the interstitial habitat of the sand filters were members of the oligochaeta, which were commonly found in mature filters when

detritus was present. Likewise, the nematoda, gastrotrichia and turbellaria were only abundant in mature beds when detritus had penetrated 2-10 cm. The turbellaria consumed a variety of algae when algal cells penetrated the filters.

The ecology of the meiofauna and particularly the oligochaete species were examined by Lodge (1979) in sand filter beds at the Hampton water treatment works. The horizontal and vertical distributions of organic carbon (OC) in the filter were also quantified. The horizontal distribution of OC was highly variable and was characterised by a lognormal pattern. There was no significant vertical difference in the amount of carbon at the start of a filter run. However, the amount of carbon increased with time and decreased with depth. Depth analysis of the carbon data in the cores suggested that the main cause of filter headloss was the accumulation of detritus material in the top 1 cm, and to a lesser extent at 2 cm. Headloss was also attributed to the development of large populations of chironomid larvae in the surface layer of the sand.

Richards (1974) studied the vertical distribution of protozoa in slow sand filters at the Walton treatment works and observed a marked decline in numbers of protozoa with increasing depth in the sand. However, small populations of all groups were present as deep as 20 cm and small amoebae were also collected at a depth of 30 cm. Goddard (1980) also examined the vertical distribution of protozoa and particularly the flagellate and ciliate species in slow sand filter beds at the Hampton water treatment works, England. Maximum population densities of ciliates and flagellates, and variations in mean body size of the ciliates were related to temperature. Maximum ciliate densities were also associated with surface accumulation of carbon, headloss and on two occasions, with the onset of a dissolved oxygen deficit in the filtrate water. The vertical distribution of ciliate and flagellate populations varied with time during the filtration runs, and deeper penetration into the sand bed occurred in the filter bed with the highest water filtration rate.

The vertical distribution of ciliated protozoan and bacterial populations with depth was investigated by Galal (1989) in slow sand filters at the Ashford Common water treatment works, as well as the abundance of particulate organic carbon (POC) and chlorophyll-a. The densities of ciliate organisms were largest in the top few centimetres

of the sand and sharply declined with depth. The bacterial populations and the concentrations of POC and chlorophyll-a showed similar patterns of depth distribution with time.

Similar trend to the population and vertical distribution of microorganisms inhabiting slow sand filters of the Thames Water was also observed in other countries. Protozoa, algae, rotifers, and invertebrates were abundant in the top 1 cm of sand in a pilot SSF plant in Australia (Bowles *et al.*, 1983). The numbers of microorganisms present in the sand decreased rapidly to a depth of 8 cm and below 8 cm few organisms were present. Small flagellates were the most abundant protozoa and ciliated species were commonly found, but amoebas were rarely found.

2.2.3.2 - Characteristics of the schmutzdecke

The schmutzdecke apparently has an important role in water purification by SSF, as well as in distributing organic matter and impacting headloss (Huisman and Wood, 1974; Bellinger, 1979; Bellamy *et al.*, 1985ab). However, the mechanisms responsible for these processes in the schmutzdecke are poorly understood. This is partially explained by the ambiguous definition and complexity of the schmutzdecke layer. This sub-section describes the main characteristics of the schmutzdecke and provides a background to understanding of its role in SSF processes.

Various definitions of the term 'schmutzdecke' have been given by different authors. For example, Huisman and Wood (1974) described the schmutzdecke as a thin slimy matting of material, largely organic in origin, consisting of filamentous algae and numerous other forms of life, including diatoms, protozoa, rotifers, and bacteria. According to Bellamy *et al.* (1985a), schmutzdecke is a layer of inert deposits and biological material which forms on the surface of the sand bed after two weeks of filter operation. Ellis (1985) described the schmutzdecke as a layer that is in intimate contact with the top of the sand consisting of alluvial mud, organic waste, bacterial matter, algae, etc., which adds substantial effectiveness to the straining process. Hendricks (1988) defined the schmutzdecke as the biological growth on the top of the sand, which acts as a surface for retaining particles. Nakamoto (1993) defined schmutzdecke as a sticky algal mat formed on the sand surface of a slow sand filter. Wotton and

Hirabayashi (1999) described the *schmutzdecke* as a layer of detritus and microorganisms with complex architecture.

It is generally agreed that *schmutzdecke* is absent in covered slow sand filters. However, few works describe *schmutzdecke* of covered slow sand filters. For example, *schmutzdecke* on slow sand filters in Colorado, USA, was described by Barret *et al.* (1991) as a light, easily suspended, inert, black carbonaceous deposit of about 1 mm in thickness. According to Eighmy *et al.* (1994), the *schmutzdecke* in three municipal slow sand filters in Massachusetts and Connecticut, USA, had a moderate density of bacteria and extracellular polymeric material was present. However, polymeric material not affiliated with bacteria was also present. Ghost cells (lysed cells) were also observed, indicating oligotrophic conditions in the *schmutzdecke*.

The various descriptions available for *schmutzdecke* developed in uncovered filters indicate that its characteristics vary significantly either from site to site and seasonally. For example, Bowles *et al.* (1983) found that *Melosira* and two other diatoms (*Navicula* sp and *Nitzschia acicularis*) were predominant species of algae in the *schmutzdecke* during the winter in a pilot plant in Australia. However, a thick mat of the green filamentous algae *Zygnema* sp developed with increasing temperature and solar radiation in the spring. The algal mat compacted to a thickness of approximately 2 mm when the filters were drained for cleaning,

McNair *et al.* (1987) examined the growth and composition of the *schmutzdecke* in clinoptilolite⁴ amended slow sand filters at the Utah Water Research Laboratory and found four distinct zones (see Figure 2.4). Zone A was almost entirely of comprised filamentous algae and had a thickness of approximately 15 mm. Zone B was characterised by a thin layer of single cell algae mixed with sediment and was also approximately 15 mm thick. Zone C contained accumulated sediment and contributed an additional thickness of 15 mm to the *schmutzdecke*. Zone D consisted of a thin layer

⁴ Clinoptilolite is a naturally occurring ion exchange mineral that has been used for the treatment of wastewater for removal of ammonium ion in the presence of other cations, including calcium and magnesium, which are commonly found in raw water (Semmes and Goodrich, 1977).

of sediment and a few single cell algae between the clinoptilolite surface and sand.

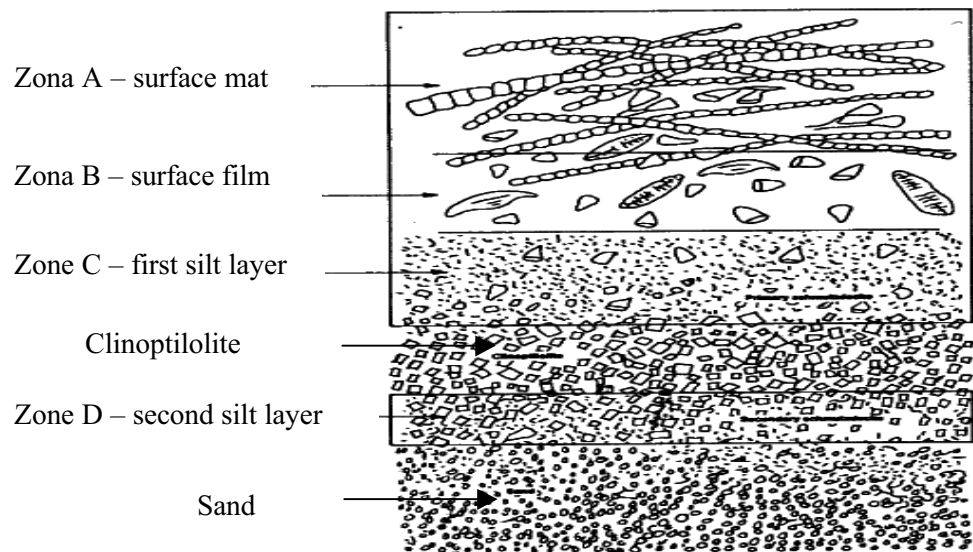


Figure 2.4 - Vertical cross section of schmutzdecke development in a clinoptilolite-amended slow sand filter (adapted from McNair *et al.*, 1987)

During the cold winter season, the surface mud on the sand bed of slow sand filters at the Someya waterworks in Ueda, Japan formed a hard thin layer composed of periphyton algae (i.e. attached algae) similar to those growing on the stones of eutrophic surface water (Nakamoto *et al.*, 1996a). Despite low concentrations of suspended matter, the filters rapidly clogged. By contrast, in the influent water, filamentous algae grew on the sand surface during the warmer summer season, forming an algal mat similar to a down blanket, and the filter was less prone to clogging in spite of a significantly increased suspended matter load. Therefore, Nakamoto *et al.* (1996a) suggested that schmutzdecke may prevent the filter from clogging and acts as a remover of suspended matter (Plate 2.3) which is consistent with other practical observations on SSF (Hirschi and Sims, 1991; McNair *et al.*, 1987).

According to Bellingier (1979), the biomass of algae on the surface of a slow sand filter in early summer in Southeast England was equivalent to $158,000 \text{ mg m}^{-2}$ (fresh weight) after 30 days of operation. Similar measurements were made by Nakamoto (1995) on filters at Ashford Common and Coppermills treatment works in London. The amount of biomass on the sand surface after 50 days of filter operation at Ashford Common bed was approximately $600 \text{ mg Chla m}^{-2}$, whereas at Coppermills the amount was 1000 mg

Chla m^{-2} (Figure 2.5). Whilst the values of biomass chlorophyll-a varied between different filter beds and run times, the accumulation of schmutzdecke biomass was summarised as a linear function with time.

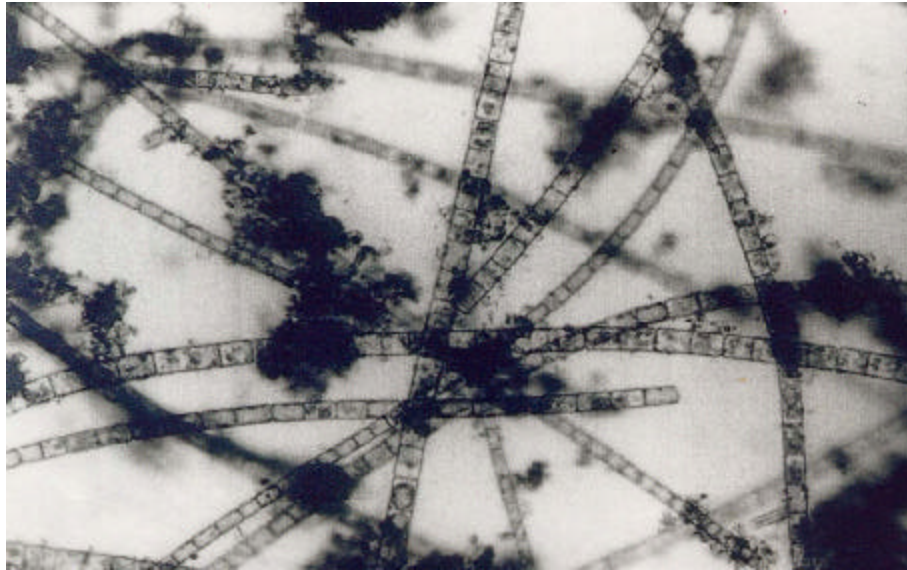


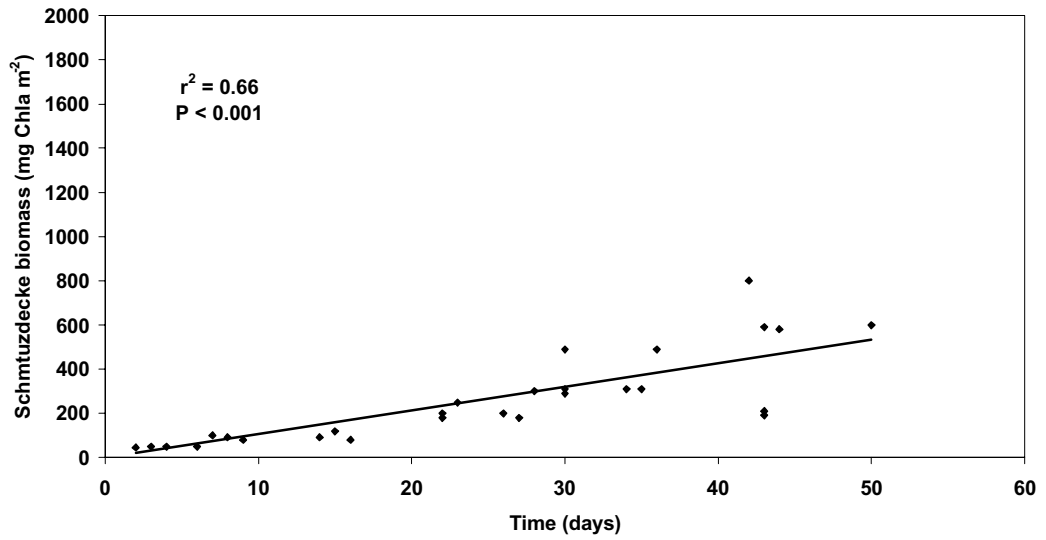
Plate 2.3 - Suspended matter trapped within the schmutzdecke (Nakamoto, 1996a)

Similar linear schmutzdecke growth with time was observed by Hirschi and Sims (1991). Schmutzdecke biomass was measured by volatile solids analysis in a laboratory scale slow sand filter. The schmutzdecke biomass increased in linear relation with time during a 55-day experimental period (Figure 2.6). At the end of the experiment, the schmutzdecke biomass was approximately 0.014 g cm^{-2} (dry weight). McNair *et al.* (1987) observed a similar trend in schmutzdecke growth during 40 days of a filter operation, and in this case, the accumulation of volatile solids was approximately 0.02 g cm^{-2} at the end of the run.

2.2.3.3 - Characteristics of the sand biomass

Knowledge of biomass in sand bed is important to understanding of headloss development in SSF systems, as too much biomass accumulation can clog filters (Eighmy *et al.*, 1994). However, similar to the schmutzdecke, the contribution of the biomass in the sand bed to the filter performance is also unquantified. This sub-section summarises published information on SSF biomass, describing the adopted techniques for measuring sand biomass and the biomass concentrations present in sand.

(a)



(b)

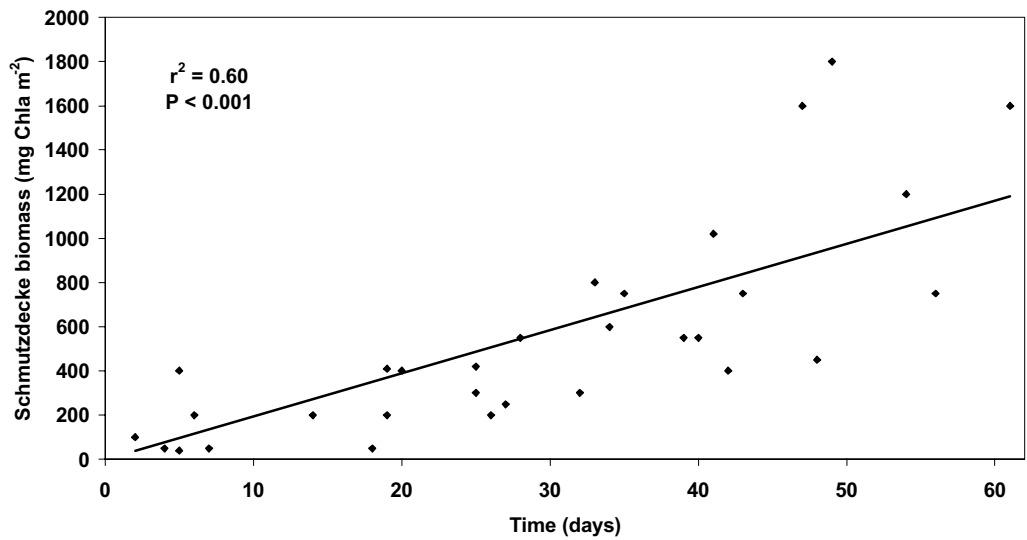


Figure 2.5 - Schmutzdecke biomass development on slow sand filter beds at (a) Ashford Common and (b) Coppermills works during February and March 1995 (Note: Data taken from Nakamoto, 1995)

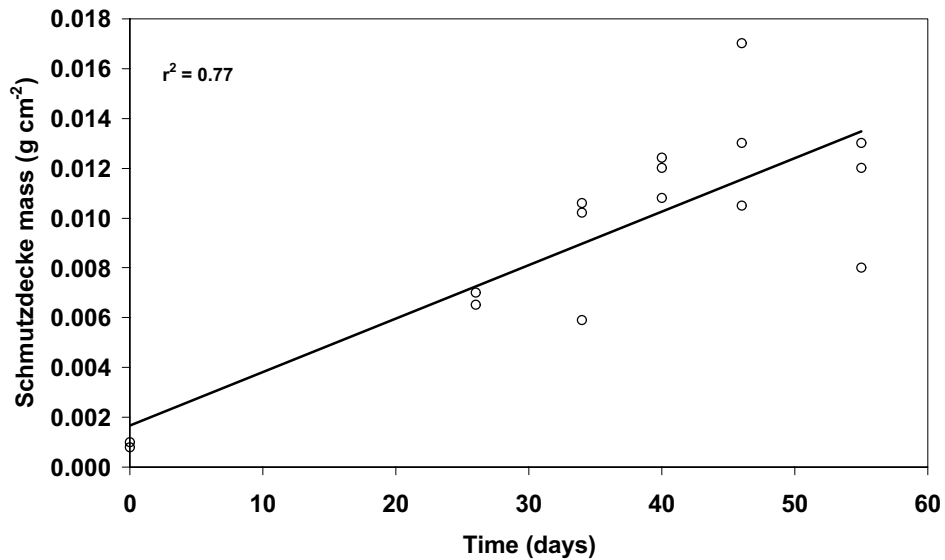


Figure 2.6 - Schmutzdecke growth with time (adapted from Hirschi and Sims, 1991)

Eighmy *et al.* (1988, 1992, 1994) and Collins *et al.* (1994) extensively investigated the distribution and activity of microbial populations within the media of covered slow sand filters in Massachusetts and Connecticut, USA. Samples were collected from the filter beds to a depth of 30 cm and bacteria populations were quantified by acriflavine direct cell counts (AFDC)⁵, whilst biomass was measured as Folin-reactive material (FRM)⁶. High bacterial populations were present in the schmutzdecke and markedly declined with filter depth. In the schmutzdecke bacteria population counts were $1 \times 10^9 \text{ g}^{-1}$ dry weight of media and the biomass content of the filter bed was 2.5-4.5 mg g^{-1} dry weight. Filter biomass was significantly correlated to bacteria counts. Eighmy *et al.* (1988) and Collins *et al.* (1994) demonstrated that slow sand filters contain extensive microbial populations that are nutritionally diverse and capable of biodegrading soluble organic matter. In addition, they suggested that filter harrowing maintains high rates of metabolic activity and stimulates biomass growth in the filter. Harrowing is a method of cleaning slow sand filters carried out by a rubber-tyred tractor equipped with a comb-tooth harrow (Collins *et al.*, 1991).

⁵ The acriflavine direct cell counts (AFDC) method utilises acriflavine (DNA-specific stain) for easy enumeration of bacteria in clear and humic waters (Bergstrom *et al.*, 1986).

⁶ The folin-reactive material (FRM) method applies a standard solution (e.g. bovine albumin) and folin reagents (e.g. Folin-Ciocalteu phenol) to measure cell protein through spectrophotometric analysis (Lowry *et al.*, 1951).

Biomass carbon concentration was determined indirectly by Duncan (1988) in slow sand filter beds at Hampton and Ashford water treatment works, using numerical conversion factors. Microorganisms in the sand were isolated and counted, and a factor of 0.0311 pg C per cell was used to convert bacteria cell density to carbon biomass per cm³ of sand. Cell volumes of ciliate species were converted to carbon biomass using 0.106 pg C per μm³. A weighted average biomass concentration of approximately 0.03 mg C cm⁻³ dry sand was observed in the first two weeks of filter operation. Biomass increased with time and decreased with sand depth. The maximum amount of biomass measured during the filter run coincided with the terminal headloss and, consequently, with the clogging of the filter.

Similar trend in biomass distribution in covered slow sand filters was also observed by Yordanov *et al.* (1996) in a pilot-scale plant in Aberdeen. The results of Yordanov *et al.* (1996) agree with the findings of Eighmy *et al.* (1988, 1992, 1994) and Collins *et al.* (1994), although the filters under study were subjected to a pretreatment using ozone. Microbial counts were higher in the surface 2.5 cm (3.8×10^8 g⁻¹ dry weight) in the filters receiving ozonated water, and decreased with depth (1.2×10^7 g⁻¹ dry weight in 10 cm). In the unozonated control filters, bacteria counts were similar to those measured in ozonated filters at 10 cm depth, but were 4-5 times lower at the surface. An increase in the headloss of the ozonated filters and corresponding shorter time of the filter runs was observed and the development of biomass was suggested as the major factor explaining the headloss development. Reduction of filter run lengths due to increased biological activity in slow sand filters receiving ozonated water was also reported by Graham (1999) and Malley *et al.* (1994).

Biological activity in slow sand filters receiving ozonated water was also characterised by Seger and Rothman (1996). However, Seger and Rothman (1996) measured adenosine triphosphate (ATP)⁷ content in uncovered slow sand filters receiving ozonated water at the Norsborg waterworks, Sweden. The reduction in total organic

⁷ The adenosine triphosphate (ATP) occurs in all living organisms and it is either consumed or regenerated in every metabolic sequence. It can be measured readily by means of the firefly luciferin-luciferase-system and the most frequently used extraction substances are based either on trichloroacetic acid (TCA) or on nucleotide releasing agent (NBR) (Zelles *et al.*, 1985).

carbon (TOC) concentration increased with the temperature of the raw water and ATP concentration in the sand beds and filters receiving ozonated water supported higher biological activities than the unozonated control filter. The biological activity decreased rapidly with depth and was not observed below 20 cm. The maximum amount of ATP in the top 5 cm of the ozonated filter was approximately 7.5×10^{-8} g g⁻¹ dry weight (at 17 °C), while in the unozonated filter ATP content was 6.0×10^{-8} g g⁻¹ dry weight (at 17 °C).

2.3 - Microbial growth

Microorganisms play an important role in water purification by SSF (Sub-section 2.2.3). However, microbial biomass accumulation in the filter has a major contribution to headloss development (Yordanov *et al.*, 1996; Graham, 1991). Therefore, information on the types of microorganisms present and an understanding of their nutritional requirements, interactions, growth kinetics and the influence of environment on these parameters is important for the development of numerical models of SSF process. These characteristics are described here for algae, bacteria, and protozoa. Additional details on the aquatic microorganisms can be found Lynch and Poole (1979), Panikov (1995) and Atlas and Bartha (1997).

2.3.1 - Nutrition and growth conditions

Algae

Algae are chemosynthetic autotrophs utilising energy and CO₂ for carbon fixation and biomass growth. Oxygen is liberated as a by-product of photosynthesis, but in the absence of sunlight, algae are chemosynthetic and consume oxygen. Therefore, water containing algal populations has diurnal variations in dissolved oxygen (DO) concentration (Tebbut, 1998) and supersaturation may occur during the day, but significant oxygen depletion is possible at night. Other inorganic compounds essential for growth include ammonia, nitrate and phosphates. There is a significant volume of literature dealing with growth factors based on nitrogen and phosphorus (Di Toro *et al.*, 1975; Horner *et al.*, 1983; Varis *et al.*, 1988). Mathematical models of algae growth incorporate terms for temperature, solar radiation intensity, and nutrient concentrations as the primary variables affecting the growth kinetics of these microorganisms (Park *et al.*, 1974; Di Toro *et al.*, 1975).

In the absence of organic compounds, algae growth depends upon the mineral content of the water and in hard water, algae obtain CO₂ from bicarbonates, which reduces the hardness and usually increases the pH value (Tebbut, 1998). Since algae use carbon dioxide as a carbon source during photosynthesis, this nutrient may limit the growth rate when alkalinity is low and concentrations of other nutrients are high (Goldman *et al.*, 1972). Kuentzel (1969) pointed out that both aerobic and anaerobic bacteria degrade organic matter at the bottom of lakes to produce high concentrations of CO₂ so that the relationship between bacteria and algae may be responsible for the rapid growth that result in blooms when other mineral nutrients are in excess.

A variety of phenomena reduce the size of algal populations in water environments, including respiration, excretion, settling, grazing losses, and decomposition. Respiration and excretion are important components of nutrient recycling, and include the conversion of algal phosphorus to inorganic phosphorus and the conversion of algal nitrogen to inorganic nitrogen (Brown and Barnwell, 1987). Settling rates depend on the density, size, shape, and physiological state of algae cells, the viscosity and density of the water, and the turbulence and velocities of the water flow (Bowie *et al.*, 1985). Algae are destroyed by grazing activities of protozoa and the rate of removal is approximately proportional to the protozoa concentration, increasing as a function of temperature (Di Toro *et al.*, 1975). Decomposition includes processes such as senescence, bacterial decomposition of cells (parasitism), and stress-induced mortality due to severe nutrient deficiencies, extreme environmental conditions, or toxic substances (Bowie *et al.*, 1985).

Bacteria

Bacteria demonstrate a remarkable range of metabolic activities and exist in most environmental conditions. The environment must supply the chemical elements to produce new cells and provide sufficient energy to permit cellular synthesis (McKinney, 1962). A significant proportion of the carbon fixed by algae is processed through a microbial food web in which planktonic bacteria assimilate and channel extracellular DOC to higher levels of the food chain (Wehr *et al.*, 1994). Indeed, bacterial growth is influenced strongly by the OC exudates produced by algae and availability of this substrate is probably the main factor limiting bacterial growth in water environments

(Cole *et al.*, 1982). Phosphorus availability may also be an important limitation to bacterial growth. For example, investigations of whole community behaviour in fresh water have shown that bacterial abundance and production is directly limited by concentration of dissolved phosphorus (Currie, 1990; Le *et al.*, 1994; Alden *et al.*, 2001). Information is also available concerning the utilisation of mixtures of substrates by bacteria (Stumm-Zollinger, 1966; Curds, 1974). For example, Stumm-Zollinger, (1966) observed that when glucose and benzoate singly and glucose/benzoate mixtures were given to bacteria, the utilisation of substrate was unaffected by the presence or absence of the other substrate, but the maximum specific growth rate was greater for a mixture of substrates than when grown on either substrate alone. Therefore, experimental evidence (e.g. Cole *et al.*, 1982; Currie, 1990) suggests that carbon and phosphorus may be concurrently important substrates for bacterial growth.

Bacteria attach firmly to almost any submerged surface in aqueous environments (Characklis *et al.*, 1982). Cells grow and reproduce at the attached bacteria colony, increasing the amount of biomass and associated polysaccharide material. The entire deposit is termed the biofilm. Attached bacteria play crucial roles in the biodegradation of contaminants and the clogging of porous media (Rittman, 1993). Biofilm accumulation in slow sand filters also causes headloss by reducing the pore size and porosity, since the biofilm is relatively impermeable to water flow.

The net accumulation of bacteria in porous media is controlled by four processes: growth, deposition, decay, and detachment. Growth is proportional to the rate of substrate utilisation, which depends on the amount of attached biomass already present and on the utilisation and mass-transport kinetics of different substrates (Rittmann and McCarty, 1980). Deposition of suspended bacteria, which also increases the accumulation of attached biomass, is controlled by the concentration of suspended bacteria and physico-chemical parameters affecting transport and adherence to the surface (Rittmann and Wirtel, 1991). Biomass decay, which supplies energy for maintenance, reduces the attached biomass and occurs in proportion to the amount of active biomass (Rittmann and McCarty, 1980). Finally, detachment can be a major loss mechanism for attached biomass and a major source of suspended biomass in water. Detachment rates are generally proportional to the amount of attached biomass and the

hydrodynamic shear stress (Rittmann, 1982), although other factors affect this complicated phenomenon (Rittmann, 1989).

Protozoa

Protozoa are aerobic holozoic heterotrophic feeders and derive their nutrition by grazing on algae and bacteria, in some cases, on smaller protozoa and by ingesting particulate organic material (Di Toro *et al.*, 1975, Tebbutt, 1998).

Dissolved oxygen concentration is critical for the survival of protozoa species as most protozoa are obligate aerobes, with only a few examples of anaerobic and facultative anaerobic species. Most of the work concerning protozoa in anaerobic digestion tanks is confined to Imhoff tanks (Lackey, 1938). A list of protozoa found in such tanks can be found in Curds (1975) and some of the more common species include *Saprodinium putrinum*, *Hexamitus inflata*, *Metopus sigmoides* and *Trimyema compressa*. Only aerobic species exist in slow sand filters and some of the most common species are *Vorticella campanula*, *V. convallaria*, *Aspidisca costata* (Lloyd, 1974; Goddard, 1980).

The growth rate of protozoa depends on the amount of food which is ingested and assimilated, and is therefore a function of food densities, grazing rates, and assimilation efficiencies (Bowie *et al.*, 1985). The assimilated food goes into individual growth, metabolic losses, and into reproduction. Grazing rates are proportional to the food supply at low food concentrations. However, at high food concentrations, the grazing rates eventually become saturated and level off at some maximum value after which the grazing rate becomes independent of the food supply (Fenchel, 1980). The grazing rate is also raised by increased temperature.

The assimilation efficiencies for different food types vary with the energy content, digestibility, and quality of the food (Bowie *et al.*, 1985). For examples, the assimilation efficiencies for algae are typically higher than for detritus and bacteria, although the assimilation efficiencies for blue-green algae are generally low. Assimilation efficiencies may decrease with increases in grazing rate at high food concentrations since the retention time in the gut decreases, resulting in incomplete digestion and reduced assimilation (Brown and Barnwell, 1987).

The rate of loss of protozoa is a function of respiratory activity, which increases as temperatures rise, and also predation by higher organisms (Di Toro *et al.*, 1975).

2.3.2 - Modelling microbial dynamics

The survival and growth of different types of microorganisms within a microbial community depends on the availability of nutrients required and on the nature and extent of competitive interactions with other species. A classification and description of the types of interactions, which occur between different species, can be found in Updegraff (1991) and Atlas and Barth (1997). This sub-section presents a description of the basic kinetic relationships used to model the main microbial dynamics, including growth and non-predatory and predatory losses.

Growth

In environmental and sanitary engineering, typical mathematical functions representing microbial growth include the exponential and logistic functions. The exponential function is the most commonly applied growth equation (Equation 2.11), which states that the rate of change of the number of microorganisms is proportional to the concentration of microorganisms.

$$\frac{dM}{dt} = k_{gm} M \quad (2.11)$$

where:

M = microorganism concentration (mg l⁻¹)

k_{gm} = specific growth rate (h⁻¹)

Monod (1949) showed that microbial growth rate was also a function of the concentration of the most limiting nutrient in the environment.

$$k_{gm} = k_{g \max} \frac{N_c}{k_s + N_c} \quad (2.12)$$

where:

N_c = nutrient concentration (mg l^{-1})

$k_{g\max}$ = maximum specific growth rate (h^{-1})

k_s = half-saturation constant (mg l^{-1})

This relationship is described as a hyperbolic function similar to the Michaelis-Menton equation used to describe enzyme-substrate interactions (Chapra, 1997). The replacement of the specific growth rate in Equation 2.11 by the Monod equation (Equation 2.12) produces an expression for growth rate (Equation 2.13), which is a first order relation with respect to microorganism concentration and variable order (zero to first) with respect to substrate concentration (Andrews, 1983).

$$\frac{dM}{dt} = k_{g\max} \frac{N_c}{k_s + N_c} M \quad (2.13)$$

At high food concentrations ($N_c \gg k_s$) the growth rate is independent of substrate concentration and the expression for growth reduces to a zero order with respect to N_c :

$$\frac{dM}{dt} = k_{g\max} M \quad (2.14)$$

At low food concentrations ($N_c \ll k_s$), the growth rate is directly proportional to the substrate concentration, or first order with respect to N_c :

$$\frac{dM}{dt} = k_{g\max} \frac{N_c}{k_s} M \quad (2.15)$$

Chapra (1997) showed that the Monod equation could be used to model microbial growth in both the batch reactor and continuous reactor. The classic curve representing the growth of microorganisms in batch culture is shown in Figure 2.7.

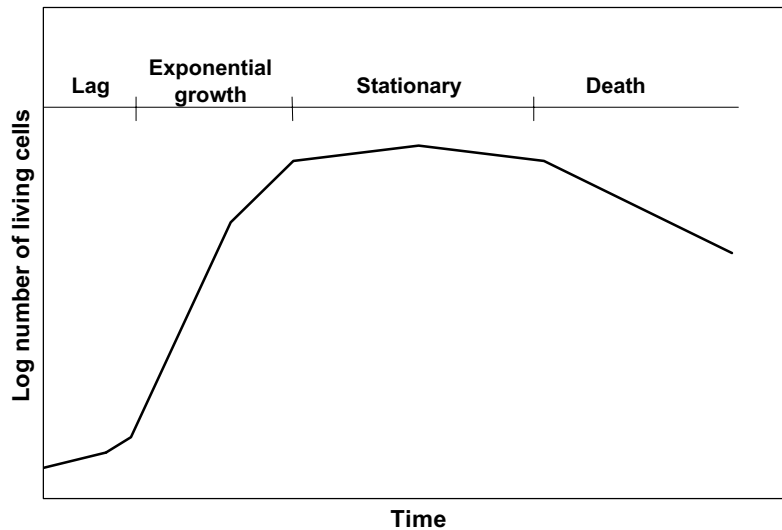


Figure 2.7 - Growth of microorganisms in a batch reactor (adapted from Chapra, 1997)

The form of the growth-decay curve depends upon many factors, such as environmental conditions in the batch reactor, the type of microorganism species, physiological condition of the inoculum, initial concentrations of microorganisms, substrates, etc (Andrews, 1983). In the case of batch reactors with high initial substrate concentrations, the zero-order reaction (Equation 2.14) predominates and the declining growth rate, approaching the stationary phase, may be hardly detectable. Lower substrate concentrations are usually encountered in SSF (continuous-flow reactor) and the declining growth rate is likely to be of considerable significance under these conditions.

Non-predatory losses

The non-predatory losses in microbial dynamics are a result of death and decay in the microbial population. Death represents losses whereby cellular OC is released back into the substrate pool. Decay represents losses of microbial biomass and the removal of substrates from the system by for example respiration, preventing its release as OC and the synthesis of new cellular material (Chapra, 1997). Equation 2.16 can be modified to incorporate these losses as follows:

$$\frac{dM}{dt} = k_{g \max} \frac{N_c}{k_s + N_c} M - k_d M \quad (2.16)$$

where:

k_d = specific loss rate (h^{-1})

The specific loss rate is usually at least an order of magnitude smaller than the specific growth rate, and is generally not important in most short-term laboratory incubation experiments (Andrews, 1983). In the case of SSF, however, although the water retention time in the sand filter bed is comparatively short (3 h), the period of operation is relatively long and extends to about 60-90 days (Haarhoff and Cleasby, 1991). Therefore, the loss rate may be important under these circumstances and must be considered in calculating the net accumulation of microbial biomass SSF.

Predatory losses

There is extensive literature on mathematical models describing predator-prey population dynamics. The Lotka-Volterra equations show the earliest relationships which are based on the logistic equation (Slater, 1979). According to these equations, the interactions of predator and prey species are represented by regular cyclic fluctuations between the two populations (Figure 2.8).

In each cycle (Figure 2.8), as the prey population increases, the predator population subsequently increases, exceeding the prey population, eventually causing a decline in the prey. The predator population then collapses allowing the prey population to recover and increase again, which stimulates the next cycle. The amplitude of the cycle is determined by the initial density of prey and predator populations, and remains constant if environmental conditions remain unchanged (Atlas and Bartha, 1997).

Proper and Garver (1966) studied the feeding and growth of the ciliate *Colpoda steinni* on the bacterium *E. coli* and suggested that the growth rate of the ciliate was dependent upon the concentration of bacteria. The relationship between the specific growth rate of the ciliate and the bacterial concentration was described by the Monod equation. Later, Curds (1971ab) confirmed the suitability of the Monod equation at describing the relationship between the specific growth rate of protozoa and the concentration of bacteria.

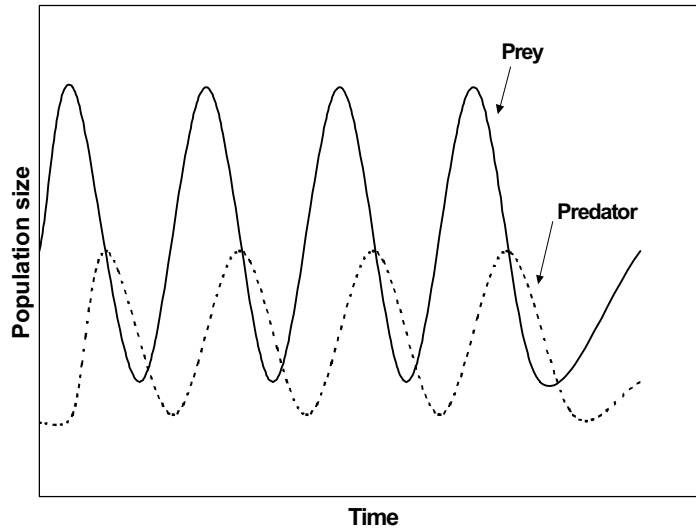


Figure 2.8 - Prey-predator relationship based on the Lotka-Volterra model
(adapted from Slater, 1979)

Prey-predator population dynamics in a continuous-flow reactor have been described by incorporating the Monod equation in the Lotka-Volterra relationship (Slater, 1979). The Monod term describes the growth rate limitation of the prey which acts as the limiting substrate for the growth of the predator population. Therefore, it is necessary to consider two basic equations which describe the development of the two populations. Equation 2.17 represents the rate of change of the predator population, whilst Equation 2.18 describes the dynamics of the prey population.

$$\frac{dP_r}{dt} = k_{g \max pr} \frac{S_c}{k_{ss} + S_c} P_r - k_{dpr} P_r \quad (2.17)$$

$$\frac{dS_c}{dt} = k_{g \max s} \frac{N_c}{k_s + N_c} S_c - k_{ds} S_c - \frac{1}{Y_{pr}} \frac{S_c}{k_{ss} + S_c} P_r \quad (2.18)$$

where:

P_r = predator concentration (mg l^{-1})

S_c = prey concentration (mg l^{-1})

$k_{g \max pr}$ = maximum specific growth rate of the predator (h^{-1})

$k_{g \max s}$ = maximum specific growth rate of prey (h^{-1})

- k_{ss} = half-saturation constant for prey (mg l^{-1})
 k_{dpr} = specific loss rate of predator (h^{-1})
 k_{ds} = specific loss rate of prey (h^{-1})
 Y_{pr} = growth yield coefficient for the predator ($\text{g predator biomass g}^{-1}$ prey biomass)

The growth yield is defined as the quantity of biomass produced per unit time by the utilisation of a unit amount of the limiting nutrient during the same time period. The yield coefficient is a function of the species of microorganism, type of substrate, and environmental conditions under which the cells metabolise the carbon source (Andrews, 1983). Therefore, the values of the yield coefficient vary for populations even when they are grown on the same substrate under identical growth conditions (Gaudy and Gaudy, 1980). Typically, the yield coefficient of heterotrophic microorganisms is $0.4 \text{ g biomass dry weight g}^{-1}$ substrate consumed, indicating that 60 % of the substrate is utilised in metabolic process primarily for energy generation (Slater, 1979).

Substrate balance

Nutrients are important in water quality modelling for several reasons. For example, nutrient dynamics are critical components of eutrophication models since nutrient availability is usually the main factor controlling algal blooms. There are other reasons for including nutrient cycles in water quality modelling rather than their role in microbial growth. For example, the oxidation of ammonia to nitrate during the nitrification process consumes oxygen and may represent a significant amount of the total biochemical oxygen demand (BOD). Also, high concentrations of unionised ammonia can be toxic to fish and other aquatic organisms.

The importance of nutrients for slow sand filter operation has been demonstrated by controlling their concentrations as a routine process. Because algal growth is typically limited by phosphorus and nitrogen (Di Toro *et al.*, 1975; Chapra, 1997), apart from other water quality parameter measurements, ammonia, nitrate, nitrite and phosphate concentrations in influent and treated water from slow sand filter beds are monitored routinely in water treatment plants (Chipps, 2000). Many species of algae are a problem in water supply systems, since they contribute to tastes and odours, clog water intakes, shorten filtration run lengths and cause high chlorine demand in the disinfection

process. Algae also release toxins that can be fatal to wild and domestic animals if they consume water that supports a significant algal population (Tebbutt, 1998). Human deaths have not been reported as a result of ingestion of algae toxins, but treated water containing residual toxins have been associated with gastrointestinal illness and skin irritation (Montgomery, 1985).

In aquatic systems, each nutrient undergoes continuous recycling between their existent forms including dissolved inorganic nutrients, dissolved organic nutrients and particulate organic nutrients (detritus). For example, dissolved inorganic nutrients are removed from water environments by algae and aquatic plants during photosynthesis. These nutrients are also distributed to the other aquatic organisms through the food chain. Dissolved inorganic nutrients are returned to the water through the soluble excretions of all organisms, the decomposition of organic detritus and sediments, and the hydrolysis of dissolved organic nutrients (Bowie *et al.*, 1985). In addition, dissolved CO₂ and N₂ gases exchange with the atmosphere. Decomposition of suspended organic detritus and organic sediment releases both dissolved organic and dissolved inorganic. In the case of SSF systems, although the cycle of the nutrients in slow sand filter beds is still undefined and unquantified, nitrogen and phosphorus are believed to be utilised for microbial growth during filter operation (Di Bernardo *et al.*, 1990).

Nutrients are modelled by using a system of mass balance equations describing each nutrient form (dissolved, particulate) and each process (e.g. uptake, detritus decomposition), plus the transport processes. The general equation for each nutrient, omitting the transport and external loading terms, can be expressed as follows:

$$\frac{dN_c}{dt} = -\frac{1}{Y_M} k_{g_{\max}} \frac{N_c}{k_s + N_c} M + k_d M \quad (2.19)$$

where:

Y_M = growth yield term for microorganism (g cells g⁻¹ substrate)

Equation 2.19 (Slater, 1979) represents the substrate balance incorporating the loss term, represented here by microbial uptake, and the gain term described by the microbial loss (e.g. excretion, death).

Nutrient models differ primarily in the specific nutrient simulated (e.g. C, N, P) and in the number of equations used to describe each nutrient cycle (e.g. dissolved inorganic forms such as NH_3 , NO_2^- and NO_3^-). In addition, the nutrient cycles in water quality modelling are often simplified by combining or omitting some of their processes. For example, both algae and protozoa excrete phosphorus, nitrogen and OC (Jorgensen, 1976). However, these processes are not often accounted for these organisms. In most models protozoa excretion is omitted, as it is considered not important for the nutrient budget (Jorgensen, 1983a), and algae excretion and respiration are always combined and modelled as a single term (Di Toro *et al.*, 1975, Chapra, 1997). Furthermore, nitrogen models differ in the forms of inorganic nitrogen that are included, as well as in some processes modelled. For example, some models include only ammonia and nitrate, rather than the full oxidation sequence of ammonia to nitrite to nitrate (Chapra, 1997). Whilst most models include the nitrification reactions (Di Toro *et al.*, 1975), only a few include denitrification (Jorgensen, 1976; Brown and Barnwell, 1987).

Effect of temperature on process rates

Temperature is a primary environmental factor affecting microbial growth and activity (Gaudy and Gaudy, 1980). Each microorganism is able to grow only within a specific range of temperature. The maximum and minimum temperatures define the limits of the temperature range within which growth is possible. At lower or higher temperatures than the maximum and minimum temperatures, no growth occurs (Hawker and Linton, 1971). There is an optimum temperature at which the growth is most rapid, i.e. the growth rate reaches its maximum value (Gaudy and Gaudy, 1980). For most microorganisms the optimum temperature is much closer to the maximum than to the minimum temperature (Hawker and Linton, 1971). Growth at minimum temperature is typically quite slow. In general, the minimum temperature for growth is in the range 10-15 °C and the optimum is 24-40 °C within maximum value range of 35-45 °C (Hawker and Linton, 1971).

Therefore, temperature influences the rates of nutrient transformations and microbial growth processes discussed above. All of the rate coefficients in Equations 2.11 through 2.19 are temperature dependent. Almost all water quality models (Bowie *et al.*, 1985; Chapra, 1997) use the exponential Arrhenius relationship (Equation 2.20) to describe temperature effects.

$$k_{(T)} = k_{20} \theta^{T-20} \quad (2.20)$$

where:

$k_{(T)}$ = process rate at temperature T °C (h^{-1})

k_{20} = process rate at 20 °C (h^{-1})

θ = temperature coefficient (dimensionless)

In water quality modelling, a temperature reference of 20 °C is usually assumed since many kinetic rates are reported at this value (Bowie *et al.*, 1985; Chapra, 1997). Table 2.3 summarises some commonly used values for θ in different processes.

Table 2.3 - Typical values of θ in water quality modelling
(adapted from Chapra, 1997)

θ	Reaction
1.024	Oxygen reaeration
1.047	BOD decomposition
1.066	Algae growth
1.08	Sediment oxygen demand

Most water quality models use a temperature correction factor of 1.047 to adjust growth of protozoa and bacteria, and 1.08 for decay process (Bowie *et al.*, 1985; Brown and Barnwell, 1987; Jorgensen, 1983a; Chapra, 1997).

2.4 - Summary

- (1) Slow sand filters support a substantial biological life due to the long hydraulic retention time of water above and across the filter bed. Particles, including mainly algae and other microorganisms, deposit on the top of the sand and contribute to the development of an algal mat (schmutzdecke) on the sand surface.

- (2) Slow sand filters for potable water treatment are usually operated without covering. In few cases the filter is covered to minimise winter freezing problems and to reduce algae growth (Sub-section 2.2.1). The different benefits of covered/uncovered filters are certain. However, research is required on understanding and quantifying the filtration mechanisms operating in these filters.
- (3) Particle removal mechanisms in SSF can be described by the same filtration mechanisms applied to rapid sand filtration (Sub-section 2.2.2.1). However, the biological mechanisms, which are the most important mechanisms affecting the performance of SSF process, are poorly understood and unquantified.
- (4) Slow sand filtration is effective at removing algae and pathogenic microorganisms from raw potable surface water supplies. Among the several biological processes occurring within slow sand filter beds, predatory action, maturity of sand bed, and schmutzdecke development are very important for water purification. The removal of bacteria and algae is primarily attributed to the grazing of protozoa (Sub-section 2.2.2.2).
- (5) There are few mathematical models describing the capture mechanisms and headloss development in SSF (Chapter 1 and Sub-section 2.2.2.3). The combination of Equations 2.3 with 2.9 has been successfully used to simulate the distribution of headloss with time and filter depth in SSF (Ojha and Graham, 1994). However, model calibration making use of these equations was not possible due to lack of experimental data.
- (6) Among those microorganisms inhabiting slow sand filters, algae, bacteria, and protozoa are the most numerous (Sub-section 2.2.3.1). In general, these microorganisms accumulate in the top few centimetres of sand and their distribution declines sharply with depth. Algal flora inhabits the supernatant water, the top of the sand and the filter bed. The fact that algae are found entering the sand bed (Bellinger, 1968, 1979; Haarhoff and Cleasby, 1991) does not give evidence that they are capable of growing in the sand bed.
- (7) Definitions have been developed to explain the nature and characteristics of the schmutzdecke. These show that the characteristics of the schmutzdecke vary from

SSF system to system depending on the incoming water quality, as well as the environmental and operation conditions (Sub-section 2.2.3.2). The schmutzdecke increases the specific bed surface and enhances particle removal efficiency, contributing to the water purification processes (Hirschi and Sims, 1991; McNair *et al.*, 1987).

- (8) The research on biological aspects of slow sand filters has focused on qualification and quantification of microorganisms present within sand beds (Sub-section 2.2.3). However, more detailed studies are needed to describe and quantify the relative importance of main groups of microorganisms in water purification by SSF, as well as the dynamics of these microorganisms within the filter.
- (9) Understanding the distribution, composition and metabolic activity of microbial populations present in slow sand filters would help to optimise management practices and better understand the role of biomass in the water purification process. For example, Eighmy *et al.* (1994) observed that too much biomass accumulation can clog the filter, but high amounts of biomass are needed to decrease non-purgeable dissolved organic carbon (NPDOC), trihalomethane formation potential (THMFP) and biodegradable organic carbon (BDOC) to minimum levels. On the other hand, biomass growth in slow sand filters can be stimulated by cleaning techniques, e.g. harrowing (Collins *et al.*, 1994). Therefore, the knowledge of population and biomass distributions in slow sand filters is important in evaluating the efficacy of natural organic matter (NOM) removal, as well as in controlling headloss, filtration rate, and filtration run (Sub-section 2.2.3).
- (10) Different approaches have been used to measure microbial biomass concentrations and the inconsistent units and sampling intervals adopted confound inter-study comparisons of biomass development and behaviour during SSF (Sub-section 2.2.3.3). Most reports are of single measurements of the net biomass production at the end of a filter run prior to cleaning, and emphasise the significant variability in schmutzdecke and sand biomass accumulated in operational slow sand filters.
- (11) Detailed analyses of biomass growth in the schmutzdecke and within the sand bed during filter operation would improve understanding of the complex and fundamental interactions between the biological and physico-chemical processes

operating in slow sand filter systems. This information would enable the development of mechanistic models of SSF systems to potentially improve the operational management of filters through the prediction of headloss rate, and the frequency of sand cleaning and renewal.

- (12) Little information is available regarding the development of schmutzdecke with time and depth (Sub-section 2.2.3.2). This is mainly due to difficulties in sampling schmutzdecke during filter operation, particularly, in full-scale plants (Campos *et al.*, 2002). In the works of Hirschi and Sims (1991) and Nakamoto (1995), the schmutzdecke presented a linear growth with time (Figures 2.5 and 2.6).
- (13) The review of nutrition and growth conditions of algae, bacteria and protozoa explained that concentrations of inorganic compounds concentrations (i.e. nitrogen and phosphorus), temperature and light are the main variables affecting algal growth (Sub-section 2.3.1). Bacterial growth is related to DOC and phosphorus concentrations, while protozoa utilise bacteria and algae as their main food source. Microbial dynamics can be represented by growth and loss processes. The loss of microbial biomass is associated with predatory and non-predatory losses. Non-predatory loss includes processes such as death and decay.

3 - CHARACTERISTICS OF THE EXPERIMENTAL DATA FROM KEMPTON PARK AWT PILOT PLANT

3.1 - Introduction

Whilst lack of experimental data has been identified as a critical constraint to model development and calibration of SSF processes (Chapter 1), a unique and most comprehensive data set was provided by Thames Water for the development of the SSF model.

The data sets which are part of an extensive investigation at the Kempton Park AWT pilot plant was collected from July 1991 to July 1993. The experimental data consist of long-time scale measurements of physico-chemical and biological water quality parameters monitored routinely in the influent and effluent of the slow sand filters during the experimental period. The data sets also contain measurements of headloss and flow during consecutive filtration runs which had a complete operation cycle and ended when terminal headloss was reached. All operational performance information was recorded from the pilot plant commissioning period onwards. The Thames Water data are therefore potentially amenable to SSF model development and offer an unprecedented opportunity for model calibration and verification to this work.

3.2 - Kempton Park AWT pilot plant

Thames Water supplies on average 2,600 Mld of drinking water in the Greater London area and approximately 75 % of this supply is produced by five key treatment works treating lowland surface water abstracted from the Rivers Thames and Lee (Rachwal *et al.*, 1993; Bauer *et al.*, 1996). These works (Ashford Common, Walton, Kempton Park, Hampton, and Coppermills) are operated based on SSF process with a total treatment capacity of 2,000 Mld.

The conventional treatment processes (reservoir storage followed by rapid gravity filters (RGFs), slow sand filters, and disinfection) are unable to consistently meet the standards for pesticides in the UK ($\leq 0.1 \mu\text{g l}^{-1}$; HMSO, 1989). The issues of controlling pesticides and organics in drinking water and the need of reducing the use of chlorine and the production of its by-products led Thames Water to seek for more advanced

treatment processes (Rachwal *et al.*, 1993). Thus, in 1980 Thames Water recommenced studies on ozonation prior to slow sand filters (Rachwal *et al.*, 1986). Ten years later, a pilot-scale plant, Kempton Park AWT, was constructed to provide a facility for investigating the combined use of ozone, advanced oxidation processes (e.g. peroxide) and activated carbon with SSF (Rachwal *et al.*, 1993).

The Kempton Park AWT pilot plant was designed and constructed between April 1990 and May 1991, and was commissioned in July 1991 (Rachwal *et al.*, 1993). The pilot plant has two parallel process streams with a total capacity of approximately 5 Mld (Figure 3.1). Both process streams include two stages of ozonation in combination with rapid gravity filtration, SSF and granular activated carbon (GAC).

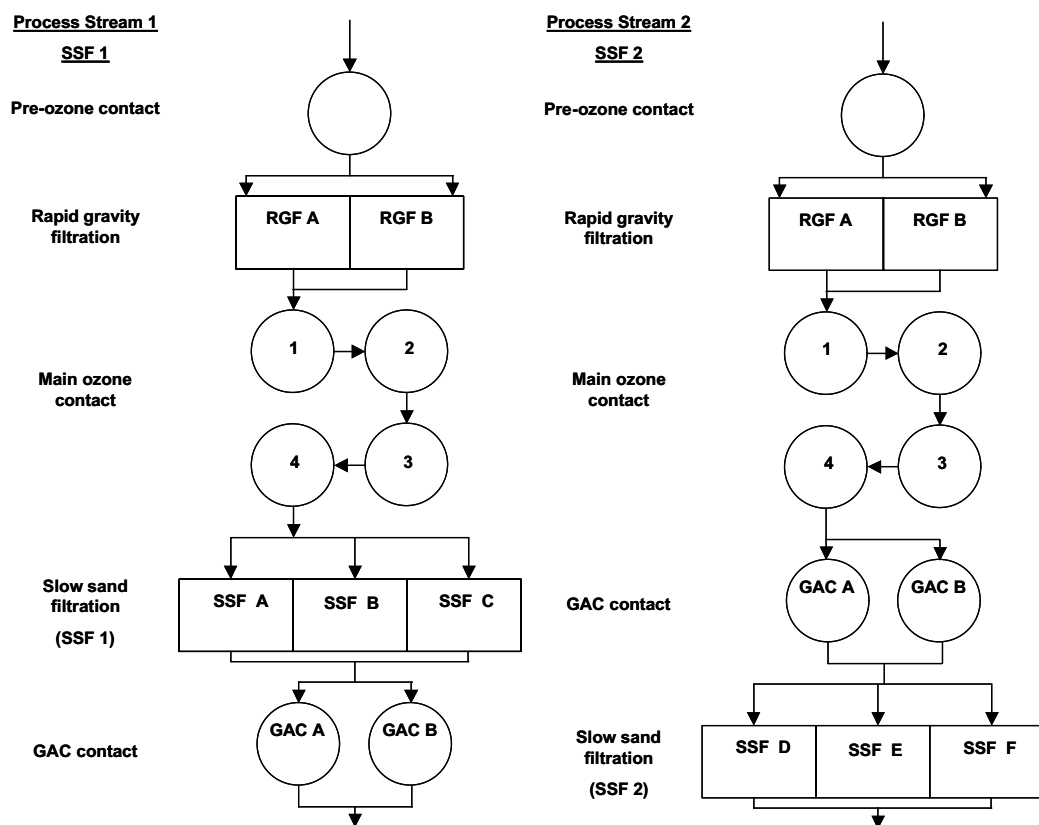


Figure 3.1 - Schematics of process stream 1 (SSF 1) and stream 2 (SSF 2) at Kempton Park AWT pilot plant (Rachwal *et al.*, 1993)

Each stream has two rapid filters, two GAC filters and three slow sand filters, with the total flow being split between the individual filters. The pre-ozone contactor is a single stage tank, while each main ozone contactor is made up of four tanks in series. In stream

1 (SSF 1), the GAC filters follow the slow sand filters, while in stream 2 (SSF 2) they come before them. The feed water to the Kempton Park AWT plant is reservoir stored River Thames which raw water characteristics are given in Table 3.1.

Table 3.1 - Characteristics of raw water treated from the River Thames by Kempton Park AWT pilot plant during the period of September/1991 and March/1993

Parameter	Unit	Average	Range
Colour	Hazen	8.5	5.1 - 14.7
Turbidity	NTU	2.1	0.4 - 6.7
pH		8.4	7.8 - 9.1
Coliforms	cells per 100 ml	119.4	0.1 - 1000
Algae	mg l ⁻¹	9.2	0.7 - 71.0
Ammonia	mg l ⁻¹	0.058	0.002 - 0.126
Phosphate (PO ₄)	mg l ⁻¹	1.83	0.66 - 3.93
POC	mg l ⁻¹	627	150 - 3514
TOC	mg l ⁻¹	5.2	2.1 - 11.8
Alkalinity	mg l ⁻¹ CaCO ₃	200	170 - 220
Hardness	mg l ⁻¹ CaCO ₃	305	274 - 364

Raw water turbidity in Kempton Park was relatively low during the period of 1991-1993, varying from 0.4 NTU to 6.7 NTU, whilst colour concentration ranges from 5.1 to 14.7 Hazen units (Table 3.1). Values of raw water turbidity smaller than 10 NTU and maximum true colour concentration of 5 CU have been suggested as appropriate for water being treated by conventional SSF processes (Di Bernardo, 1993; Galvis *et al.* 1998). The chlorophyll-a concentration of the raw water at Kempton Park was maximum 71 mg l⁻¹ which is larger than the maximum concentration of 5 mg l⁻¹ recommended for SSF processes (Galvis *et al.*, 1998).

Regarding the operation mode of the slow sand filters, four are uncovered and two are covered (Table 3.2). Detailed information was also collected of the influent and effluent water quality from the slow sand filters. The data provided by Thames Water included physico-chemical and microbiological water quality parameters, headloss, flow, inlet channel level, and depth of the sand beds (Table 3.3). The data related to headloss, flow, turbidity, and temperature were recorded every 15 minutes, whilst the chemical and microbiological parameters determined on a daily, weekly or monthly sampling basis. All this information forms the basis of the data used for the development, calibration and verification of the SSF model in this thesis.

Table 3.2 - Mode of operation of the slow sand filters at the Kempton Park AWT

Stream	Filter	Form of operation
SSF 1	SSF A	uncovered
	SSF B	uncovered
	SSF C	covered
SSF 2	SSF D	covered
	SSF E	uncovered
	SSF F	uncovered

Table 3.3 - Measured parameters for the slow sand filters at Kempton Park

Parameter	Unit
<i>Physical:</i>	
Temperature	°C
Flow rate	m ³ h ⁻¹
Headloss	m
Inlet channel level	m
Filter media depth	m
Turbidity	NTU
<i>Chemical and microbiological:</i>	
Ammonia	mg l ⁻¹
Nitrate ^(*)	mg l ⁻¹
Phosphate	mg l ⁻¹
Bacteria counts	cell ml ⁻¹
Chlorophyll-a	µg l ⁻¹
TOC	mg l ⁻¹
POC	µg l ⁻¹

^(*) measured from 1993 onwards

Three consecutive filtration runs of each filter were selected for model calibration and verification. The aim of selecting three filtration runs was to access the performance of successive filtration runs and have an annual representation of the seasonal variation of each filter. In general, all filters, except the covered filter SSF D, had a average filtration run length of about 100-150 days (Table 3.4). The first filtration run length of the covered SSF D was 373 days, and the second filtration run was about 789 days ending in September/1994. As Thames Water provided information during the period of 1991-1993, the data set of the second filtration run of SSF D is incomplete.

Table 3.4 - Duration period of the filtration runs at Kempton Park

Filter	Run	Date of operation	Duration of the run	
			(day)	(hour)
SSF A	1	16/07/1991 to 30/10/1991	106	2544
	2	17/12/1991 to 20/03/1992	94	2256
	3	20/03/1992 to 15/08/1992	148	3552
SSFB	1	16/07/1991 to 23/10/1991	99	2376
	2	25/10/1991 to 25/03/1992	152	3648
	3	26/03/1992 to 15/08/1992	142	3408
	4 ^(*)	26/08/1993 to 05/01/1993	132	1320
SSF C	1	16/07/1991 to 14/09/1991	60	1440
	2	15/10/1991 to 25/03/1992	162	3888
	3	26/03/1992 to 21/12/1992	270	6480
	4 ^(*)	22/12/1992 to 15/02/1993	55	1320
SSF D	1	16/10/1991 to 23/07/1992	373	8952
	2	31/07/1992 to 28/09/1994	789 ^(**)	18936 ^(**)
SSF E	1	16/07/1991 to 09/10/1991	85	2040
	2	09/10/1991 to 19/05/1992	223	5352
	3	19/05/1992 to 04/09/1992	108	2592
SSF F	1	16/07/1991 to 24/10/1991	100	2400
	2	24/10/1991 to 19/05/1992	208	4992
	3	25/06/1992 to 17/08/1992	53	1272

^(*) Filtration runs reserved

^(**) Data set until March 1993

3.3 - Physico-chemical and biological parameters

Table 3.5 shows the mean values for influent and effluent concentrations for both SSF 1 and SSF 2. The relationships between influent and water quality parameters were examined using a t-test statistic and t value was significant at $P \leq 0.05$.

The influent water quality to SSF 1 in terms of particulates and TOC (Table 3.5) was larger than that to SSF 2 and this was probably explained by the GAC pretreatment located in SSF 2 since it is effective at removing biodegradable organic matter (Klevens *et al.* 1996; Graham, 1999). On the other hand, the treatment efficiency for removal of turbidity, chlorophyll-a, POC, and TOC was, generally, more significant in SSF 1 ($P < 0.05$) than in SSF 2. This suggests that the ozonation pretreatment increased the biodegradable organic carbon (NDOC) content increasing efficiency of organic matter removal in SSF 1 (Malley *et al.*, 1994; Yordanov *et al.*, 1996).

Table 3.5 - Mean values for influent and effluent concentrations for SSF 1 and SSF 2

Parameter	SSF 1			SSF 2		
	Influent	Effluent	t-Test	Influent	Effluent	t-Test
Turbidity (NTU)	0.79	0.09	P < 0.05	0.12	0.08	P < 0.05
Chlorophyll-a (mg l ⁻¹)	3.9x10 ⁻³	1.21x10 ⁻⁴	P < 0.05	5.23x10 ⁻⁴	2.81x10 ⁻⁴	P = 0.10
B. counts (cells per ml)	13.2	3.9	P = 0.05	12.8	3.4	P = 0.05
POC (mg l ⁻¹)	0.29	0.18	P < 0.05	0.07	0.13	P < 0.05
TOC (mg l ⁻¹)	4.9	3.9	P < 0.05	3.7	3.6	P = 0.24
Phosphate (mg l ⁻¹)	0.50	0.56	P = 0.13	0.44	0.45	P = 0.45
Ammonia (mg l ⁻¹)	3.0x10 ⁻³	3.5x10 ⁻³	P = 0.43	5.4x10 ⁻³	1.7x10 ⁻³	P = 0.06
Nitrate ^(*) (mg l ⁻¹)	6.49	6.66	P = 0.19	6.49	6.71	P = 0.12

3.3.1 - Level of the supernatant water

The channel level of both streams on average was 1 m and the minimum level measured was 0.40 m. This channel keeps the level of the supernatant water in the slow sand filters approximately constant.

3.3.2 - Temperature

Temperature was measured only at the influent water to the treatment process (Figure 3.2). The water temperature varied from 4.8 to 24.3 °C and presented on average 12.2 °C over the period of 1991-1993. The highest temperatures were measured between July and September, whilst the lowest temperatures occurred from December to March.

3.3.3 - Headloss and influent flow

Figures A.1.1 to A.1.6 (Appendix A.1) show the variations in headloss and flow with time during three filtration runs for the slow sand filters in SSF 1 and SSF 2. From these figures (Appendix A.1) the following aspects are observed:

- Headloss was proportional to flow and an increase or decrease in flow was followed by an increase or decrease in headloss. Although headloss increased over the entire

filtration run, variations were observed with time, which is consistent with Toms and Bayley (1988).

- b) In all filters, high intermittent values of headloss were larger than the maximum available hydraulic head, 1.8 m (e.g. Figures A.1.2b and A.1.3b).
- c) Missing values were evident for both flow and headloss in all filtration runs. The majority of the filters showed more than 50 % (52 days) of missing values at the beginning of the first filtration run. More than 80 % of the data in the first filtration run of SSF C (Figure A.1.3a) and 40 % in the second run of SSF A (Figure A.1.1b) were not available.
- d) The constant flow recorded for SSF C in filtration Run 1 and Run 2 (Figures A.1.3ab) suggested that there were operational problems with the measuring equipment.

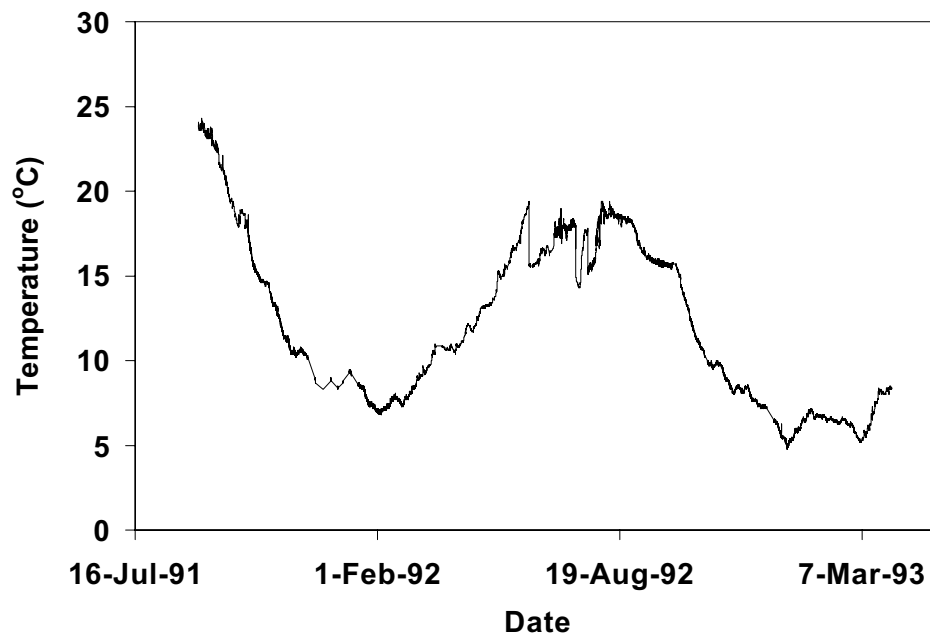


Figure 3.2 - Raw water temperature at Kempton Park.

3.3.4 - Turbidity

The influent turbidity at SSF 2 was apparently lower than for SSF 1 and on average the turbidity of the filtrate from both SSF streams was less than 0.1 NTU (Figure 3.3). Both streams had significant removal efficiency of turbidity of approximately 87 % in SSF 1 and 35 % in SSF 2 ($P < 0.05$).

Figure 3.3 - Influent and effluent turbidity for (a) SSF 1 and (b) SSF 2

The turbidity meters were set to measure maximums of 2 NTU and 1 NTU in the influent and effluent, respectively. However, turbidity occasionally exceeded these upper limits of the monitoring apparatus possibly due to passage of flocs through the rapid filters caused by inadequate dosage of coagulant (Chipps, 2000). Some turbidity data were missing at the beginning and also during the monitoring period (Figure 3.3a).

3.3.5 - Chlorophyll-a

The chlorophyll-a influent concentration of SSF 2 was apparently smaller than for SSF 1 (Figure 3.4). The influent chlorophyll-a of SSF 1 varied from 0.0005 to 0.016 mg l⁻¹, while 0.006 mg l⁻¹ was the maximum influent concentration for SSF 2. A very significant chlorophyll-a removal of 96 % was evident in SSF 1 ($P < 0.05$), whilst SSF 2 only 46 % of chlorophyll-a was removed.

3.3.6 - Bacteria counts

Bacteria data consisted of total bacteria counts, *E. coli* counts, and coliform counts. Because *E. coli* and coliforms represent a small proportion of the total bacteria concentration in water, bacteria counts were selected for the SSF modelling. The variation of influent and effluent bacteria counts were similar in both streams containing on average 13 cells per 100 ml in the influent and 3.6 cells per 100 ml (Figure 3.5). The efficiency of bacterial removal of 75 % was significant in both streams ($P = 0.05$).

3.3.7 - Particulate organic carbon

The influent POC (Figure 3.6) concentration of SSF 1 was larger than that of SSF 2. On average, POC influent to SSF 1 and SSF 2 contained 0.29 mg l⁻¹ and 0.07 mg l⁻¹, respectively. The POC removal of approximately 38 % in SSF 1 was very significant ($P < 0.05$). However, in SSF 2 POC concentration in the effluent was considerably larger ($P < 0.05$) than that in the influent, presenting an increase of approximately 86 % of POC.

3.3.8 - Total organic carbon

On average, TOC influent concentrations were 4.9 mg l⁻¹ in SSF 1 and 3.7 mg l⁻¹ in SSF 2, and the effluent concentrations were 3.9 mg l⁻¹ and 3.6 mg l⁻¹ in SSF 1 and SSF 2, respectively (Figure 3.7). The removal of 20 % of TOC in SSF 1 was very

significant ($P < 0.05$) compared to 3 % removed in SSF 2 ($P = 0.24$). Similar removal of TOC (24 %) was observed at Walton (Campos *et al.*, 2002), which has analogous advanced water treatment to SSF 1.

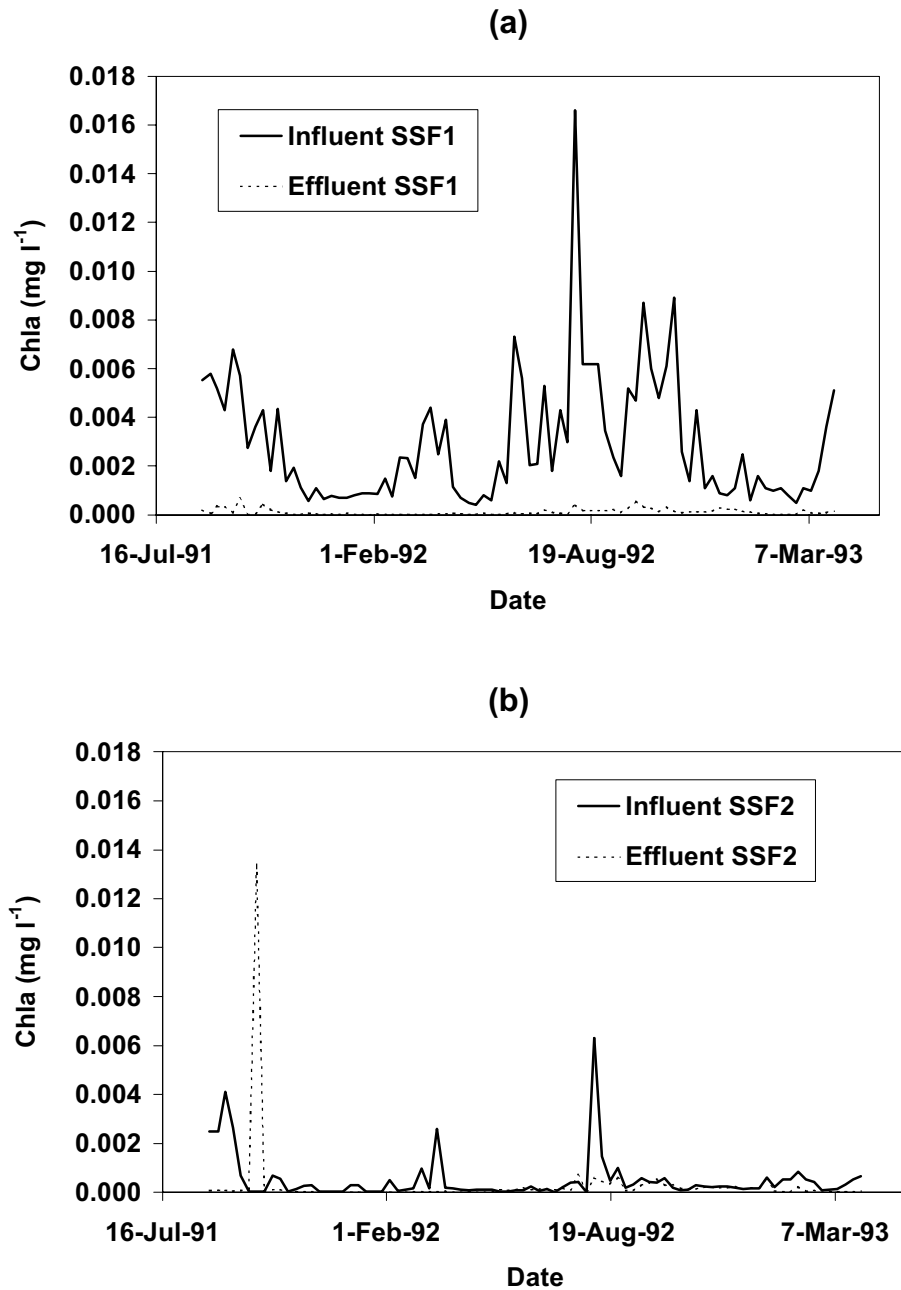


Figure 3.4 - Influent and effluent chlorophyll-a contents for (a) SSF 1 and (b) SSF 2

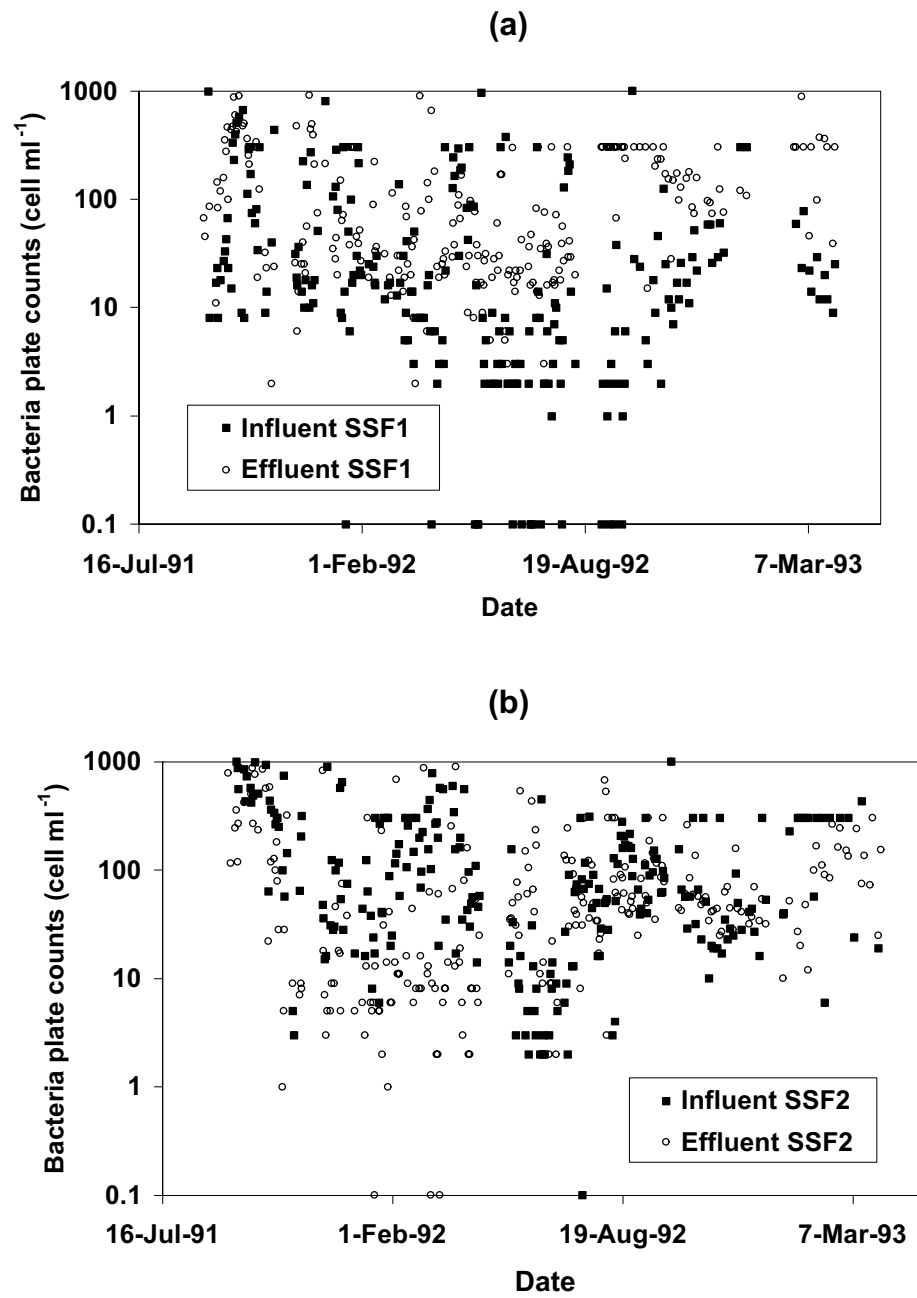


Figure 3.5 - Influent and effluent bacteria counts for (a) SSF 1 and (b) SSF 2
(Note: Bacteria counts plotted on logarithm scale)

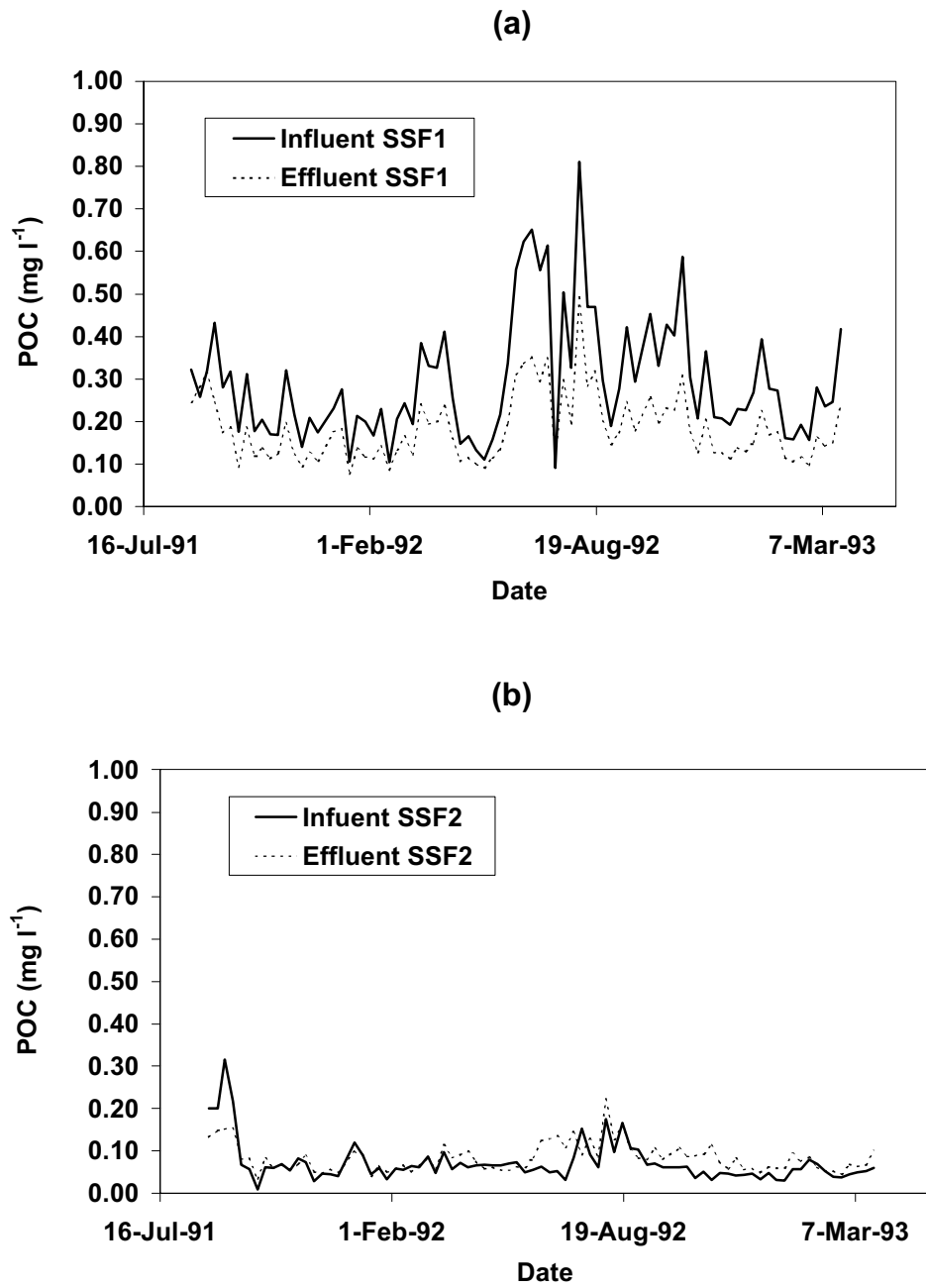


Figure 3.6 - Influent and effluent POC concentrations for (a) SSF1 and (b) SSF 2

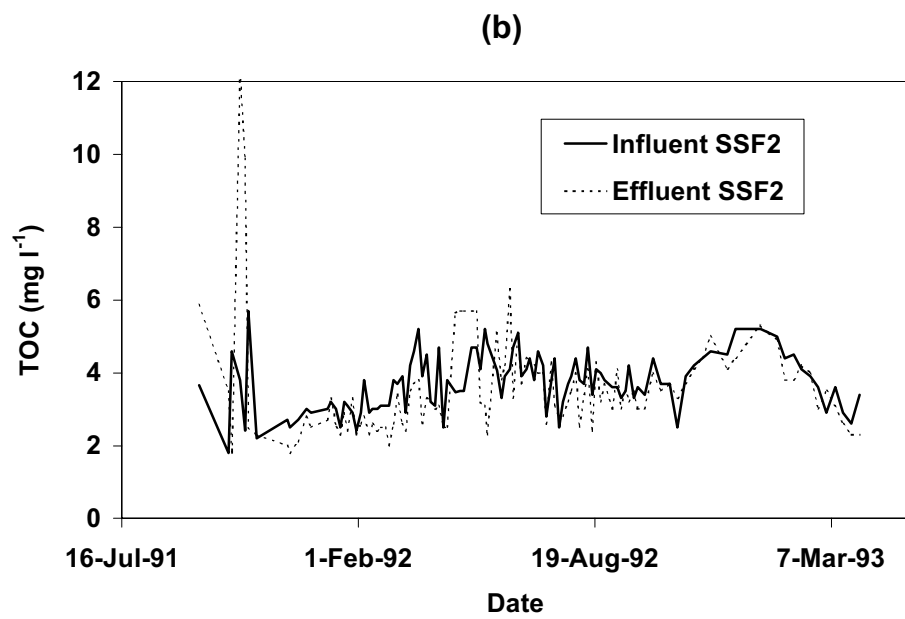
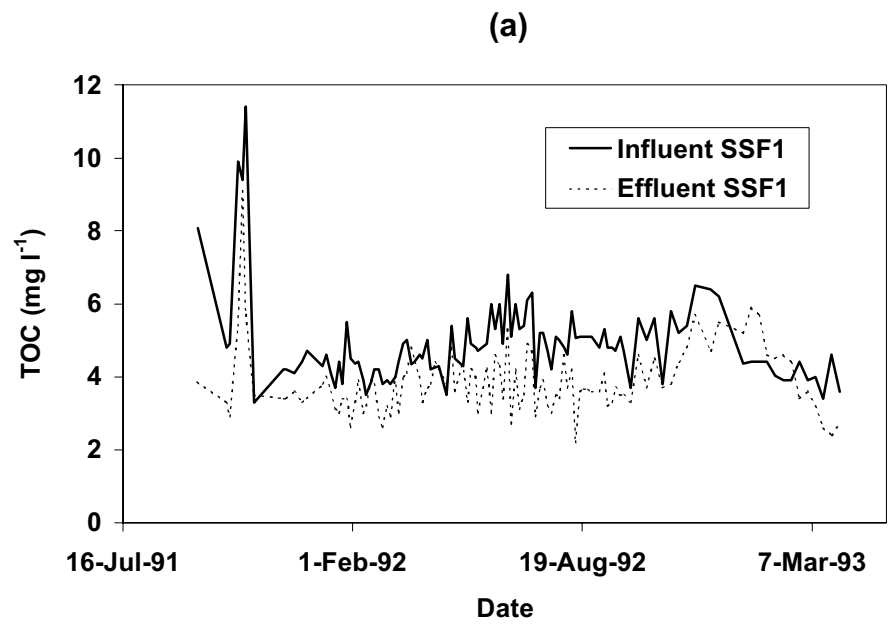


Figure 3.7 - Influent and effluent TOC concentrations for (a) SSF 1 and (b) SSF 2

3.3.9 - Ammonia, nitrate, and phosphate

The data provided by Thames Water consist of the inorganic forms of nitrogen (nitrate NO_3^- and ammonia NH_3) and phosphorus as orthophosphates ions PO_4^{3-} .

Nitrate (NO_3^-) concentration was not monitored during the experimental period, but on average influent nitrate concentration of the raw water was approximately 5.79 mg l^{-1} during the period of August/1993 and May/1998 (Figure 3.8). During this period, there was no significant removal of nitrate ($P = 0.19$ for SSF 1, $P = 0.12$ for SSF 2) in both streams. Excluding those values of the effluent that exceed the corresponding influent values (for reasons unknown) only 4 % of nitrate was removed in both streams during the period of 1993 - 1998.

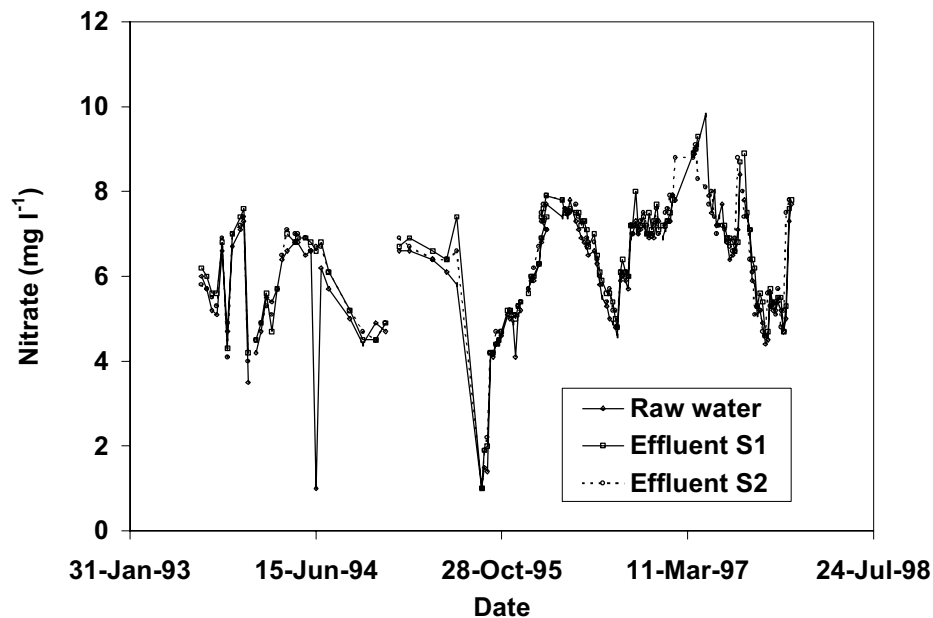


Figure 3.8 - Raw water and effluent nitrate concentrations for SSF 1 and SSF 2 from 1993 to 1998

Similar to nitrate, ammonia (Figure 3.9) also exhibited a variable pattern with time and no difference between influent and effluent was apparent ($P = 0.43$ for SSF 1, $P = 0.06$ for SSF 2). On average, the influent and effluent ammonia concentrations in SSF 1 were 0.003 mg l^{-1} , whilst in SSF 2 the influent and effluent concentrations were 0.005 mg l^{-1} and 0.002 mg l^{-1} , respectively.

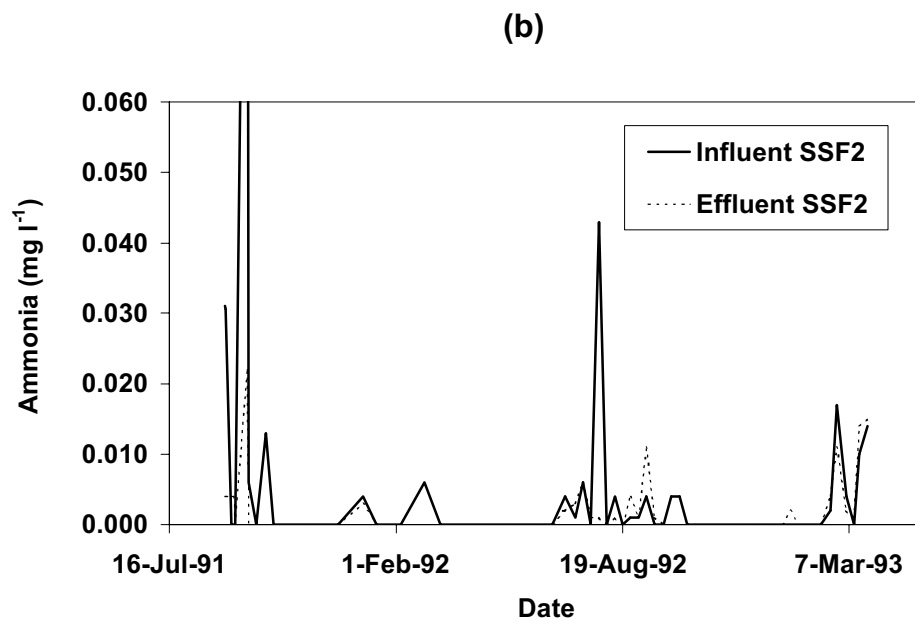
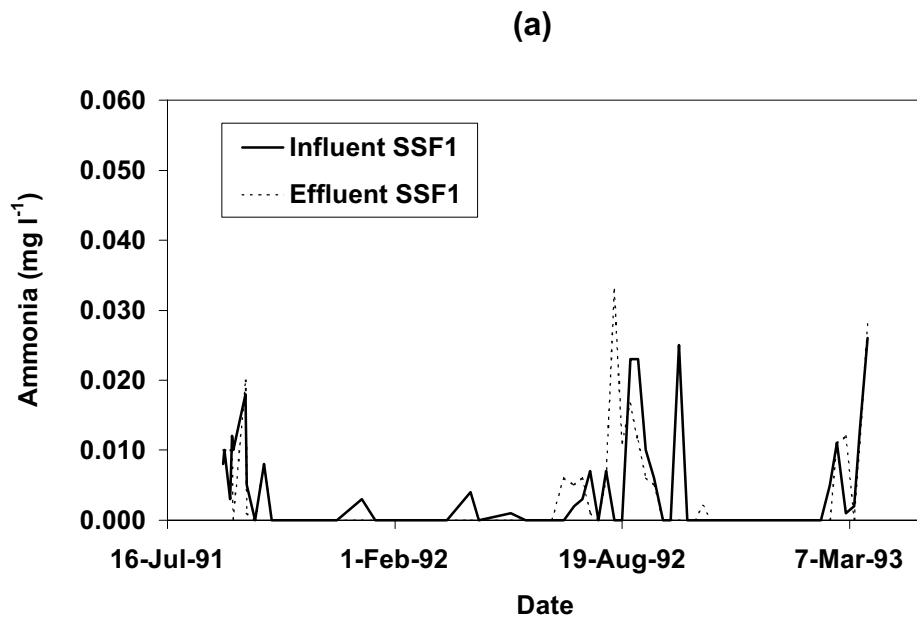


Figure 3.9 - Influent and effluent ammonia concentrations for (a) SSF 1 and (b) SSF 2

The influent and effluent concentrations of phosphate (Figure 3.10) in SSF 1 were, on average, 0.44 mg l^{-1} and 0.45 mg l^{-1} , respectively. The influent and effluent concentrations in SSF 2 were slightly higher than in SSF 1, containing on average 0.50 mg l^{-1} and 0.56 mg l^{-1} , respectively. Therefore, no significant ($P = 0.13$ for SSF 1, $P = 0.45$ for SSF 2) difference between influent and effluent of both SSF streams was apparent.

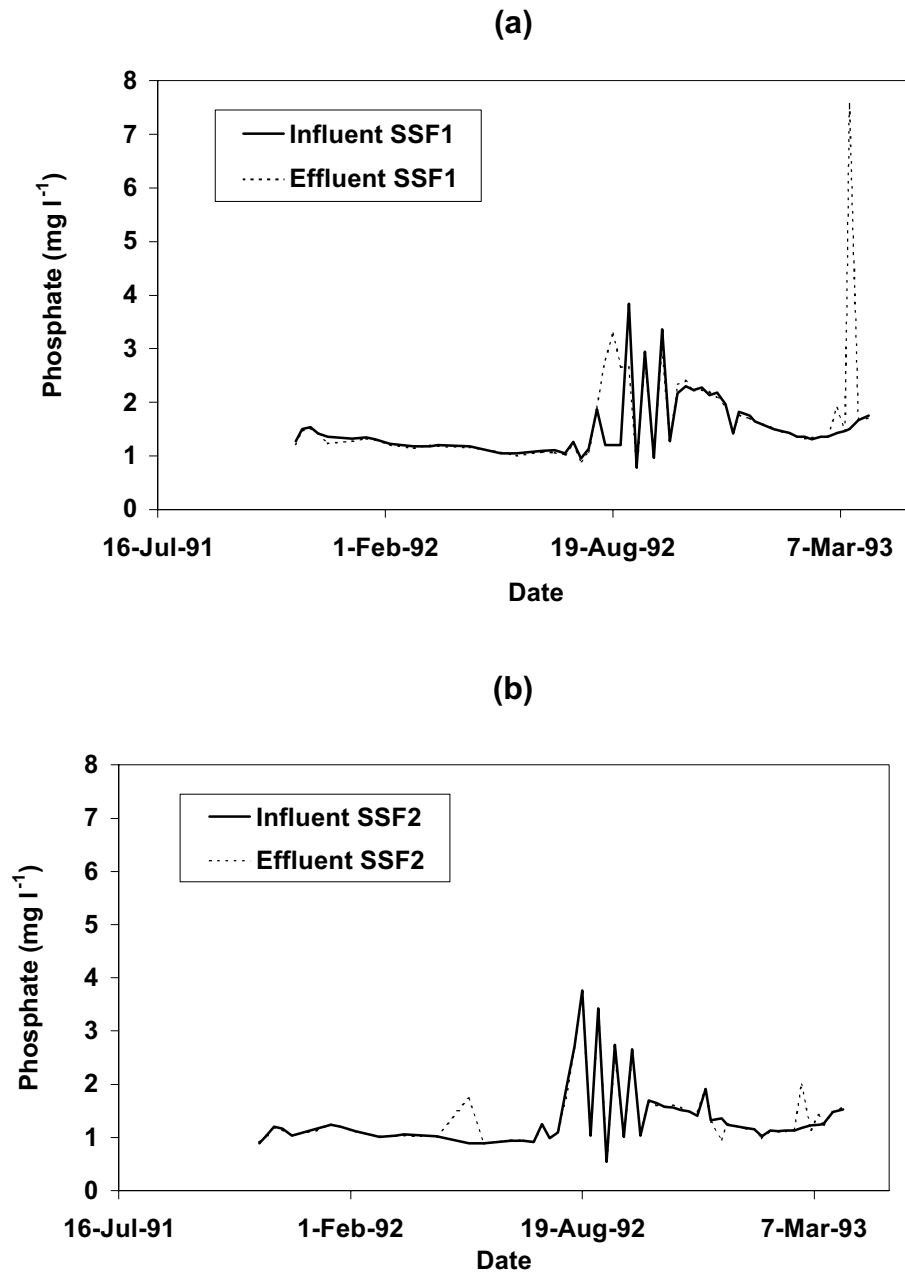


Figure 3.10 - Influent and effluent phosphate concentrations for (a) SSF 1 and (b) SSF 2

3.3.10 - Filter media depth

At the beginning of the experimental period the initial depth of the sand layer was 0.70 m in all slow sand filters. On average 5 cm was removed during filter cleaning and the sand depth was measured after each skimming (Table 3.6).

Table 3.6 - Filter media depth (m) of the slow sand filters at Kempton Park

Filter	Run 1	Run 2	Run 3	Run 4
SSF A	0.70	0.66	0.63	NP
SSF B	0.70	0.65	0.59	0.59
SSF C	0.70	0.63	0.59	0.54
SSF D	0.70	0.64	NP	NP
SSF E	0.70	0.60	0.56	NP
SSF F	0.70	0.69	0.62	NP

NP: Not Provided

3.4 - Relationships between water quality parameters

The quantitative relationships between water quality parameters were examined via determination of correlation coefficient. The correlation coefficient was obtained from the daily variation of the parameters, and it was based on the period of July 1991 and July 1993. Tables A.2.1 and A.2.2 (Appendix A.2) present the summary of the regression analysis between the influent water quality parameters of SSF 1 and SSF 2.

A very significant relationship was observed between influent POC and chlorophyll-a (Figure 3.11) of both SSF 1 ($r = 0.75$, $P < 0.001$) and SSF 2 ($r = 0.72$, $P < 0.001$). This suggests that an increase in algae may lead to an increase in POC and that algae may be a significant part of POC content in the influent water of both SSF streams. In contrast, the relationship between bacteria and POC contents in the influent water (Figure 3.12) was very significant only in SSF 2 ($r = 0.72$, $P < 0.001$) and this may be explained by the location of GAC treatment prior to SSF 2.

Turbidity was expected to have a positive and strong correlation with chlorophyll-a, bacteria counts, and POC since turbidity is caused by the presence of suspended solids including organic and inorganic matter (Sadar, 1998). However, there was no significant

relation between turbidity and particulates in the influent for both SSF 1 and SSF 2 (see Tables A.2.1 and A.2.2, Appendix A.2) which contrasts other observations in conventional SSF systems (Graham, 1982, Demby, 1988, Mbwette, 1989). This suggested that in Kempton Park AWT plant turbidity consisted mainly of inert and non-living POC, although a significant correlation was observed between turbidity and chlorophyll-a for SSF 2 ($r = 0.25$, $P = 0.03$). Therefore, it was possible that inert and non-living POC particles were the principal part to contribute to the bulk specific deposit within the filters.

The correlation of water temperature with the bio-chemical parameters influent to both streams was generally positive, indicating that these parameters were proportional to temperature (see Tables A.2.1 and A.2.2, Appendix A.2). Total organic carbon in raw waters was found to increase with increasing temperature as reported by Seger and Rothman (1996). In contrast, the correlation between water temperature and influent turbidity (Figure 3.13) in SSF 1 was negative and very strong ($r = -0.38$, $P < 0.001$). This unexplained negative correlation between influent turbidity and water temperature was not expected because temperature increase led to chlorophyll-a and POC increase in both SSF streams (Figure 3.14 and Figure 3.15). However, this negative correlation may be related to the efficiency of the advanced pretreatment prior to slow sand filters and to the particle types present in water.

No significant correlation was found between algae and ammonia ($r = 0.17$ and $P = 0.27$ for SSF 1, $r = -0.13$ and $P = 0.43$ for SSF 2), and phosphate ($r = 0.10$ and $P = 0.53$ for SSF 1, $r = 0.16$ and $P = 0.41$ for SSF 2) for both SSF streams. In addition, the relationship between phosphate and bacteria was negative and not significant ($r = -0.02$ and $P = 0.92$ for SSF 1, $r = -0.06$ and $P = 0.71$ for SSF 2) in the influent to both streams (see Tables A.2.1 and A.2.2, Appendix A.2).

A very strong correlation ($P < 0.001$) was found between headloss and influent flow for the covered filters SSF C and SSF D and uncovered filter SSF E (Figure 3.16). The positive correlation coefficient values between headloss and influent flow (Table A.2.3, Appendix A.2) confirmed that headloss was directly proportional to flow as described in Sub-section 3.3.3.

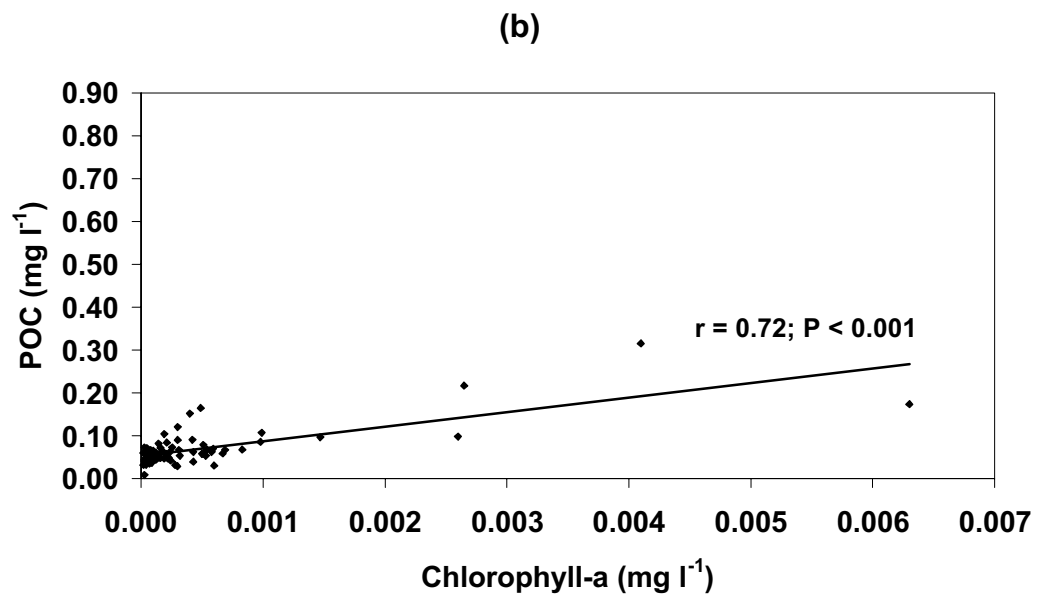
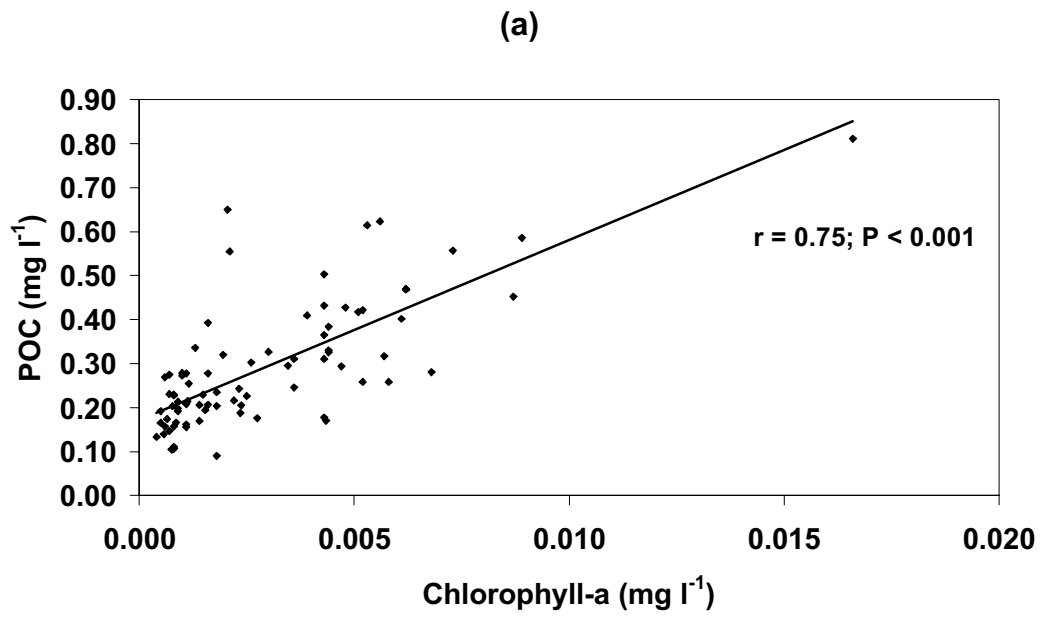


Figure 3.11 - Correlation between POC and chlorophyll-a for (a) SSF 1 and (b) SSF 2

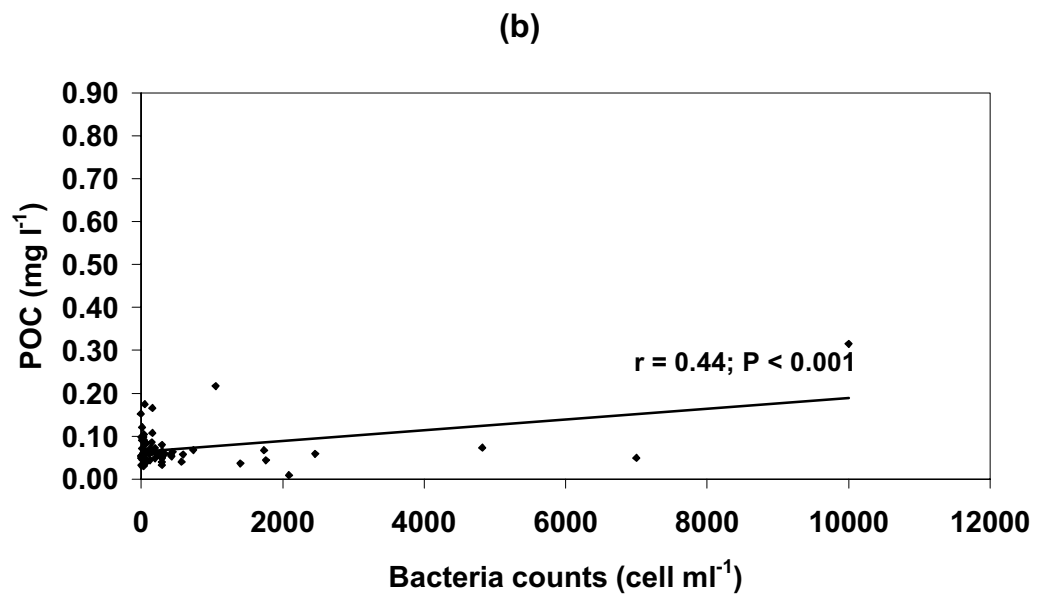
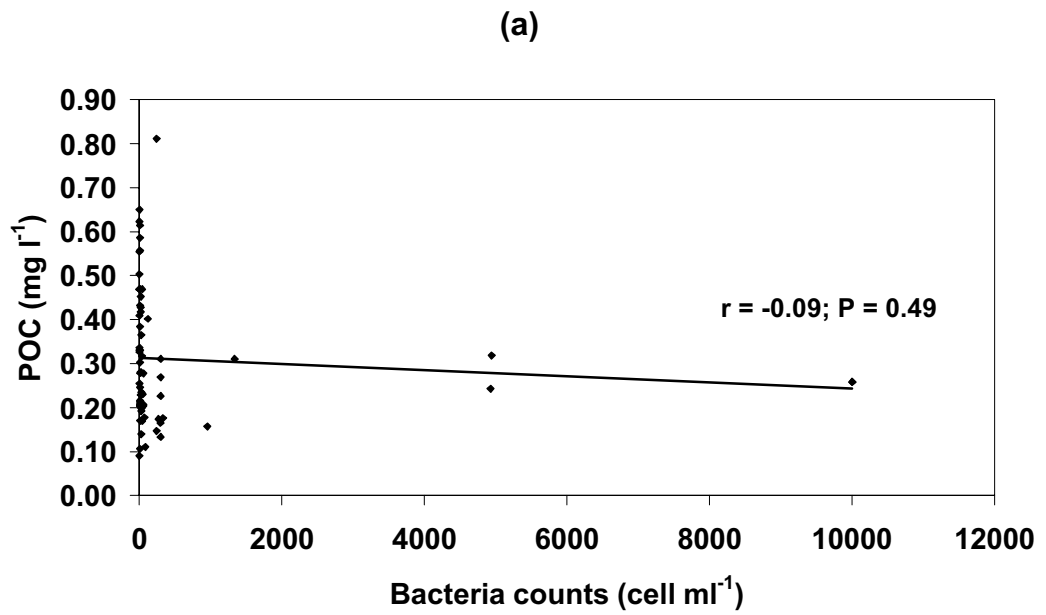


Figure 3.12 - Correlation between POC and bacteria counts for (a) SSF 1 and (b) SSF 2

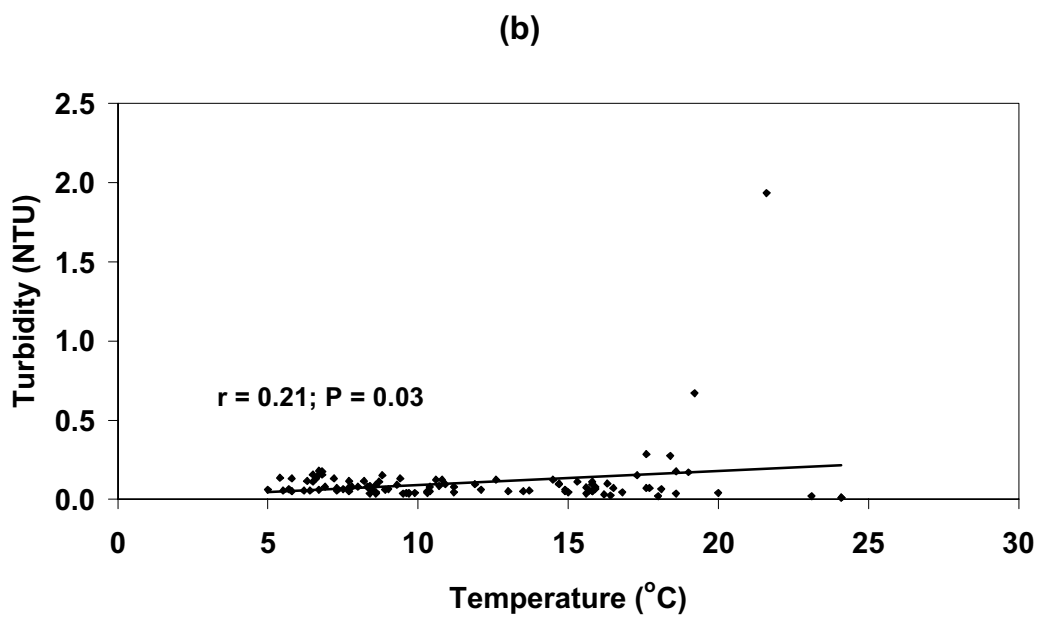
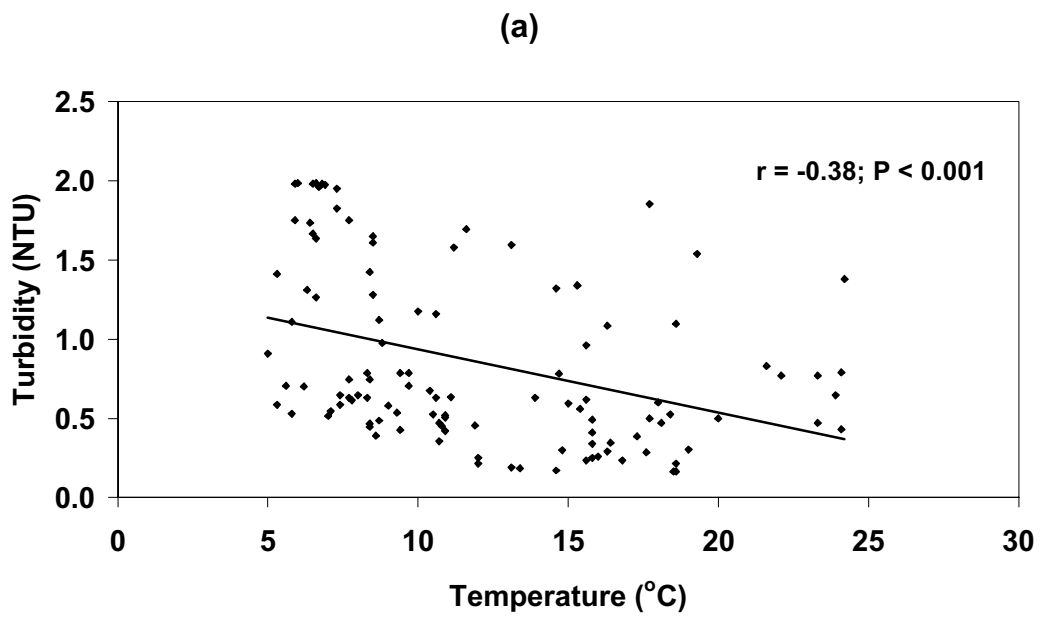


Figure 3.13 - Correlation between turbidity and temperature for (a) SSF 1 and (b) SSF 2

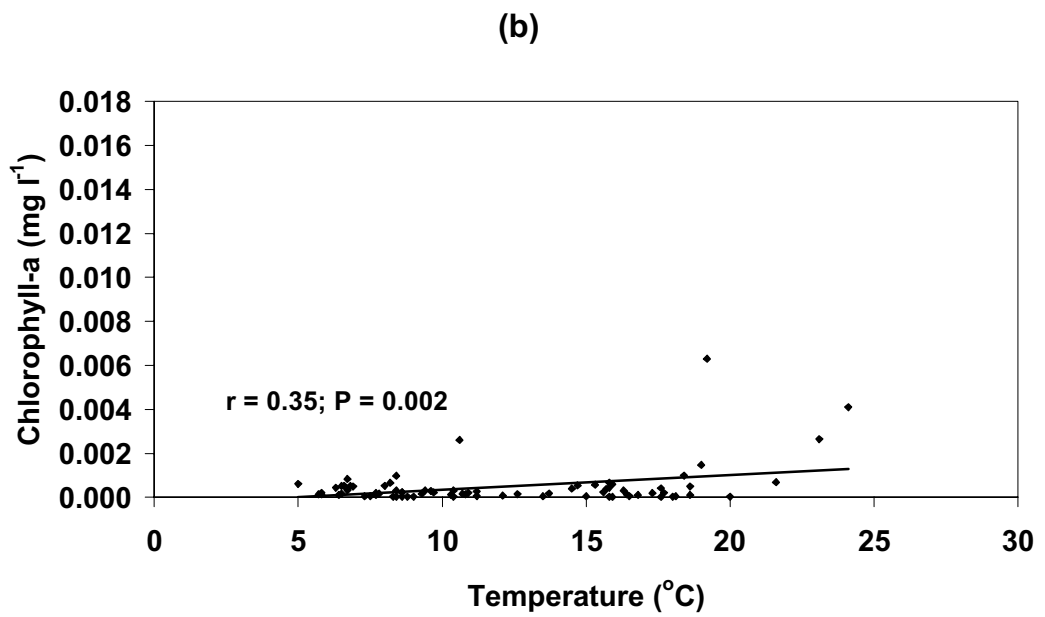
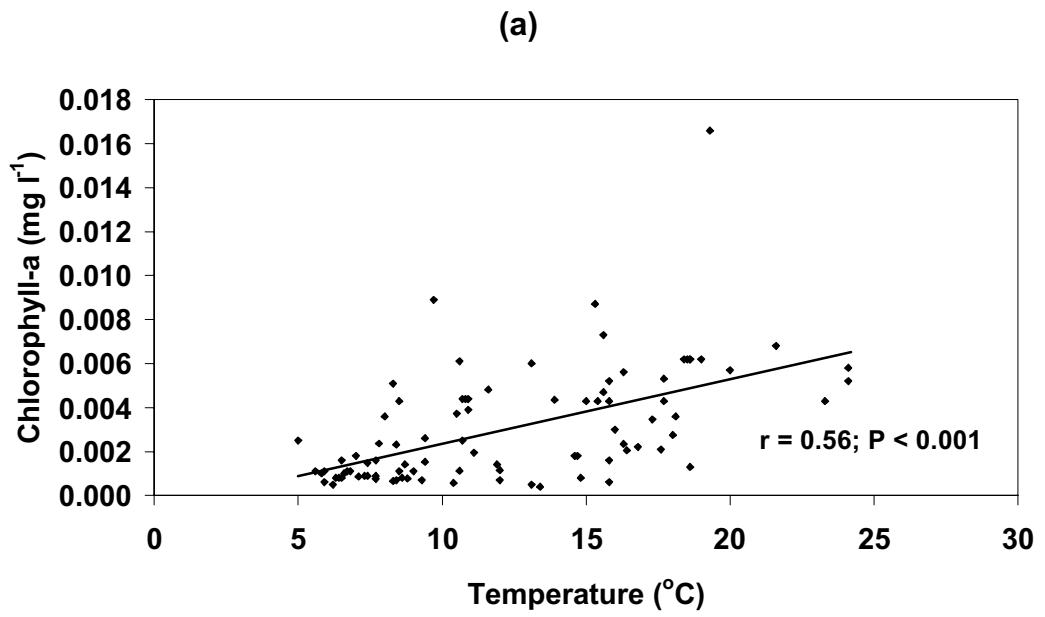


Figure 3.14 - Correlation between chlorophyll-a and temperature for
(a) SSF 1 and (b) SSF 2

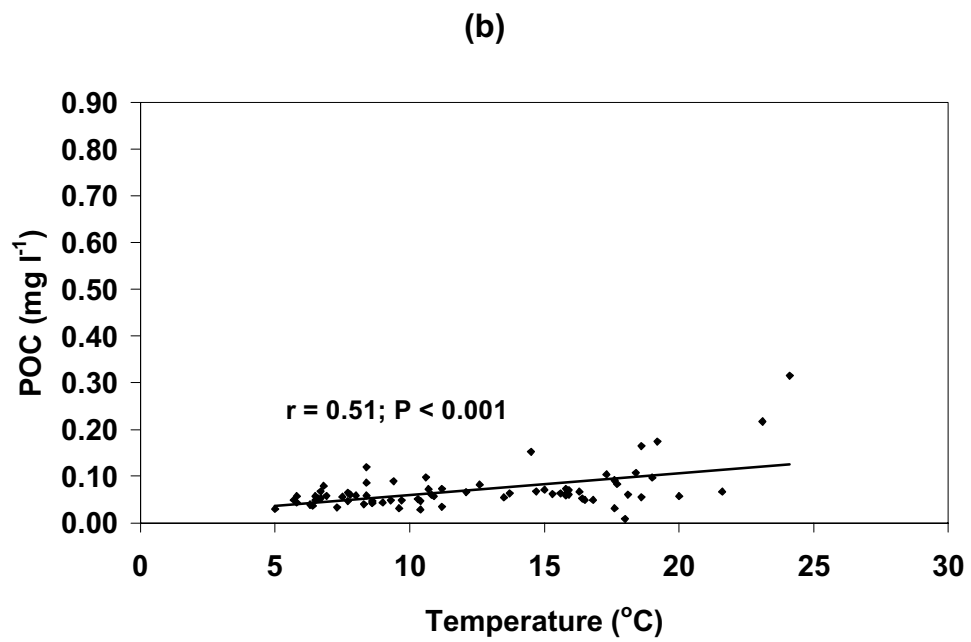
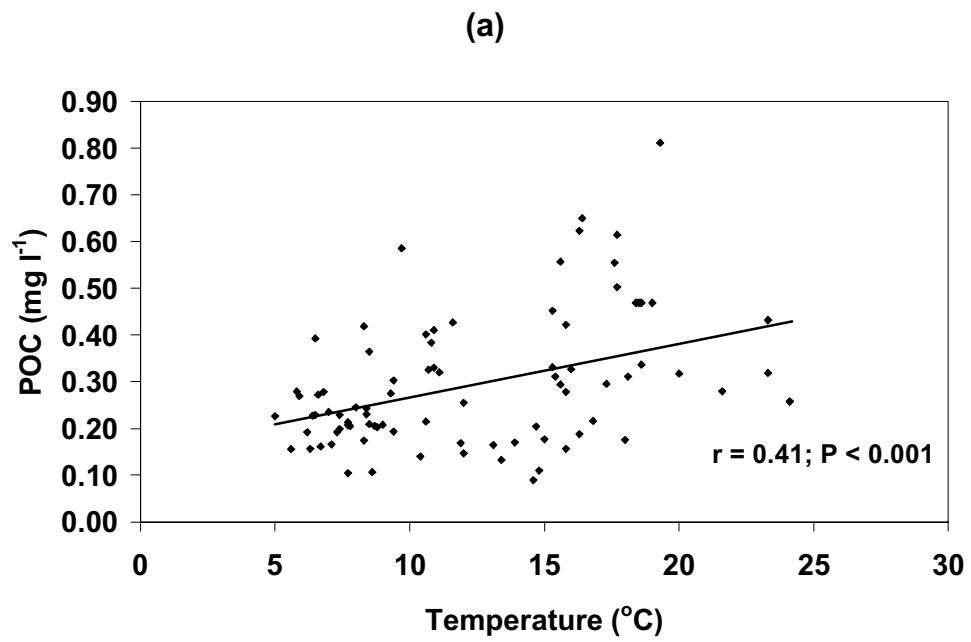


Figure 3.15 - Correlation between POC and temperature for (a) SSF 1 and (b) SSF 2

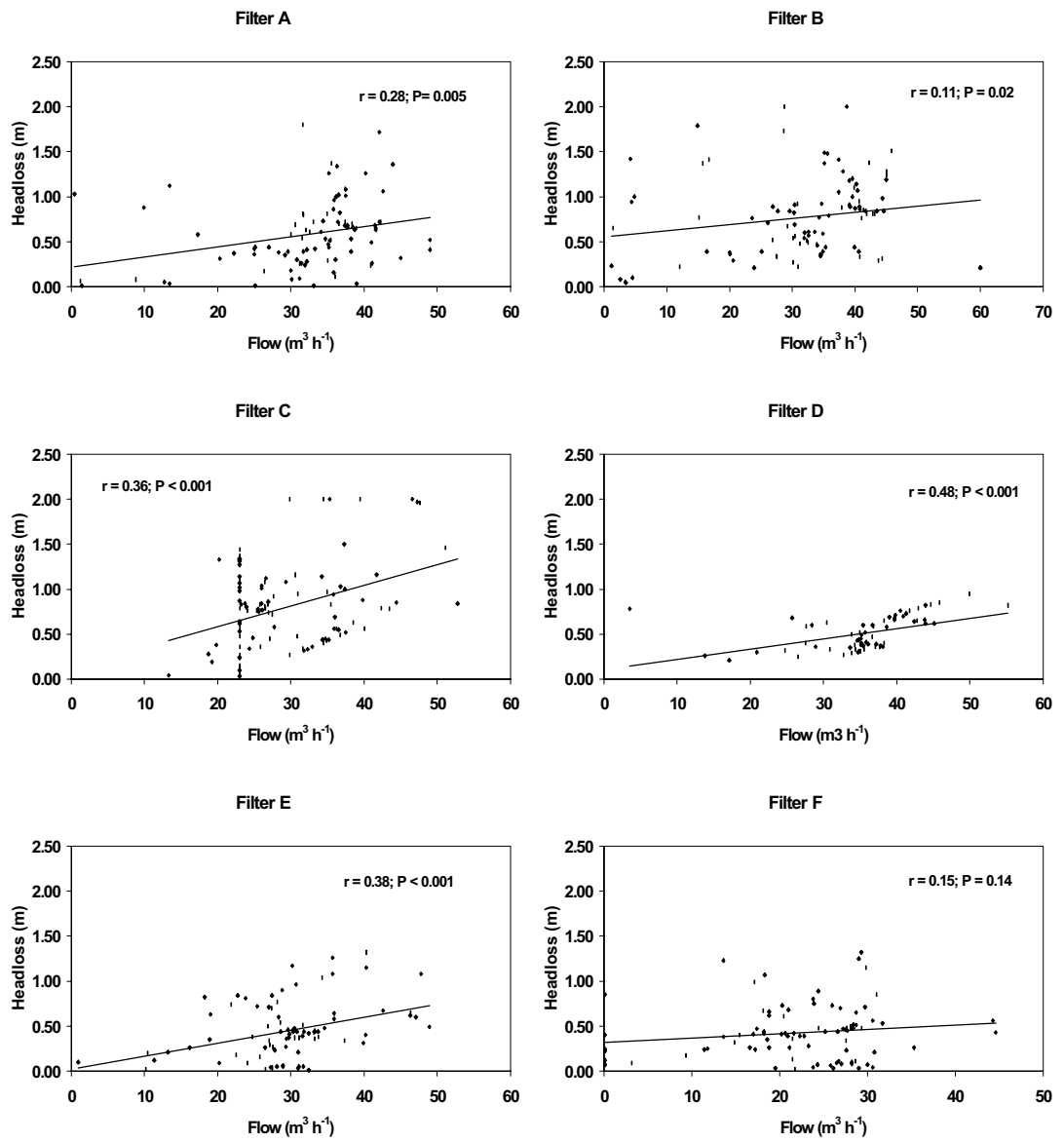


Figure 3.16 - Correlation between headloss and influent flow

The correlation between headloss and influent water temperature was negative in all filters (Figure 3.17), except SSF E and SSF F, suggesting that an increase in temperature may cause a decrease in headloss rate due to decreased viscosity and reduced flow resistance of the fluid (see Equation 2.7). However, this negative correlation between headloss and influent water temperature may be also related to the negative correlation between influent turbidity and influent water temperature (Figure 3.13). This suggests that a positive correlation between headloss and turbidity may exist.

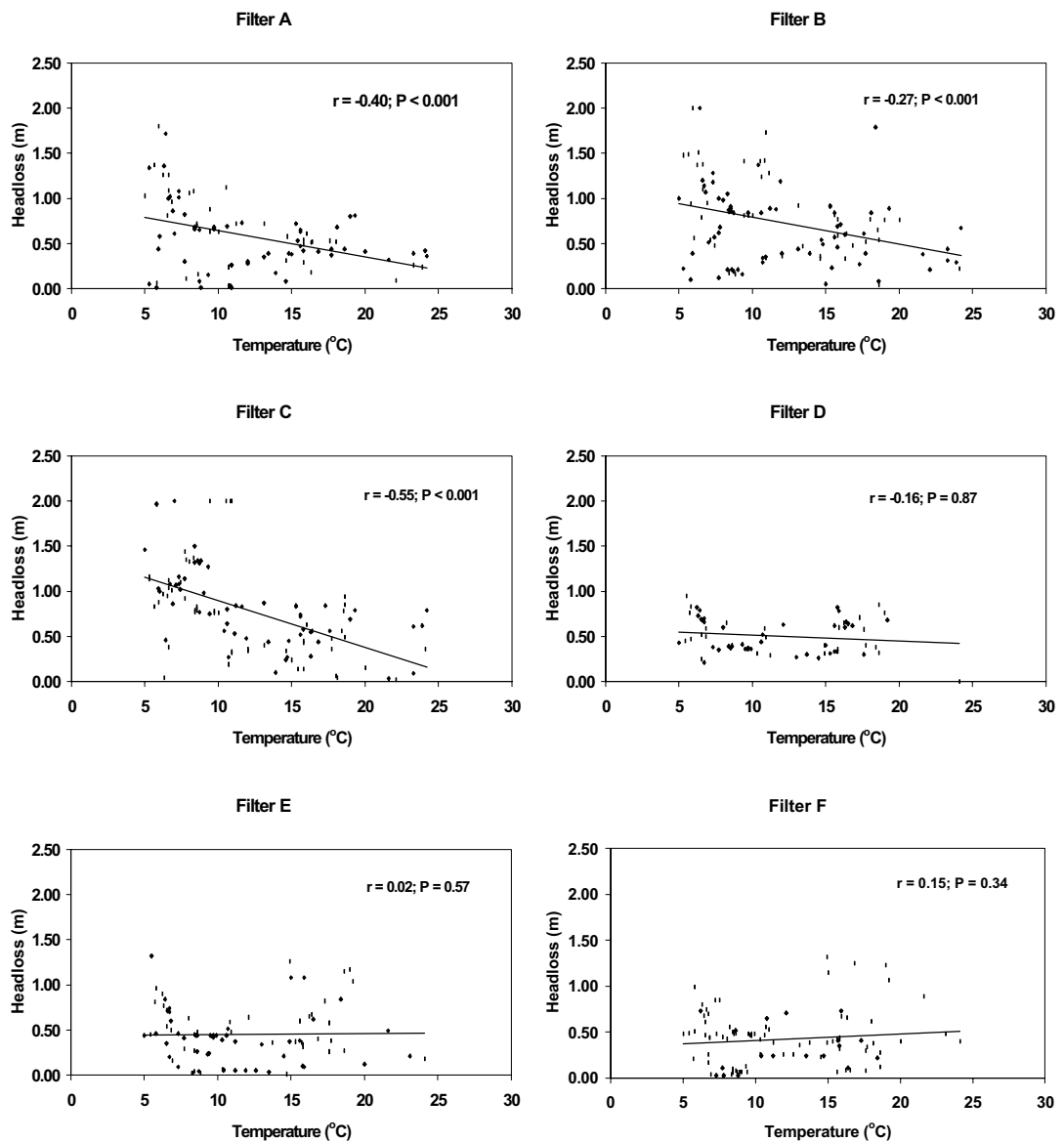


Figure 3.17 - Correlation between headloss and water temperature

Indeed, there was a positive relationship between influent turbidity and headloss (Figure 3.18), although this correlation was more significant in SSF 1 ($r = 0.44$ and $P < 0.001$ for SSF A, $r = 0.32$ and $P < 0.001$ for SSF B) than SSF 2. This indicates that headloss performance was probably affected by the influent turbidity concentration to the filters, which is emphasised by the significant removal efficiency of turbidity of approximately 87 % in SSF 1 and 35 % in SSF 2 (Table 3.5).

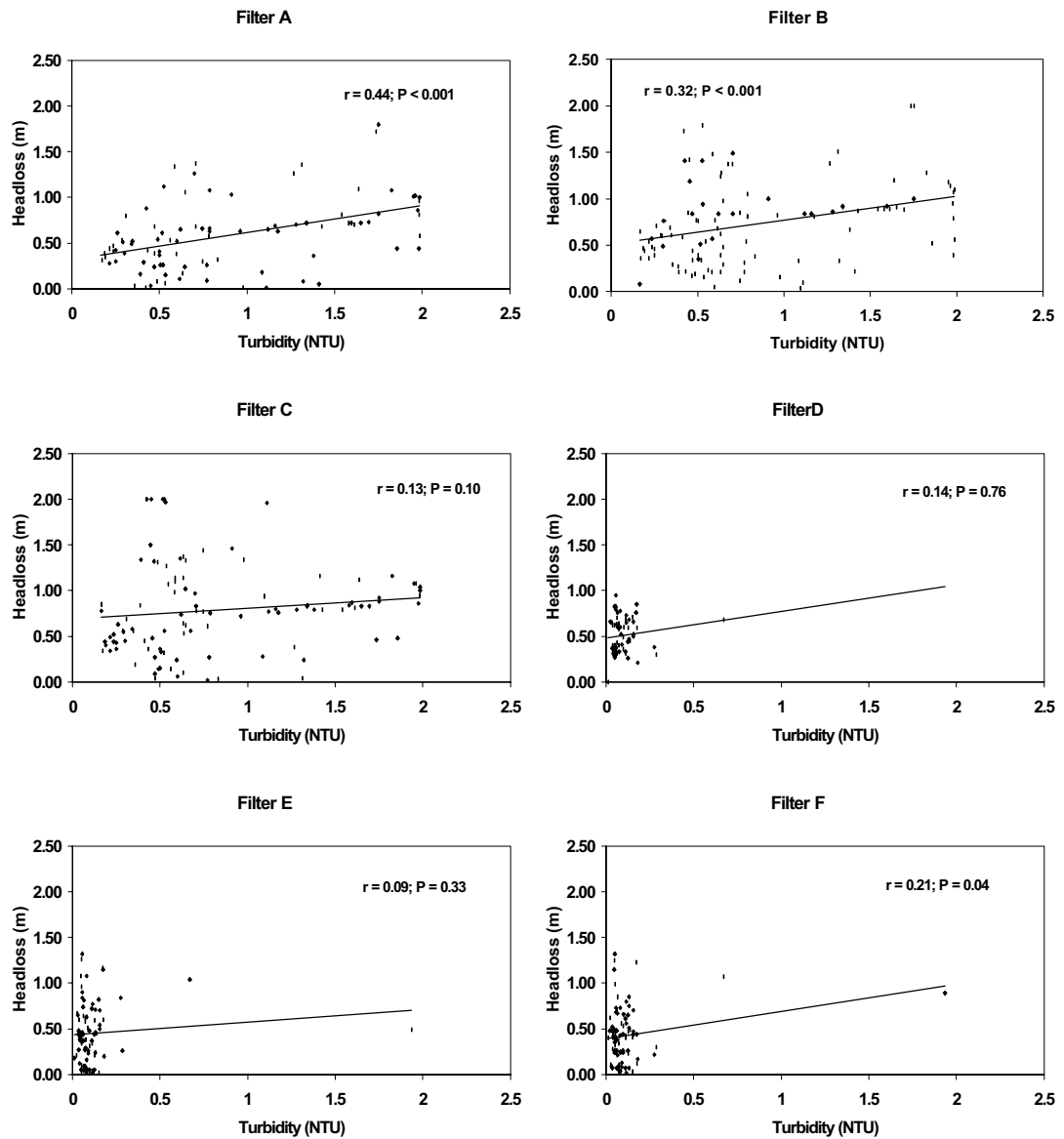


Figure 3.18 - Correlation between headloss and turbidity

The fact that there was no strong relationship between turbidity and algae, bacteria, and POC in the influent water to the filters (suggesting that inert material and non-living POC were the principal part to contribute to turbidity) indicates that headloss in slow sand filters in advanced water treatment works may be strongly related to the amount of inert and non-living POC particles present in the influent water. This may be confirmed by the weak correlation coefficients ($P > 0.01$) between headloss and influent chlorophyll-a, bacteria, TOC, and POC concentrations (Table A.2.3, Appendix A.2). Therefore, these results suggest that influent TOC and living organism concentrations may be not a major cause of headloss by blocking the filter directly.

3.5 - Data processing

For the purposes of model development, it was necessary to transform and process the raw data collected from Kempton Park into a suitable form for the SSF model input data.

3.5.1 - Headloss

The headloss models makes use of a constant flow (Sub-section 2.2.2.4) and, since headloss is proportional to flow, actual headloss was corrected to a standard flow rate to produce a normalised headloss, NHL. The normalised headloss was calculated using a standardised flow rate of 0.2 m h^{-1} by Equation 3.1 (Woodward and Ta, 1988). The normalised headloss of uncovered SSF B and covered SSF C are presented in Figures A.3.1 to A.3.2 (Appendix A.3).

$$\text{NHL} = H \frac{q_s}{q} \quad (3.1)$$

where:

q_s = standard flow rate (0.2 m h^{-1})

3.5.2 - Level of the supernatant water

The inlet channel level was assumed to be the depth of the supernatant water in the slow sand filters. This depth is important to calculate the spatial variation of light through the water column when considering algae growth in the supernatant water.

3.5.3 - Turbidity, suspended solids and inert particles

The accumulation of captured inert material and microorganisms, together with the growth of biological populations, gives rise to increasing hydraulic resistance to flow manifested as an increasing process pressure headloss (Graham *et al.* 1994). In previous works on SSF modelling (Ojha and Graham, 1994-1996ab), the concentration of inert material was assumed to be equivalent to turbidity measurements (i.e. 1 NTU = 1 mg l⁻¹). However, turbidity is not a direct measure of suspended particles in water, but a measure of the scattering effect of the particles on a light source (Sadar, 1998). In addition, turbidity is caused by the presence of suspended solids including inorganic matter such as clay, silt, calcium carbonate, silica, and organic matter such as phytoplankton and other microorganisms. Therefore, the inert material concentration can be determined from the turbidity measurements transformed to suspended solids. For this, a correlation between turbidity and suspended solids was determined and the percentage of inert material contributing to the total amount of suspended solids estimated.

Determinations of the correlation of turbidity with the gravimetric concentration of kaolin suspensions (mg l⁻¹) have been reported previously (Graham, 1982, Demby, 1988, Mbvette, 1989). Contrary to the experimental findings of Demby (1988) but in reasonable agreement with Graham (1982), Mbvette (1989) found that 1 NTU corresponded to approximately 1.6 mg l⁻¹ for particles ranging from 1 to 160 µm. The suspended solids concentration found in treated wastewater has also been correlated to turbidity measurements. A typical relationship (Metcalf and Eddy, 1991) for the effluent from an activated sludge process between suspended solids and turbidity is 1:2.35 (suspended solids:turbidity). In the case of treated effluent, the particles fell into two distinct size ranges, small particles varying in diameter from 1 to 15 µm and large particles varying in size from 50 to 150 µm. These results suggest that there is always a significant correlation between turbidity and suspended solids, but the relationship varies between water sources and the characteristics of the suspended solids in these waters. For this reason, the correlation between turbidity and suspended solids was experimentally determined specifically for influent water to slow sand filters in advanced water treatment. This experiment was carried out at the Walton AWT works and is described later in Chapter 4.

The percentage of inert material contributing to the total amount of suspended solids was estimated based on experimental data of Mbwette (1989) who determined the variation of POC and silt contents in the filter beds at the Ashford Common pilot plant from Thames Water. Table 3.7 shows the profile sand sample analysis for POC and silt content taken at the end of the filter runs.

Table 3.7 - SSF sand profile POC and silt content at the end of filter runs at Ashford Common (adapted from Mbwette, 1989)

	Run	Depth (cm)			
		0-25	25-50	50-75	75-100
POC mg C cm ⁻³ sand	1	1.82	0.29	0.18	0.13
Silt µg cm ⁻³ sand	1	21.94	2.94	1.67	1.16
POC mg C cm ⁻³ sand	2	4.88	0.82	0.4	0.28
Silt µg cm ⁻³ sand	2	40.92	6.13	2.31	1.58

Assuming that the total suspended solids was equivalent to the POC plus silt content, and that carbon was 50 % of the dry weight, the amount of suspended solids was determined for each filtration run (Tables 3.8 and 3.9). The amount of silt was mainly located in the top 25 cm of the sand and decreased with sand depth. The percentage of silt in relation to suspended solids in the top 25 cm of sand was 0.51 % and 0.35 % for Run 1 and Run 2, respectively. On average the silt content in the top 25 cm of sand was 0.43 % of the suspended solids. Since this percentage was equivalent only to the amount of silt in relation to suspended solids within the sand bed, it was assumed that 2 % of the influent suspended solid concentrations was inert material. This percentage was then used to determine the amount of inert particles present in the influent water to the slow sand filters at the Kempton Park AWT pilot plant.

3.5.4 - Bacteria

The bacteria data provided by Thames Water were reported in terms of cell counts (Sub-section 3.3.6), and a conversion of these into mass concentration was necessary for the SSF model. The bacterial counts were transformed to bacteria concentration using a conversion factor of 0.0311 pg C per cell as suggested by Duncan (1988).

Table 3.8 - Percentage of silt in relation to suspended solids at Run1 (Ashford Common)

	Depth (cm)			
	0-25	25-50	50-75	75-100
POC mg cm ⁻³ sand	3.640	0.580	0.360	0.260
Silt µg cm ⁻³ sand	0.022	0.003	0.002	0.001
Suspended solids	3.662	0.583	0.362	0.261
% Silt	0.60	0.51	0.55	0.38

Table 3.9 - Percentage of silt in relation to suspended solids at Run 2 (Ashford Common)

	Depth (cm)			
	0-25	25-50	50-75	75-100
POC mg cm ⁻³ sand	9.760	1.640	0.800	0.560
Silt µg cm ⁻³ sand	0.041	0.006	0.002	0.002
Suspended solids	9.801	1.646	0.802	0.562
% Silt	0.42	0.36	0.25	0.36

3.5.5 - Dissolved organic carbon and non-living POC

Dissolved organic carbon (DOC) and non-living POC concentrations were not provided by Thames Water and their concentrations are required by the SSF model. Thus, relationships were derived from other water quality parameters to obtain the concentrations of DOC and non-living POC.

Total organic carbon can be fractionated to provide DOC and POC based on the fractions that pass through, and are retained by a 0.45 µm pore diameter filter (APHA *et al.*, 1995). Therefore, the DOC concentration was assumed to be the difference between TOC and POC concentrations.

The amount of non-living POC was determined based on the concentration of living organisms present in the POC content. The contribution of living organisms towards POC content was estimated based on bacterial and algal carbon concentrations

(Figure 3.19). Algae concentration was converted from chlorophyll-a to carbon using a stoichiometric factor of 25 mg C mg⁻¹ Chla (Chapra, 1997).

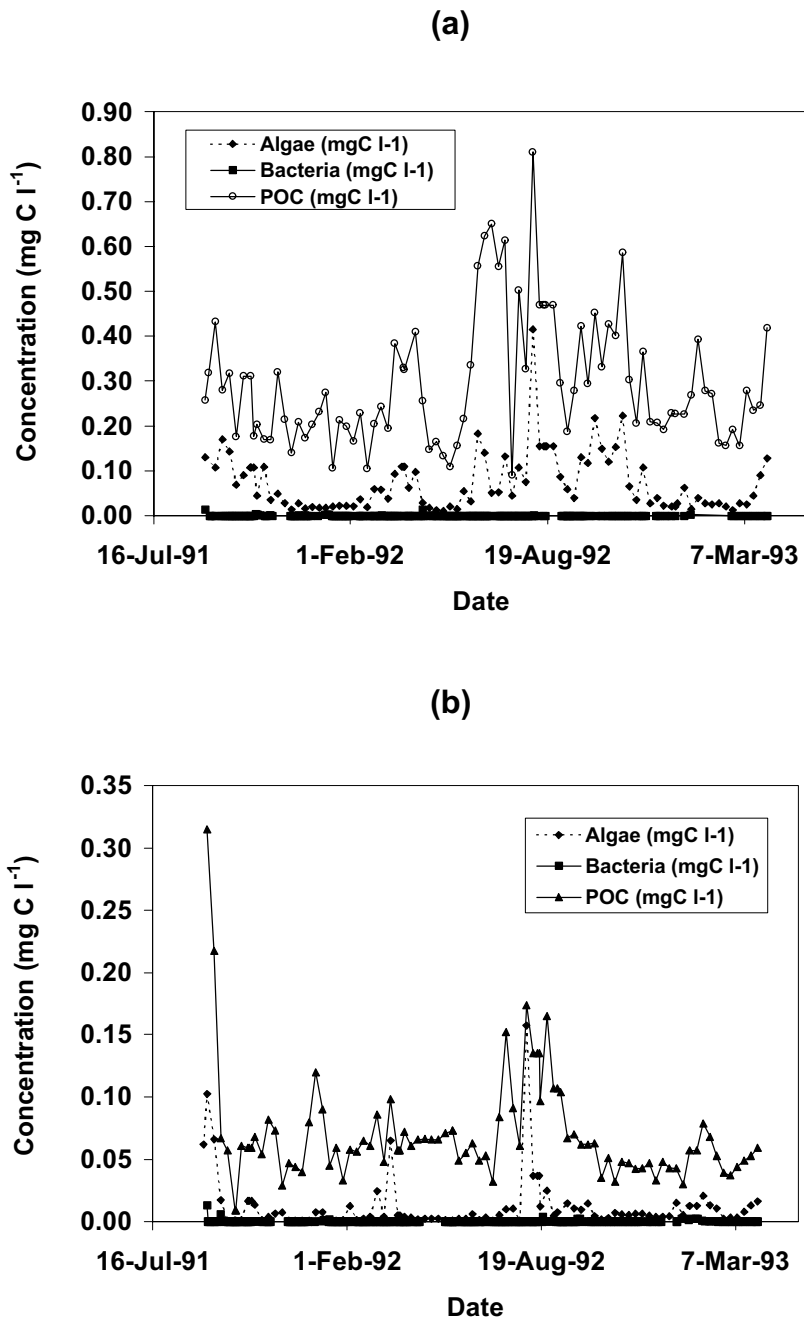


Figure 3.19 - Influent algae, bacteria, and POC at (a) SSF 1 and (b) SSF 2

As expected, POC was the largest amount of particulate matter present in both influent of the SSF 1 and SSF 2 (Figure 3.19). Chlorophyll-a concentration was lower than POC followed by bacteria. Bacteria contribution to POC concentration was almost negligible

compared with chlorophyll-a concentration, emphasising that POC may be composed mainly of algae (see Figure 3.11). Thus, the non-living POC concentration was assumed to be the difference between POC and algae content.

3.5.6 - Nitrogen and phosphorus

The concentration of nitrogen was reported as nitrate (NO_3^-), ammonia (NH_3), and phosphorus as orthophosphates (PO_4^{3-}), and the soluble amount of these nutrients for the SSF model was determined using stoichiometric factors (Table 3.10).

Table 3.10 - Conversion factors

Multiply	by	to get
NH_3	0.777	$\text{NH}_4\text{-N}$
NO_3^-	0.226	$\text{NO}_3^- \text{-N}$
PO_4^{3-}	0.3261	$\text{PO}_4^{3-} \text{-P}$

Nitrate concentration from July 1991 to July 1993 was not provided and no differences were observed between influent and effluent nitrate concentrations during 1993 and 1998 (Figure 3.8). Thus, a constant concentration equal to 5.79 mg l^{-1} was assumed for the whole period of 1991-1993, based on the average value measured in 1993.

3.5.7 - Protozoa

Protozoa counts were not provided by Thames Water and had to be determined for the SSF modelling. Protozoa concentration was determined based on the work of Galal (1989) who showed that the bacteria biomass predominated in the slow sand filters at the Ashford Common works, followed by algae and protozoa. In the uncovered filter, the ratios of bacteria:algae:protozoa varied from 1:1.4:0.1 at the beginning of the filtration run to 1:16:0.2 later in the run. Comparable ratios for the covered filter were 1:0.6:0.1 which were similar to the ratios initially observed for the uncovered filter. Thus, protozoa biomass varies from 10 to 20 % of the bacteria biomass. Assuming that influent protozoa concentration was 15 % of the influent bacteria concentration, a range from 5.8×10^{-11} to $2.8 \times 10^{-5} \text{ mg C l}^{-1}$ was determined for protozoa.

3.5.8 - Depth of the sand beds

Knowledge of the depth of the sand bed at the starting up of each filtration run (Table 3.6) can be used to determine the sand depth scraped off during filter cleaning, and allows that consecutive filtration runs be simulated. Table 3.11 shows the sand depth removed during each filter cleaning based on the difference between filter depths given in Table 3.6.

Table 3.11 - Sand depth removed during filter cleaning at Kempton Park

Filter	Cleaning period and depth removed (cm)	
	Run 1 – Run 2	Run 2 – Run 3
SSF A	4.0	3.0
SSF B	5.0	6.0
SSF C	7.0	4.0
SSF D	6.0	NP
SSF E	10	4.0
SSF F	1.0	7.0

NP: Not Provided

The sand depth removed at each filter cleaning was larger than the amount generally recommended in the literature, which is usually nearer to 2-3 cm (Sub-section 2.2.1). For example, for SSF E, 10 cm of sand was removed between Run 1 and Run 2. Nevertheless the actual sand depths and removals were considered to be realistic of operational practice at Kempton Park.

3.5.9 - Missing data, erroneous values and unequal spacing values

Missing values, unequal spacing and erroneous values were present inevitably in the data series provided by Thames Water, and a number of approaches were followed to overcome these limitations. However, it is emphasised that the Thames Water data were amongst the most comprehensive available for modelling the physico-chemical and biological dynamics of SSF.

A probabilistic approach to identify missing values was attempted using ARIMA⁸ model. However, the use of this autoregressive process was not successful because of the extent of the missing data, particularly during the first filtration run (52 days). Therefore, a pragmatic approach to managing missing data was adopted by replacing missing values with the mean result from the available observed data.

For the input data (water quality parameters), this initial period of missing data was replaced by the mean value from the following month when a more or less complete set of data was collected. Other intermittent missing values were interpolated since the amount of missing data was comparatively small. In the case of the headloss data, the initial 52 days and intermittent missing values could be ignored during model calibration because the error between the calculated and observed headloss was only determined using collected data records.

Unequal spacing values (i.e. time period between measurements) were also ignored when comparing observed and calculated headloss during model calibration. However, for the influent water quality parameters, the intermittent unequal spacing values were interpolated.

3.6 - Summary

The main aspects related to the amount and quality of the Thames Water data are summarised as follows:

- (1) A considerable amount of data was provided by Thames Water which was part of an extensive investigation in the Kempton Park AWT pilot plant from July 1991 to July 1993 (Sections 3.1 and 3.2).
- (2) Detailed information was collected describing the influent and effluent water quality from the slow sand filters. The data included physico-chemical and microbiological water quality parameters, headloss, flow, inlet channel level, and depth of the sand beds. These data are potentially amenable to SSF model

⁸ Autoregressive Integrated Moving Average (ARIMA) is a probability process for time series (Chatfield, 1989).

development and offer an unprecedented opportunity for model calibration and verification.

- (3) The aim of the Thames Water investigation was not set out to develop a computer model, but to determine the optimum ozone/biological filtration process conditions for the removal of pesticides, reduction of chlorine demand and minimisation of chlorination by-products such as trihalomethanes (Rachwal *et al.*, 1993).
- (4) From the data set, three filtration runs were selected for model calibration and verification (Table 3.4) since it was the aim of this thesis to evaluate the performance of the model using successive filtration runs.
- (5) The data was subject to errors and missing values due to variations in sampling regimes and the recording apparatus. Approximately 52 days of data were missing at the beginning of the monitoring period. In addition, intermittent missing values were also observed (Section 3.3). Despite all these problems, the Thames Water data were the best and most complete that could be found anywhere for the SSF model development.
- (6) Nitrate data were not available from July 1991 to July 1993, but were measured in the raw water and effluents from Aug/1993 (Sub-sections 3.3.9). In addition, protozoa counts were not provided by Thames Water (Sub-section 3.5.7).
- (7) Although the Thames Water data set was comprehensive, it did not include schmutzdecke and sand biomass. These data would be essential to development of the model and understanding the complex interactions between biological component and filter performance. Therefore, it was necessary to collect additional information in biomass growth at the Walton AWT works, as described later in Chapter 4.

The analysis of water quality data and headloss information from Kempton Park showed that:

- (1) The influent water quality to SSF 1 in terms of particulates and TOC was larger than that to SSF 2 and this suggested that the GAC pretreatment located in SSF 2 was effective at removing biodegradable organic matter (Klevens *et al.* 1996; Graham, 1999). In contrast, the treatment efficiency for removal of turbidity,

chlorophyll-a, POC, and TOC was, generally, more significant in SSF 1 than in SSF 2. This suggested that the ozonation pretreatment increased the NDOC content increasing efficiency of organic matter removal in SSF 1 (Malley *et al.*, 1994; Yordanov *et al.*, 1996).

- (2) A very strong relationship was observed between influent POC and chlorophyll-a concentrations of both streams (Figure 3.11), suggesting that algae may be the principal part of POC content in the influent water to the slow sand filters at Kempton Park.
- (3) A strong correlation was found between headloss and influent flow confirming that headloss was directly proportional to flow (Sub-section 3.3.3).
- (4) Significant negative correlations were observed between both headloss and water temperature and influent turbidity and water temperature. This was shown to be due to the positive correlation between headloss and turbidity, which was emphasised by the significant removal efficiency of turbidity in both streams.
- (5) The fact that there was no strong relationships between turbidity and algae, bacteria, and POC in the influent water to the filters suggested that headloss in slow sand filters in advanced water treatment works may be strongly related to the amount of inert and non-living POC particles present in the influent water. This may be confirmed by the weak correlation between headloss and influent chlorophyll-a, bacteria, TOC and POC concentrations, indicating that influent TOC and living organism concentrations may be not a major cause of headloss by blocking the filter directly.

The Thames Water data were not amenable to be used directly for simulation input data. The data were transformed and manipulated into a form that was suitable for application in the SSF model as summarised here:

- (1) Actual headloss values were corrected to a standard flow rate to produce a normalised headloss (Sub-section 3.5.1).
- (2) Turbidity measurements were used to determine the amount of inert material in the influent water. For this, a correlation between turbidity and suspended solids was experimentally determined at the Walton AWT works, as described later in Chapter

4. The concentration of inert material present in the influent was assumed to be 2 % of the suspended solids (Sub-section 3.5.3).
- (3) Dissolved organic carbon concentration was calculated as the difference between TOC and POC concentrations, while non-living POC was assumed to be POC minus algae concentration (Sub-section 3.5.5).
- (4) Bacteria counts were converted to a concentration value using a factor of 0.0311 pg C per cell (Sub-section 3.5.4) and protozoa concentration was assumed to be 15 % of the bacteria concentration varying from 5.8×10^{-11} to 2.8×10^{-5} mg C l⁻¹ (Sub-section 3.5.7).
- (5) Concentrations of ammonia, nitrate, and phosphates were converted into ammonium-nitrogen (NH₄ – N), nitrate-nitrogen (NO₃⁻ – N) and soluble phosphorus (PO₄⁻³ – P), using conversion factors of 0.777, 0.226 and 0.3261, respectively (Table 3.10). Nitrate concentration was assumed to be constant and equal to 5.79 mg l⁻¹ based on the average value of the year 1993.
- (6) The sand depth removed during filter cleaning was estimated based on the depth of the filter beds provided by Thames Water (Sub-section 3.5.8).
- (7) Missing values at the beginning of the first filtration runs were replaced by the mean water quality data from the following month. Intermittent missing values were interpolated (Sub-section 3.5.9). Missing headloss data were ignored during calibration of the model because the error between calculated and observed headloss was only estimated using collected data records (Sub-section 3.5.9).

4 - BIOMASS DEVELOPMENT IN SLOW SAND FILTERS

4.1 - Introduction

Microbial biomass in the schmutzdecke and filter sand bed has been quantified using a range of different microbiological methods (Duncan, 1988; Nakamoto, 1993; Yordanov *et al.*, 1996). In some cases the sand biomass is determined indirectly by plate counts and numerical conversions (Duncan, 1988). The different approaches used to measure biomass concentrations and the inconsistent units and sampling intervals adopted (e.g. Bellinger, 1979; Yordanov *et al.*, 1996) confound inter-study comparisons of biomass development and behaviour during SSF. Most reports are of single measurements of the net biomass production at the end of a filter run, prior to cleaning, and these emphasise the significant variability apparent in schmutzdecke and sand biomass accumulation in operational slow sand filters (Bellinger, 1979; Yordanov *et al.*, 1996).

The collection of representative samples of schmutzdecke and sand material during filter operation is difficult in practice, and the lack of a simple routine method for measuring microbial biomass are probable reasons for the limited amount of field-scale investigation of the biological mechanisms of SSF. Detailed analyses of biomass growth in the schmutzdecke and within the sand bed during filter operation would improve understanding of the complex and fundamental interactions between the biological and physico-chemical processes operating in slow sand filter systems. This information would enable the development of mechanistic models of SSF systems which may improve the operational management of slow sand filters through the prediction of head loss rate, and the frequency of sand cleaning and renewal.

This chapter describes the temporal and spatial dynamics of schmutzdecke and sand biomass development in full-scale slow sand filter beds at the Walton AWT works, operated by Thames Water, in the UK. This experimental investigation formed an integral part of model development, providing data related to sand biomass growth with respect to time and depth, as well as information for the assumptions and simplifications of the SSF model. In addition, a correlation between turbidity and suspended solids in the influent water to the slow sand filters at Walton was determined to convert turbidity values of the Kempton Park AWT pilot plant data into mass concentration.

4.2 - Materials and methods

In this thesis, schmutzdecke layer is defined as the green algal mat formed on the top of the sand bed of the uncovered filter. The term ‘schmutzdecke biomass’ refers to the oven dry weight of the algal mat per unit area of sand bed, and includes all living organisms present in the slime layer. ‘Sand biomass’ is defined as the total microbial biomass concentration in the sand for both the uncovered and covered filters measured by a modified chloroform fumigation-extraction technique (Wu *et al.*, 1990; ISO, 1997).

The fieldwork period was carried out in two phases. In Phase I, during the period 23rd May to 22nd August 2000, microbial and schmutzdecke biomass were determined from two full-scale slow sand filters, operated with and without a light excluding cover. The experimental procedure was jointly developed with a M.Sc. project on biological investigation of slow sand filters (Su, 2000). In Phase II, samples of schmutzdecke at the end of the run were collected from four uncovered beds. This work was carried out from November 2000 to June 2001 with the purpose of obtaining the algal biomass of the schmutzdecke at the end of the run. The structure of the schmutzdecke was observed by electronic microscope. Furthermore, samples of supernatant water were collected and a correlation between turbidity and suspended solids was established.

4.2.1 - Description of the Walton AWT works

Walton is an advanced water treatment facility that receives raw water from the river Thames via large-scale storage reservoirs. The reservoir water is treated sequentially by pre-ozonation, dissolved-air flotation, rapid filtration, intermediate ozonation, and granular activated carbon (GAC) prior to SSF (Figure 4.1). The works treats between $90 \times 10^3 \text{ m}^3$ to $137 \times 10^3 \text{ m}^3$ of water per day and there are 9 slow sand filter beds in operation, each with an approximate area of 3500 m^2 .

All the slow sand filter beds at the Walton AWT plant are dimensionally identical and receive water from the same pre-treatment process. The Walton AWT plant has a similar treatment to the SSF 2 at Kempton Park (Figure 3.1). Table 4.1 describes the characteristics of the filter beds.

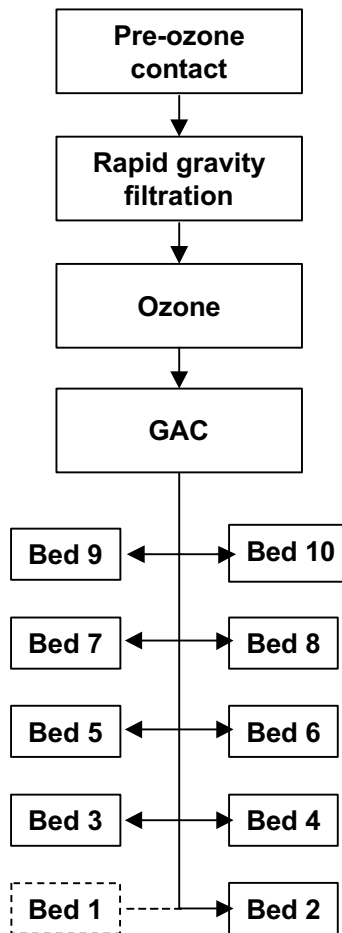


Figure 4.1 - Schematic representation of the Walton AWT works.
Bed 1 is not operated and Bed 10 is covered

Table 4.1 - Characteristics of the filter beds at the Walton AWT works

Parameter characteristics (average per filter)	
Filter bed area:	3500 m ²
Filtration rate:	0.15 m h ⁻¹
Sand depth:	0.80 m
Effective size of sand:	0.30 mm
Supernatant water:	1.5 m

Eight out of nine filter beds were uncovered permitting full light penetration to the filter, representing normal operational practice, while Bed 10 had a flexible plastic cover installed, supported by positive air pressure, to exclude light as part of a wider investigation (Figure 2.3). However, the wind blew the cover of Bed 10 away in

October 2001. As a result, Bed 10 operated for about six months as a covered filter and two months as an uncovered filter before cleaning. In Phase I of the fieldwork, Bed 10 was in a covered state throughout the period of monitoring.

4.2.2 - Determination of sand biomass

During Phase I of the fieldwork, sand and schmutzdecke samples were collected from Bed 9 (uncovered) and Bed 10 (covered). Filter Bed 10 was completely renewed with clean sand before the experimental period commenced and came into operation on the 11th May 2000. The sand surface of Bed 9 was skimmed following routine cleaning and water filtration began on 17th May 2000. Water temperature was measured during the experimental period and increased from initial values of 12 - 13 °C in May 2000 to a maximum range of 18 - 19 °C recorded after 100 days in August (Figure 4.2). Table 4.2 describes the sampling date and duration of the filtration run in the first sampling phase.

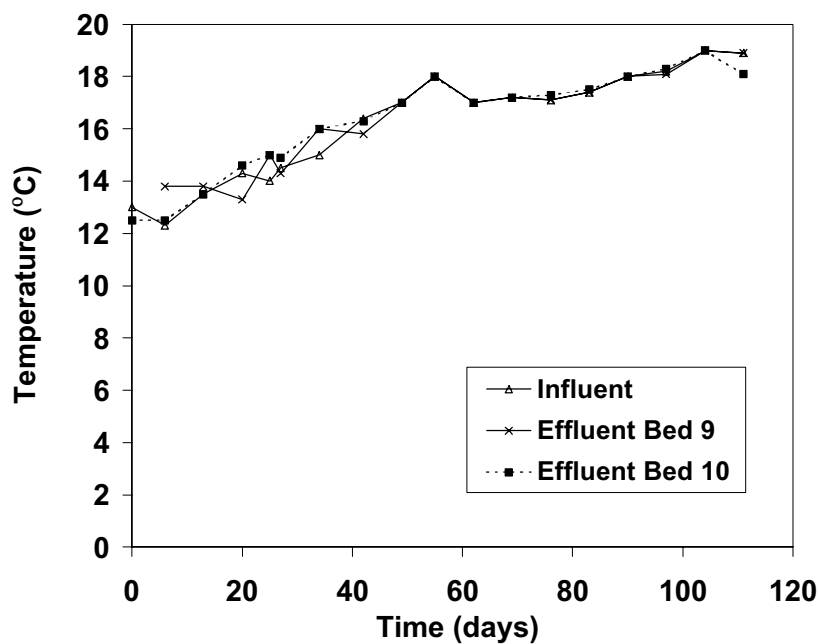


Figure 4.2 - Variation of water temperature with time during the experimental period at Walton (Phase I)

4.2.2.1 -Sampling device and technique

Sand cores were collected using a small boat, whilst the filters were operating at intervals of approximately two weeks during the monitored period. Samples were

collected using a specialised coring device developed by the Department of Geology, University College London (Wotton, 2000). The sampling device consisted of a plastic tube (75 mm in diameter and a length of approximately 2000 mm), two pistons and a rope attached to a metal karabiner (a coupling link) at one end. The main advantages of this sampler are: simple construction, capability to take undisturbed in-situ sand samples during filter operation, flexibility in the number of the sand cores taken and it also served the purpose of minimal interference with the operational functioning of the filter beds (Plate 4.1).

Table 4.2 - Sampling date and filtration run length during Phase I

	Bed 9 (uncovered)	Bed 10 (covered)
Run start date	17/05/2000	11/05/2000
Run end date	28/08/2000	(*)
Duration of the run (days)	104	103

(*) run continued beyond first study phase



Plate 4.1 - Sampling device used during the experimental period

The filter beds were divided into 140 sampling units with an approximate area of 5 m x 5 m (Figure A.4.1, Appendix A.4). There were 44 eye-bolts located at approximately 5 m apart on the internal wall of the filter beds. A rope marked with 9 points, representing the filter width, was tightly strung across the filter bed to represent the correct position of the boat and also to help stabilise the boat while samples were taken. Three replicate cores of sand were sampled to a depth of 10 cm from randomly selected locations on each sampling event.

Two people were required to be on the boat. Whilst one person stabilised the boat by holding firmly to the rope strung across the bed, the other was sampling. Before the core was placed vertically on the sand surface and pushed into the sand to approximately 15 cm depth, the sampler was filled with little supernatant water from the filter bed to help the core sink better in the sand bed. The core sampler was pulled up as quickly as possible and the second piston fixed to the bottom end of the tube to stop the sand from falling out.

The sand column was pushed up the corer and, after scraping off the schmutzdecke, undisturbed sand cores were divided into five uniform segments of 2 cm, using a ring of 2 cm depth and a slicer to cut the sand at the required thickness. The sub-samples from each section of the profile from 0-10 cm in 2 cm depth increments were pooled and thoroughly mixed to provide a representative composite for the determination of microbial biomass concentration in the sand. The pooled profile sections were transferred to plastic sample bags and both sand and schmutzdecke materials were transported to the laboratory in a cool box.

The validity of pooling replicate sections of sand profiles was examined using a t-test statistic to compare the sand biomass content of a pooled sample with three independent measurements of the biomass concentration in individual cores collected on 25th July 2000 (day 69) at the same random locations on the filter bed. The t value was not statistically significant ($P > 0.05$) indicating that the sand biomass measured in the composite sample was representative of the mean concentration measured from the analysis of individual replicate samples of sand (Figure A.4.2, Appendix A.4).

4.2.2.2 -Analytical methods

Dry matter and water content

The dry matter and water contents of the field sand samples were determined by the gravimetric method as described by ISO (1994) in which sub-samples of 10 g of field moist sand are dried in an oven maintained at 105 °C for 24 h. The difference in mass of an amount of sand before and after the drying procedure is used to calculate the dry matter and water contents on a mass basis.

Sand moisture adjustment

Sand was collected from the filter beds in a water-saturated condition and this can interfere with the efficiency of chloroform fumigation (Jenkinson and Powlson, 1976). Therefore, the moisture content of the sand was reduced to 40 - 50 % of its water holding capacity (WHC) to aid chloroform penetration by absorption into laboratory filter paper. Water-saturated sand (100 g) was uniformly distributed on to double layers of 11 µm pore size, cellulose fibre filter paper (14 x 14 cm) and moisture from the sample was absorbed by the paper for a period of 10 minutes. This procedure was repeated with fresh filter paper and the WHC and gravimetric moisture content of the dewatered sand were determined at each step (Harding and Ross, 1964). The moisture content of water-adjusted sand used for chloroform fumigation was reduced on average to 48 % of the WHC.

Chloroform fumigation extraction

A chloroform fumigation-extraction technique was adapted from a standard method for microbial biomass determination in soil (Wu *et al.*, 1990; ISO, 1997) to quantify biomass concentration in the sand from slow sand filters.

Sub-samples of sand (25 g fresh weight) of the WHC adjusted sand were transferred into four 100 ml glass bottles with plastic screw caps. A small beaker containing 30 ml of ethanol-free, amylene-stabilised chloroform (Rathburns) with 3-4 anti-bumping granules was placed in the base of a large capacity desiccator vessel fitted with a vacuum tap and lined with moist absorbent paper to prevent sample desiccation. Two of the bottles from the set of four, for each composite sample, were placed on a supporting

plate in the desiccator and up to 10 duplicate bottles could be simultaneously fumigated by this method. A high vacuum was applied to the desiccator for approximately 5 minutes until the chloroform had begun to boil. The desiccator was isolated from the vacuum after closing the gas-tight valve and incubated at room temperature in the dark for 24 hours. The vacuum was released to remove the chloroform and lining material, and the desiccator was cleaned and dried with absorbent laboratory paper. The sample bottles were replaced and the desiccator was evacuated under high vacuum for 3 minutes and ventilated. This procedure was repeated six times to remove residual chloroform from the samples. The unfumigated bottles were stored in the dark at 4 °C or were extracted immediately for the determination of TOC content.

Fumigated and unfumigated samples were extracted for 30 minutes in the sealed glass bottles with 50 ml of 0.5 M potassium sulphate solution using a laboratory shaker set at 200 revolutions min⁻¹. The sand extracts were filtered through GF/C filter paper (150 mm diameter, 1.2 µm pore size) and the TOC concentration in filtrate extracts of fumigated and unfumigated samples was measured using a Dohrmann DC80 automatic carbon analyser. The mean TOC concentration determined in the extracts of the unfumigated samples was subtracted from the mean result obtained for the fumigated sand to estimate the extractable OC fraction released from the lysis of microbial cells by chloroform fumigation. This value was converted to biomass carbon using a multiplication factor of 2.22, following the approach recommended by Wu *et al.* (1990).

4.2.3 - Schmutzdecke biomass determination

4.2.3.1 -Sampling program and technique

During Phase I of the fieldwork, the schmutzdecke and supernatant water were separated from the sand cores collected from Bed 9 and the samples placed in plastic bottles. The thickness of the green algal mat forming the schmutzdecke was measured using a graduated depth gauge before the schmutzdecke being scrapped off the sand.

In Phase II of the fieldwork, schmutzdecke biomass was sampled at the end of the filtration run after filter drainage for cleaning. A simple device consisted of a ring with 7.5 cm of diameter and 5 cm depth was used to sample the schmutzdecke on the top of the sand. The sampling technique consisted of turning the ring on the sand surface of

the filter beds at the selected sampling points in a way that the ring cut and removed the schmutzdecke off the sand surface. The samples were placed in plastic bags.

Samples were collected from Beds 4, 7, 8 and 9 on two occasions, except Bed 8 which was taken out of service for refurbishment after the first sampling. Twelve sampling points were selected for each filter bed in the first sampling occasion (Figure A.4.3a, Appendix A.4). In the second sampling occasion, the number of sampling locations was increased and twenty points were selected in each filter bed (Figure A.4.3b, Appendix A.4). Table 4.3 shows the sampling date and the duration of the filtration runs of each filter.

Table 4.3 - Sampling date and duration of the filtration run during Phase II

Filter	Sampling date		Duration of the run (days)	
	1 st Sampling	2 nd Sampling	1 st Sampling	2 nd Sampling
Bed 8	29/11/2000	-	84	-
Bed 4	07/02/2001	09/05/2001	77	91
Bed 9	13/03/2001	07/06/2001	92	87
Bed 7	20/03/2001	30/05/2001	94	71

4.2.3.2 -Dry and ash-free weights

Schmutzdecke biomass was measured as dry weight per unit area in both study phases, and in addition ‘ash free⁹’ weight was measured in Phase II to determine the chlorophyll-a content of the schmutzdecke.

A membrane filter method was used to measure dry and ash-free weight of schmutzdecke (APHA *et al.*, 1995). The schmutzdecke samples were washed with mains water and filtered through a cellulose fibre filter paper (150 mm diameter, 11 µm pore size) and were dried in a forced air oven maintained at 60 °C for 24 hours. After re-weighing, the samples were further ashed in an electronic muffle at 500°C for 24 hours for the determination of the ‘ash free’ weight. The difference in mass before

⁹ The term ‘ash free’ is the weight of biomass without combustion residues, i.e. mineral residual after removal of the volatile organic components (APHA *et al.*, 1995).

and after the drying procedure is used to calculate the dry and ash-free weight. Chlorophyll-a content was assumed to be 1.5 % of the ash-free weight of schmutzdecke (APHA *et al.*, 1995).

4.2.3.3 - Microscopy examination

One sample of the schmutzdecke collected from Bed 8 was separated and taken for examination by electronic microscope at the Department of Biological Sciences, Imperial College of Science, Technology and Medicine (Morris, 2001). The microscope utilised for the examination has the following characteristics: Philips 501(b); operating conditions 8KV, 350 Angstroms spot size (35nm), +20 tilt, 38mm working distance.

4.2.4 - Turbidity and suspended solids

Samples of approximately 5000 ml of the supernatant water were collected from Bed 9 on two different days, and one sample from Bed 7. Turbidity and suspended solid concentration of ten sub-samples of about 300 ml each were measured in laboratory.

The turbidity of each water sub-samples was measured by a nephelometric method (APHA *et al.*, 1995) using a Turbidimeter Hach, Model 2100A, 0.01 NTU of precision. The determination of the total suspended solids of each sample followed the method recommended by APHA *et al.* (1995). The sub-samples were filtered using a pre-weighed filter (47 mm diameter, 0.2 µm pore size). The filter papers were placed in an oven at 105 °C for an hour and then re-weighed

4.2.5 - Water quality parameters

The influent and treated water concentrations from the slow sand filter beds are monitored routinely at Walton. Dissolved organic carbon and TOC concentrations (Figure 4.3), and turbidity, ammonia, and coliform concentrations (Figure A.4.4, Appendix A.4) were provided by Thames Water for Bed 9 and Bed 10 for the duration of the experiment in Phase I.

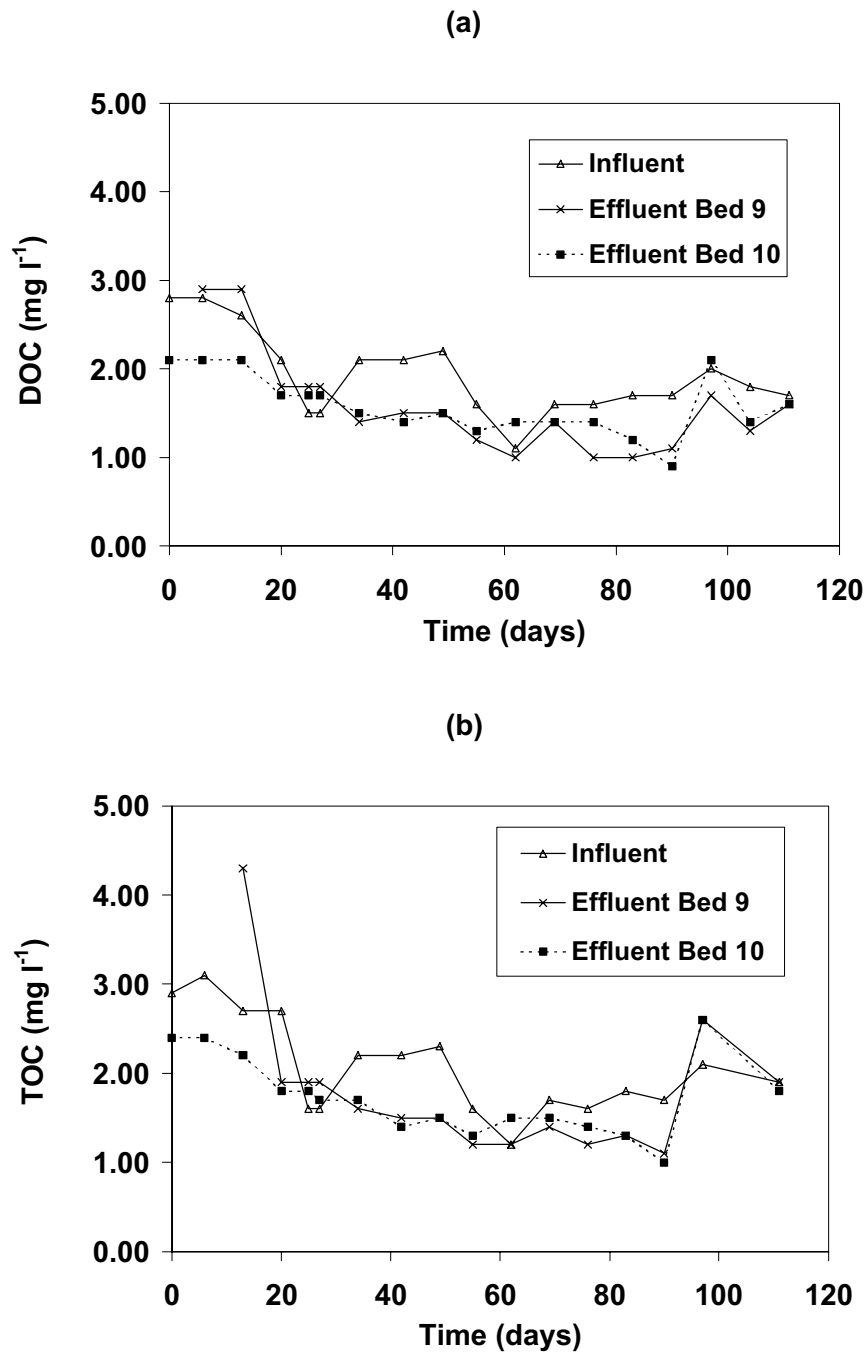


Figure 4.3 - Influent and effluent (a) DOC and (b) TOC concentrations for uncovered (Bed 9) and covered (Bed 10) filters. (Data provided by Thames Water)

4.3 - Results and discussion

4.3.1 - Sand biomass

The general patterns in interstitial microbial biomass concentrations in the sand, in relation to time and depth for both filters, are presented in Figure 4.4. In the uncovered system, sand biomass increased with time and decreased with depth (Figure 4.4a). The biomass carbon concentration measured in the top 0-2 cm of sand from the uncovered filter (Figure 4.4a), with full light interception, increased generally to a maximum value of $60 \mu\text{g C g}^{-1}$ (dry sand) in relation to filter run time, although more than $120 \mu\text{g C g}^{-1}$ was recorded in the surface sand at day 56. Biomass accumulated at a slower rate in the covered sand compared to the uncovered filter and increased to a maximum concentration of $15 \mu\text{g C g}^{-1}$ (dry sand) after 103 days (Figure 4.4b). No consistent relationship was observed between biomass concentration and depth of sampling in the covered filter.

Temporal trends in the weighted average biomass concentrations in the top 10 cm of the sand beds are shown in Figure 4.5. The weighted average biomass was calculated by summing the total biomass in the top 10 cm depth by a defined area over the defined volume. The biomass concentration increased significantly with time in the uncovered filter and was summarised by a simple logistic growth function¹⁰ ($r^2 = 0.9$; $P < 0.001$). The model predicted a maximum biomass accumulation in the sand of $71.4 \mu\text{g C g}^{-1}$ (dry sand) after 97 days of operation and the filter run ended 7 days later when the terminal head loss was reached. These observations are consistent with other reports (Duncan, 1988; Eighmy *et al.*, 1994) linking changes in headloss to biomass development in operational slow sand filters.

Biomass in the covered sand bed also increased (Figure 4.5), but at a significantly slower rate compared to the uncovered filter and in approximately linear relation with time ($r^2 = 0.70$; $P = 0.009$). The covered filter had not reached terminal headloss at the end of the monitoring period (day 103) and continued to normally operate after the final sample collection event in August 2000. Unfortunately, headloss is not routinely

¹⁰ $y = a * (1 - b * \exp(c * x))$ where a, b and c are constants and x is time (CoHort Software, 1993).

measured on the slow sand filters at the Walton AWT plant and so the relationship between biomass growth and headloss development could not be further elucidated.

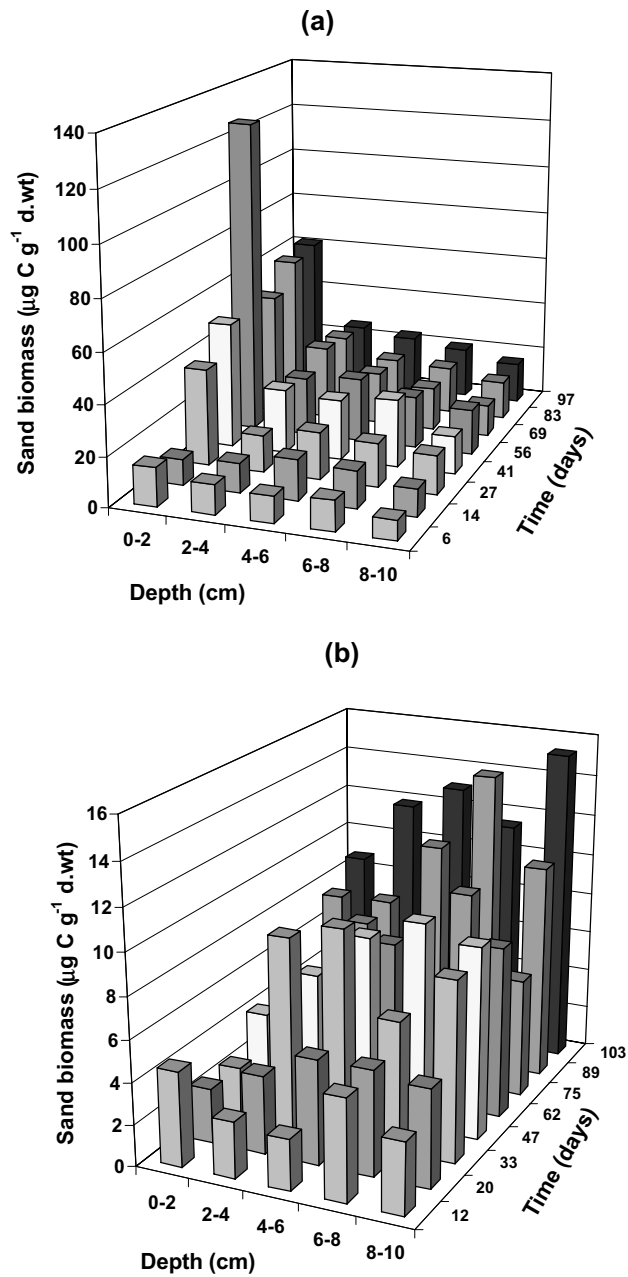


Figure 4.4 - Total microbial biomass concentration in sand from (a) uncovered (Bed 9) and (b) covered (Bed 10) slow sand filters in relation to time and depth

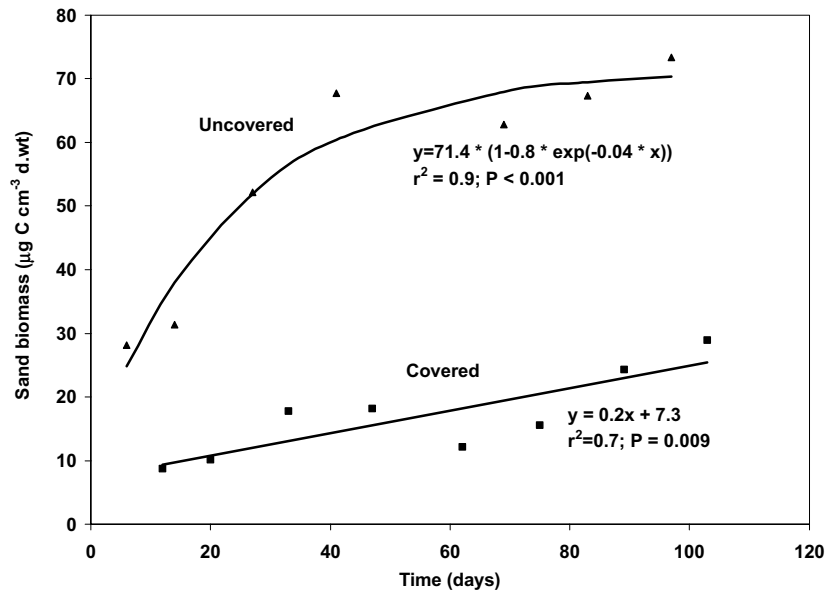


Figure 4.5 - Weighted average biomass concentrations in the 0-10 cm sand layer from slow sand filters in relation to time (Note: biomass value at 0-2 cm depth in Bed 9 for day 56 was 126.8 µg C g⁻¹ d.wt and the weighted average was omitted from the regression)

The distribution of interstitial biomass with depth in sand from the uncovered and covered filters is shown in Figure 4.6. No measurable increase in the microbial biomass content of the upper 0-2 cm sand layer was detected for the first 14 days of operation of the uncovered filter and the correlation between biomass content and depth achieved statistical significance ($P < 0.05$) after 56 days of operation for this filter. Similar patterns in biomass distribution with depth in slow sand filters have also been reported by Duncan (1988) and Yordanov *et al.* (1996). As expected, the largest accumulation of biomass in the uncovered filter was measured in the top 0-2 cm of sand. The increased production of biomass in the uncovered filter emphasised the importance of photosynthetic inputs of carbon substrates to the sand from the schmutzdecke, compared to the covered sand bed, where growth was smaller and supported only by the availability of substrates supplied in the influent water (Figure 4.3). Nevertheless, the observed reduction in biomass concentration with depth suggested there was also substrate limitation to microbial growth in the deeper layers of the uncovered filter.

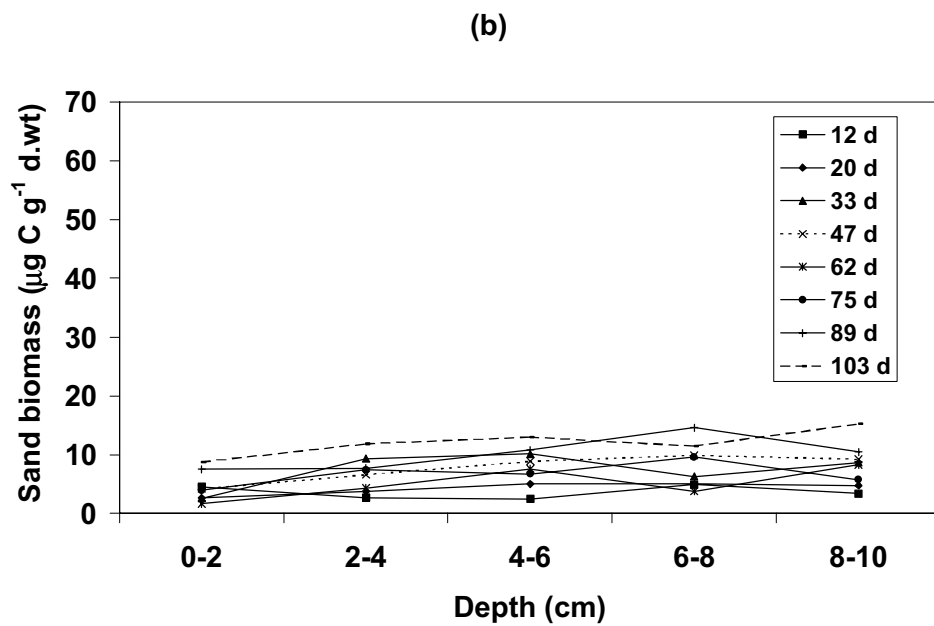
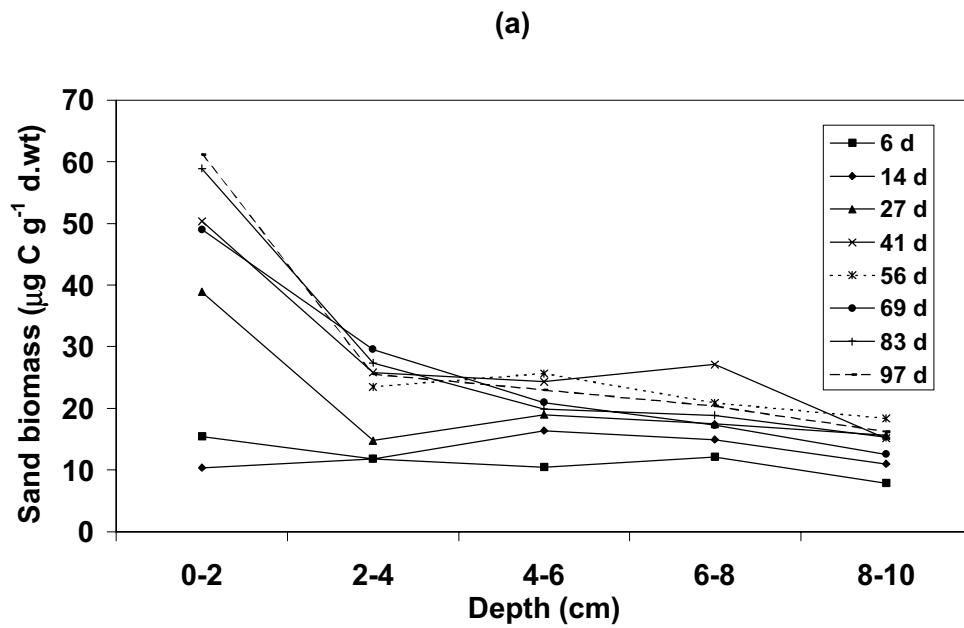


Figure 4.6 - Interstitial sand biomass concentration in relation to depth in (a) uncovered (Bed 9) and (b) covered (Bed 10) slow sand filters

The biologically active microbial community in the top few centimetres of sand in the filter bed is considered to be a major factor contributing to water purification by SSF (Bellamy *et al.*, 1985a; Hendricks and Bellamy, 1991). Interestingly, no differences were apparent in the water quality of effluents from either filter and generally consistent removals of TOC and DOC were observed throughout, despite large differences in the biological properties of the covered and uncovered filter beds (Figure 4.3). Thus, the average removals of TOC and DOC by Bed 9 (uncovered) were 25 % and 23 %, respectively, and Bed 10 removed 23 % of both TOC and DOC on average from the influent water (Note: mean values were estimated from net positive removal data for TOC/DOC presented in Figure 4.3). This behaviour contrasts with the data reported by Collins *et al.* (1994), which showed increased removals of natural organic matter (NOM) and organic precursor material in covered filters with increasing biomass concentration in the sand. These apparently conflicting observations could be explained by differences in the quality of influent water, and thus the nature of the dissolved organics, supplied to the filters. In this study the SSF was part of an advanced water treatment system involving pre-treatment by reservoir, pre-ozonation, flotation, rapid filtration, intermediate ozonation, and granular activated carbon. In view of this, it is likely that the amount of bio-available organic substrates in the influent to the filters at the Walton AWT plant would be very low. Collins *et al.* (1994) conducted their studies using a more conventional SSF system, without extensive pre-treatment of the influent water, and therefore it is likely that a greater amount of bio-available organic material was present.

4.1.2 - Schmutzdecke biomass

Phase I

Schmutzdecke was visible on the surface of the sand of Bed 9 from day 14 onwards. However, samples could not be collected until day 41 because the schmutzdecke had not developed sufficiently for it to be physically separated as a distinct layer from the sand before this period of filter operation had elapsed. By day 41, schmutzdecke had also formed on most of the filter surface and at the random locations used for collecting sand cores, increasing the possibility of sample collection.

development in Bed 9 at the Walton AWT works after 69 days of operation is shown in Plate 4.2. Although species identification was not an objective of this investigation, similar prolific algal development in uncovered slow sand filters has been widely observed (Brook, 1954, 1955; Bellinger, 1979; Nakamoto *et al.*, 1996ab).

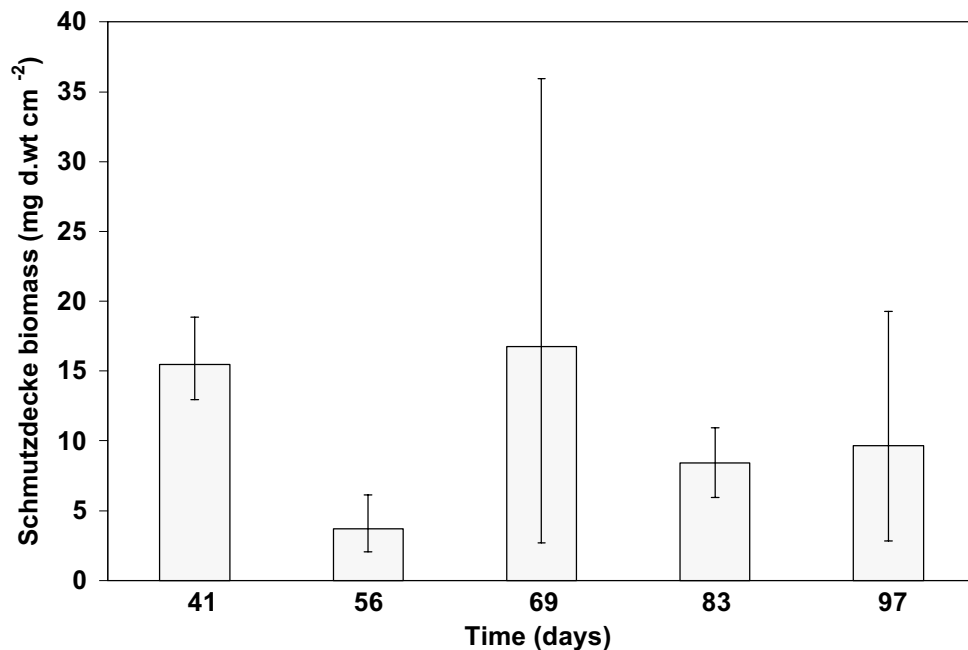


Figure 4.8 - Temporal variation in mean schmutzdecke biomass in Bed 9 (uncovered) at Walton (vertical bars represent minimum and maximum values)

Phase II

The visual characteristics of the schmutzdecke changed with time (Plate 4.3). During the period of February to March the schmutzdecke apparently presented a ‘green’ colour in all filter beds (Plate 4.3ace), and during May and June it had a dark colour (Plate 4.3bdf). Although this appears relatively inconsistent seasonal change between the periods of February/May and May/June, the mean of all chlorophyll-a contents of the schmutzdecke in the filter beds during May/June was approximately 26 % larger than that content during February/March (Table 4.4 and Tables A.4.1 to A.4.8, Appendix A.4). This increase in chlorophyll-a content was apparently very significant in Bed 4 ($P < 0.05$). In general, the increase in dry weight biomass between periods was not significant, except for Bed 9 ($P < 0.05$).

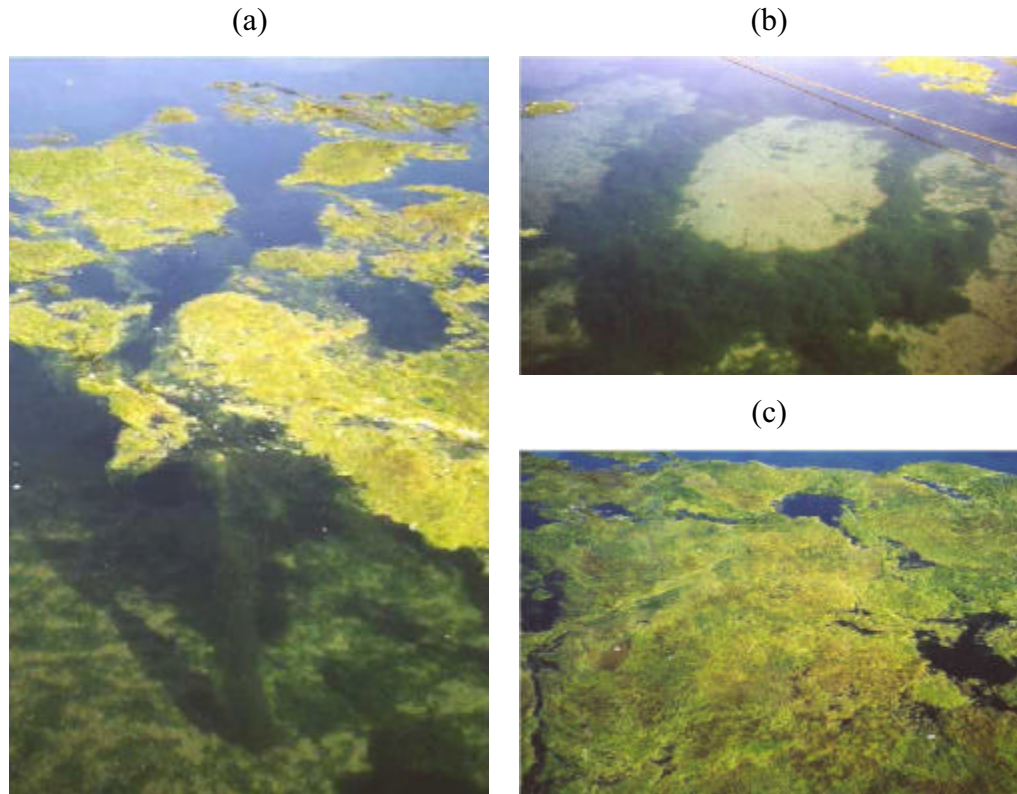


Plate 4.2 - Algae in Bed 9 (uncovered) at Walton: (a) supernatant algae; (b) benthic algae; (c) algal mat on the water surface

Table 4.4 - Mean biomass of schmutzdecke at the end of filtration run during two seasonal periods at Phase II

Filter bed	February/March		May/June		Significance	
	Dry weight ($\times 10^3$ mg m^2)	Ash-free (mgCha m^2)	Dry weight ($\times 10^3$ mg m^2)	Ash-free (mgCha m^2)	Dry weight	Ash-free
Bed 8	547	2004	NM	NM	NM	NM
Bed 4	704	2070	765	3309	P = 0.30	P < 0.05
Bed 7	828	3183	815	3467	P = 0.43	P = 0.21
Bed 9	920	3470	732	3360	P < 0.05	P = 0.38
Average	750	2682	771	3379		

NM = Not Measured

Plate 4.3 - Plate 4.3.doc Filter beds before schmutzdecke sampling in Phase II

Brook (1954,1955) observed that algae species in the supernatant water and on the top of slow sand filter beds vary over the year. Two cycles of algae growth were observed in the supernatant water, one cycle with a minimum growth in winter and maximum in spring and another for the remaining algae in summer. On the top of the sand, filamentous species were abundant from March to June and from August until December, and the maximum number of non-filamentous species was occurred in May and June and a minimum in January and February. Another interesting observation made by Brook (1954) was that towards the end of April the beds harboured other aquatic organisms as well as protozoa, rotifers, crustacea, and insect larvae. The disappearance of algae from filter beds was most marked from May to October, when insect larvae were most abundant. He suggested that the insect larvae were responsible for the disappearance of algae, and especially of the filamentous forms, from the filter beds. Midge larvae were observed on the sand surface of the drained filters and in the supernatant water of the filters in operation at the occasion of schmutzdecke sampling during the period of May to June at Walton. Therefore, the apparent differences on the schmutzdecke characteristics shown in Plate 4.2 may be explained by the species of algae and other organisms present in each seasonal cycle.

Schmutzdecke biomass data were also analysed statically to measure the amount of variation or spread in data (i.e. standard deviation, minimum, and maximum) and to describe the shape and symmetry of the distribution of biomass over the surface area of the filter (Figures A.4.5 to A.4.7, Appendix A.4). The statistics analyses were carried out for dry weight biomass and chlorophyll-a biomass of the schmutzdecke (Table A.4.9, Appendix A.4). Both contents of chlorophyll-a and dry weight biomass of schmutzdecke presented normal distribution over the surface area, suggesting that the random sample collection was satisfactory for measuring dynamics at the end of the filter run.

The algal mat (schmutzdecke) collected from the top of the sand of Bed 8 was formed mainly by filamentous algae during 84 days of operation (Plate 4.4). The schmutzdecke looked like a fibrous media consisting of multiple layers of coarse and fine meshes with pore size ranging from values smaller and larger than 100 μm (see bar lines in Plate 4.4). As such, the schmutzdecke may be expected to behave as a filter medium

involving the removal of particles and headloss development. As only one sample of the schmutzdecke filter was observed, the microscope photography does not reflect the variations in schmutzdecke development due to existing fluctuations in environmental conditions. However, similar images were seen in the micrographs of a mature schmutzdecke (40 days old) sample collected at Ivercannie water treatment works, Scotland (Law *et al.*, 2001).

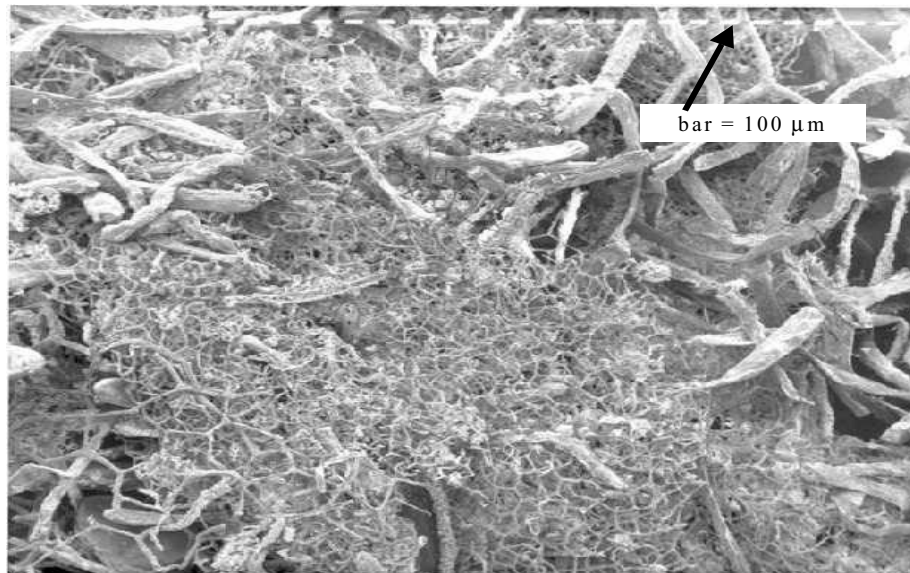


Plate 4.4 - Schmutzdecke structure at Walton (enlarged 20x, bar =100 μm)

4.1.3 - Turbidity and suspended solids relation

Figure 4.9 shows the results of turbidity and suspended solids concentration for the supernatant water of Bed 9 and Bed 7. The results are presented in terms of average values of the sub-samples collected in each filter bed, and they show that an increase in suspended solids implies an increase in turbidity. On average, 1 NTU was found to relate to 2.4 mg l⁻¹ in Bed 7, and to 5.7 mg l⁻¹ and 5.4 mg l⁻¹ in Bed 9a and Bed 9b, respectively. This figure suggests that, on average, 1 NTU is related to 5 mg l⁻¹ for the supernatant water at Walton.

4.2 - Conclusions

Interstitial microbial biomass and schmutzdecke development was determined in full-scale slow sand filters at Walton to help in the assumptions and simplifications of the simulation model. The conclusions of this study are stated as follows:

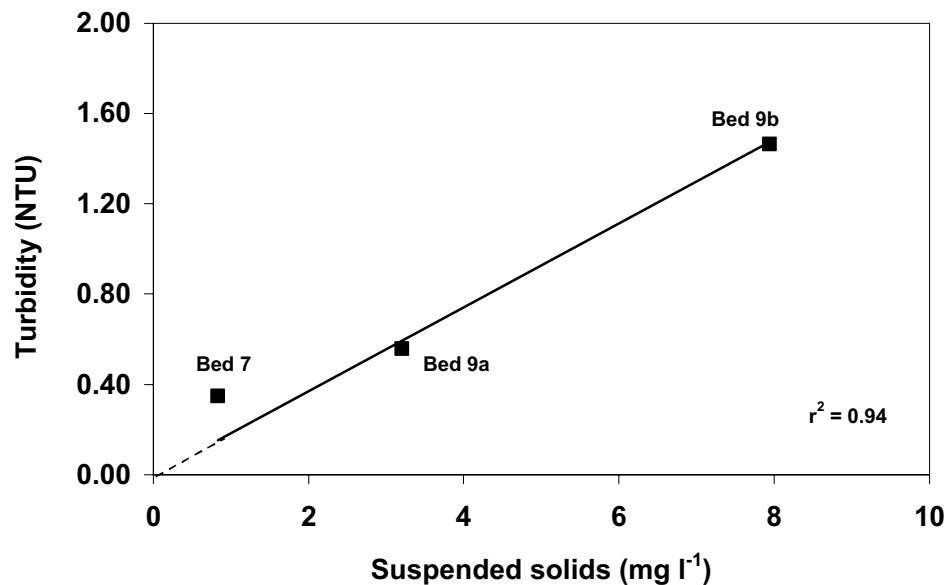


Figure 4.9 - Suspended solids vs turbidity in the supernatant water of Bed 9a (09/05/01), Bed 9b (30/05/01) and Bed 7 (07/06/01) at Walton

- (1) Biomass increased with time and decreased with depth in the uncovered filter (Bed 9), and most biomass development occurred in the upper 0-2 cm layer of the filter. By contrast, biomass content was much lower in the covered filter (Bed 10) and only a small increase was observed with time during the monitoring period, but no relationship was apparent with depth (Sub-section 4.3.1).
- (2) Temporal trends in the weighted average biomass concentrations in the top 10 cm of the sand in the uncovered filter showed that the biomass concentration increased significantly with time and was summarised by a simple logistic growth function (Figure 4.5). Biomass in the covered Bed 10 also increased, but at a significantly slower rate compared to the uncovered Bed 9 and in approximately linear relation with time. Beyond the 100-day of operation of Bed 10, biomass development was not known.
- (3) Covered and uncovered slow sand filters may achieve similar rates of OC removal in advanced water treatment systems, despite having markedly different biological properties. The results presented have suggested that, in advanced water treatment systems, labile OC is effectively removed and utilised for growth by the microbial biomass in covered slow sand filters. Uncovered filters, on the other hand, support